

Unravelling cell-particle interactions for the design of new micro- and nanoengineered systems

Doctoral Thesis presented by
Tania Patiño Padial

September 2015

UAB

Universitat Autònoma
de Barcelona



Universitat Autònoma de Barcelona

**UNRAVELLING CELL-PARTICLE
INTERACTIONS FOR
THE DESIGN OF NEW
MICRO- AND NANOENGINEERED SYSTEMS**

TANIA PATIÑO PADIAL

Memòria presentada per optar al Grau de Doctora amb Menció Internacional
en Biologia Cel·lular per la Universitat Autònoma de Barcelona

Directors:

DRA. CARMEN NOGUÉS SANMIQUEL, DR. LEONARD BARRIOS SANROMÀ
i DRA. ELENA IBÁÑEZ DE SANS

Bellaterra, 2015



Universitat Autònoma de Barcelona

Departament de Biologia Cel·lular, de Fisiologia i d'Immunologia

Unitat de Biologia Cel·lular

La Dra. **Carme Nogués Sanmiquel**, professora titular del Departament de Biologia Cel·lular, de Fisiologia i d'Immunologia de la Universitat Autònoma de Barcelona,

el Dr. **Leonard Barrios Sanromà**, catedràtic del Departament de Biologia Cel·lular, de Fisiologia i d'Immunologia de la Universitat Autònoma de Barcelona,

i la Dra. **Elena Ibáñez de Sans**, professora agregada del Departament de Biologia Cel·lular, de Fisiologia i d'Immunologia de la Universitat Autònoma de Barcelona,

CERTIFIQUEN:

Que **Tània Patiño Padial** ha realitzat sota la seva direcció el treball d'investigació que s'exposa en la memòria titulada "Unravelling cell-particle interactions for the design of new micro- and nanoengineered systems" per optar al grau de Doctora amb Menció Internacional per la Universitat Autònoma de Barcelona.

Que aquest treball s'ha dut a terme a la Unitat de Biologia Cel·lular del Departament de Biologia Cel·lular, de Fisiologia i d'Immunologia de la Universitat Autònoma de Barcelona.

I per tal que així consti, firmen el present certificat.

Bellaterra, 23 de setembre de 2015.

Dra. Carme Nogués Sanmiquel

Dr. Leonard Barrios Sanromà

Dra. Elena Ibáñez de Sans

Tania Patiño Padial

Aquesta tesi s'ha realitzat amb el finançament dels projectes MINAHE III (TEC2008-06883-C03) i MINAHE IV (TEC2011-29140-C03) del Ministerio de Ciencia y Tecnología, i el projecte 2009-SGR-282 de la Generalitat de Catalunya. Tania Patiño Padial ha gaudit d'una beca predoctoral per a la formació de personal investigador novell (FI), concedida per l'Agència de Gestió d'Ajuts Universitaris i de la Recerca de la Generalitat de Catalunya.

The unique and controllable physico-chemical properties of micro- and nanomaterials have allowed the creation of ground-breaking approaches to overcome some of the major challenges of different branches of technology and science, including modern medicine. The fast advances in micro- and nanotechnology have lead to an increasing demand for understanding the behaviour of micro- and nanomaterials within the physiological environments as well as their interactions at the bio-interface, including the cellular level, for an efficient and safe development. In this scenario, the present Thesis aimed to provide an integrated understanding about microparticle interactions with cells. First, we assessed the impact of cationic lipids and polymer coating of microparticles on their uptake by non-phagocytic (HeLa) cells. We found that non-covalently conjugated PEI at a 0.05 mM concentration offers the best balance between uptake efficiency and cytotoxicity. Second, we observed that surface modified microparticles were differently uptaken by tumoral (SKBR-3) and non-tumoral (MCF-10A) human breast epithelial cells, not only in terms of uptake efficiency but also of their endocytic pathways. Third, we demonstrated that polysilicon-chromium-gold multi-material intracellular chips (MMICCs) are suitable for biological applications due to their biocompatibility and capability of developing multiple functions through their bi-functionalization using orthogonal chemistry. Collectively, our results highlight the importance of assessing cell-particle interactions, in terms of cytotoxicity, uptake, intracellular location and cell type effect of newly designed micro- and nanomaterials, not only with respect to the target cells but also the neighbouring cells, in order to ensure their safety and efficiency.

Els micromaterials i nanomaterials presenten unes propietats fisicoquímiques úniques i controlables, les quals han permès la creació d'eines innovadores per tal d'afrontar alguns dels reptes que presenten diferents branques de la ciència i tecnologia, incloent la medicina moderna. El creixement exponencial de la microtecnologia i nanotecnologia en els últims anys ha generat la necessitat de conèixer millor el comportament dels micromaterials i nanomaterials en ambients fisiològics, especialment a nivell cel·lular, per tal d'assegurar un desenvolupament segur i eficient. En aquest context, l'objectiu principal d'aquesta tesi ha estat estudiar la interacció entre diferents tipus de micropartícules i cèl·lules. Amb aquesta finalitat, es van dur a terme tres treballs diferents. Primer, s'ha avaluat l'impacte del recobriment de micropartícules amb lípids i polímers catiónics en la seva internalització en cèl·lules no fagocítiques HeLa. En concret, s'ha observat que la utilització de PEI a una concentració de 0.05 mM presenta el millor balanç entre eficiència d'internalització i citotoxicitat. En segon lloc, s'ha analitzat si la modificació de la superfície de les micropartícules té un efecte diferent segons la línia cel·lular utilitzada. En concret, s'ha observat que les cèl·lules epitelials mamàries tumorals (SKBR-3) i no tumorals (MCF-10A) mostraven diferències significatives, tant pel que fa a la eficiència d'internalització de micropartícules com als mecanismes d'endocitosi involucrats. Finalment, s'ha demostrat que els xips intracel·lulars compostos de polisilici, crom i or, són bons candidats per a la seva utilització en aplicacions biològiques, ja que presenten una alta biocompatibilitat i són capaços de desenvolupar diferents funcions mitjançant la seva bifuncionalització. En conjunt, els resultats d'aquesta tesi posen de manifest la importància de determinar la citotoxicitat, l'eficiència d'internalització, la localització intracel·lular i l'efecte de la línia cel·lular a l'hora de dissenyar nous microsistemes i nanosistemes per tal de maximitzar la seva eficiència i minimitzar els efectes adversos.

Los micromateriales y nanomateriales presentan propiedades fisicoquímicas únicas y controlables que han permitido la creación de herramientas innovadoras para abordar algunos de los mayores retos que presentan distintas ramas de la ciencia y tecnología, incluyendo la medicina moderna. El crecimiento exponencial de la microtecnología y nanotecnología durante los últimos años ha generado la necesidad de comprender el comportamiento de los micromateriales y nanomateriales en ambientes fisiológicos, especialmente a nivel celular, para conseguir un desarrollo eficiente y seguro. En este contexto, el objetivo principal de esta tesis ha sido estudiar las interacciones entre diferentes tipos de micropartículas y células. Para ello, se han llevado a cabo tres estudios diferentes. Primero, se ha evaluado el impacto del recubrimiento de micropartículas con lípidos y polímeros catiónicos en la internalización de estas en la línea celular no fagocítica HeLa. Se ha determinado que utilización de PEI a una concentración de 0.05 mM presenta el mejor balance entre internalización y citotoxicidad. En segundo lugar, se ha analizado si la modificación de la superficie de las micropartículas tenía un efecto diferente según la línea celular utilizada. Concretamente, se ha observado que las células epiteliales mamarias tumorales (SKBR-3) y no tumorales (MCF-10A) presentaban diferencias significativas con respecto a la eficiencia de internalización y a los mecanismo de endocitosis involucrados. Finalmente, se ha demostrado que los chips intracelulares compuestos de polisilicio, cromo y oro, son buenos candidatos para su utilización en aplicaciones biológicas, ya que muestran una alta biocompatibilidad y son capaces de desempeñar distintas funciones mediante su bifuncionalización. En conjunto, los resultados de esta tesis ponen de manifiesto la importancia de determinar la citotoxicidad, eficiencia de internalización, localización intracelular y el efecto de la línea celular de los nuevos microsistemas y nanosistemas para maximizar su eficiencia y minimizar sus efectos adversos.

1. Introduction	2
1.1. Nanotechnology: a revolution “from the bottom”	5
1.2. Micro- and nanosystems for biomedical applications: opportunities and challenges of Nanomedicine	6
1.3. Understanding particle interactions at the bio-interface	14
1.3.1. Portals of particle entry into cells	16
1.3.2. Intracellular transport: endolysosomal network entrapment and cytosol delivery strategies	20
1.3.3. Effect of particle design on their interactions with cells: Size, Shape and Surface Properties	25
1.4. Impact of cell type on particle-cell interactions	30
1.5. Polystyrene particles as a model for studying particle-cell interactions	31
2. Objectives	32
3. Results	36
3.1. Enhancing microparticle internalization by nonphagocytic cells through the use of noncovalently conjugated polyethyleneimine	39
3.2. Surface modification of microparticles causes differential uptake responses in normal and tumoral human breast epithelial cells	55
3.3. Polysilicon-chromium-gold intracellular chips for multi-functional applications	71
4. Discussion	98
5. Conclusions	112
6. References	116

Abbreviations

BioMEM	Biological microelectromechanical system
BSA	Bovine serum albumin
CD	Cytochalasin D
CLSM	Confocal scanning laser microscopy
CME	Clathrin mediated endocytosis
Dyn	Dynasore
EDX	Energy-dispersive-X-ray
EE	Early endosome
EEA-1	Early endosome marker 1
FBS	Fetal bovine serum
FC	Flow cytometry
FITC	Fluorescein isothiocyanate
GNP	Gold nanoparticle
HeLa	Human cervix adenocarcinoma cell line
IgG	Immunoglobulin G
IL	Interleukin
LAMP-1	Lysosome associated membrane protein 1
LE	Late endosome
LF2000	Lipofectamine™ 2000
LPS	Lipopolysaccharide
MCF-10A	Human breast epithelial cell line
MMICC	Multi-material intracellular chip
MTT	3-(4,5-dimethylthiazol-2-yl)-2,5-diphenyltetrazolium bromide
PB	Phosphate buffer
PBS	Phosphate buffered saline
PEI	Polyethyleneimine
PFA	Paraformaldehyde
SEM	Scanning electron microscopy
siRNA	Small interference ribonucleic acid

SKBR-3	Human breast epithelial adenocarcinoma cells
TB	Trypan blue
TEM	Transmission electron microscopy
Tf	Transferrin
THP-1	Human leukemia derived monocytic cell line
TNF-(alpha)	Tumour necrosis factor (alpha)
TR-Phal	Texas Red® conjugated phalloidin



1

Introduction

The concept of nanotechnology was pioneered by the physicist Richard Feynman in 1959, with his revolutionary talk “There’s Plenty of Room at the Bottom” at the American Physical Society meeting at California Institute of Technology. During this talk, Dr. Feynman challenged his colleagues to consider the potential of the until then unexplored field of nanoscale. He envisioned the possibility of fabricating molecular machines, through control and manipulation of individual molecules and atoms: “We can arrange atoms the way we want: the very atoms, all the way down!” (FEYNMAN, 1992).

A decade later, Professor Norio Taniguchi first introduced the term **nanotechnology** as the precise manufacturing of materials, from a large to smaller scales, ultimately reaching the nanoscale (TANIGUCHI, 1974). But it was not until 1981, when single atoms could be “seen” through the scanning tunneling microscope, that modern nanotechnology was truly developed. During that time, the scientist Kim Eric Drexler popularized nanotechnology with his ideas about the construction of tiny machines that could be used for manipulating biological systems, for example as a cure to diseases (DREXLER, 1981). In 1996, one of the most relevant nanotechnology scientists, Richard Smalley, was awarded the Nobel Prize in Chemistry, shared with Harry Kroto and Robert Curl, for their discovery in 1985 of a new arrangement form of carbon structure: the *Buckminsterfullerene* (KROTO ET AL., 1985). This structure, also known as the *buckyball*, is a molecule resembling a soccerball in shape and is composed entirely of carbon, as are graphite and diamond. Their discovery was followed by other relevant findings such as colloidal semiconductor nanocrystals (quantum dots) in 1984-85 (BRUS, 1984; EKIMOV ET AL., 1985), and carbon nanotubes (FIG. 1) in 1991 (IJIMA, 1991).

The discovery of all these new materials with singular properties evidenced the usefulness and potential of nanotechnology as a tool for creating new systems and materials with unique and controllable physicochemical features.

Nanotechnology is nowadays defined as “the design, characterization, production and application of structures, devices and systems by controlling shape and size at the nanoscale” (DOWLING, 2004).

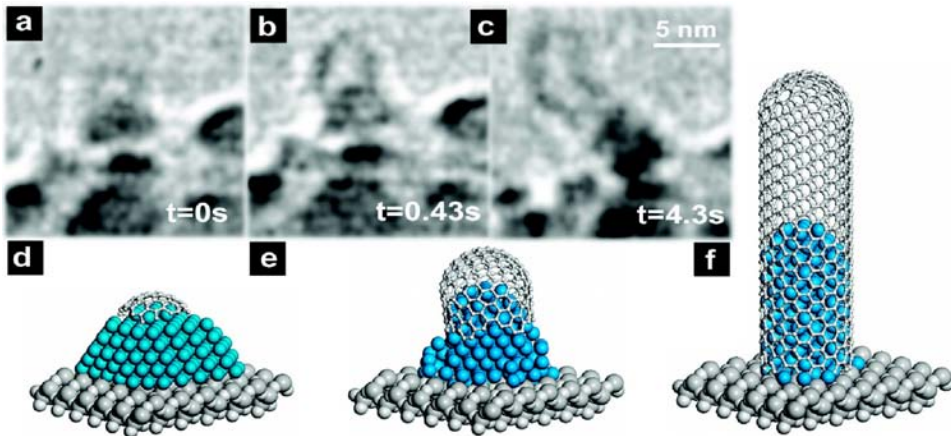


FIGURE 1. In situ transmission electron microscopy imaging of carbon nanotube's different stages of growth (a-c), with their corresponding ball-and-stick schematic model (d-f), where blue balls represent Ni, used as a catalyst, and grey rings represent carbon atoms (HOFMANN ET AL., 2007). Reproduced with permission from the copyright owner.

The development of nanotechnology is expected to have a considerable impact on society, as it offers powerful alternative approaches to overcome many limitations of different branches of technology and science (ALBANESE ET AL., 2012). Some examples are **energy**, through the use of solar cells and high-performance batteries; electronics, by the creation of data storage and single-atom transistors; or **food and agriculture**, providing improved delivery mechanisms for nutrients or screenings for contaminants (ETHERIDGE ET AL., 2013). But one the most exciting applications of nanotechnology is in the **biomedical field**, where nanotechnology is currently giving excellent and promising results that are expected to overcome the major challenges of modern medicine, including cancer research.

1.2. Micro- and nanosystems for biomedical applications: opportunities and challenges of Nanomedicine

Nanomedicine is a new emerging discipline, which has been defined by the USA National Institutes of Health as the use of micro- and nanoengineered devices for diagnosis, monitoring and treatment of a disease (MOGHIMI ET

AL., 2005). This includes the development of nanotechnology tools and nanomachines for medical research, therapeutics or diagnostics, such as cantilevers with functionalized tips (DAVID ET AL., 2014; CABALLERO ET AL., 2015), microneedles (QUINN ET AL., 2014; HAN & DAS, 2015), microchips for controlled drug delivery (STAPLES, 2010) or carbon nanotubes (MEHRA ET AL., 2015; MUNDRA ET AL., 2014).

The fast advances in the development of micro- and nanotechnology have provided a considerable number of promising new approaches to overcome several medicine challenges. This is possible thanks to the unique and controllable physicochemical properties of micro- and nanomaterials, which allow the design and tuning of “smart” systems to surpass the limitations of current diagnostics and/or therapeutic approaches (DAVIS ET AL., 2008). For example, nano-engineered materials have been shown to significantly improve the poor solubility (MERISKO-LIVERSIDGE & LIVERSIDGE, 2008) and pharmacokinetics (IMPERIALE ET AL., 2015; KAMINSKAS ET AL., 2015; WANG ET AL., 2015) of certain drugs. Moreover, nanomaterials specificity can be increased by enhancing molecular recognition of target cells through the conjugation of antibodies or peptides to the particle surface (GU ET AL., 2007; JAIN ET AL., 2013; SANNA ET AL., 2014). Particularly, the use of micro- and nanoplatforms is highly relevant in cancer treatment, where classical chemotherapies lead to a high number of undesirable side-effects due to their lack of specificity (FERRARI, 2005; PEER ET AL., 2007; CHAUHAN & JAIN, 2013; DEL BURGO ET AL., 2014). In this regard, nano-sized particles have proven to be advantageous against smaller molecules, as they present a higher efficiency to accumulate in tumor tissues, due to the enhanced permeability and retention effect (MAEDA, 2010; ACHARYA & SAHOO, 2011). Furthermore, some types of nanoparticles have shown unique photophysical properties, which can be used for the simultaneous diagnostic and treatment of cancer cells. This is the case of gold nanoparticles (GNPs), since their light absorption can be used for both imaging and photothermal ablation of cancer cells (HUANG & EL-SAYED, 2011; KENNEDY ET AL., 2011; JAIN ET AL., 2012).

Hence, the main goal in nanomedicine is the design and fabrication of multimodal systems that can integrate several functions in a single entity to be able to overcome the limitations of current medical approaches. FIGURE 2 shows a schematic representation of how different functions can be integrated in a single micro-/nanoplatfrom.

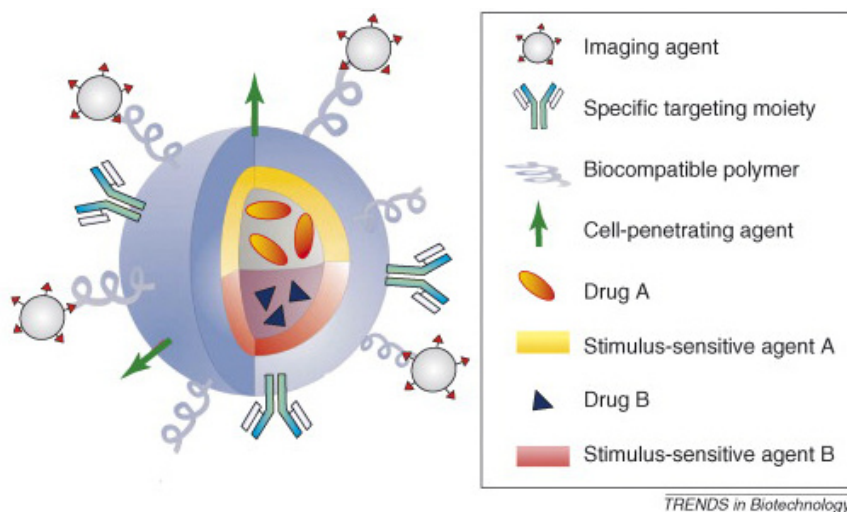


FIGURE 2. Scheme of the possibilities for particle modification in order to achieve a multi-functional platform (SANVICENS & MARCO, 2008). Reproduced with permission from the copyright owner.

In recent years, a wide range of micro- and nanoparticulate systems, either of organic or inorganic nature, have been developed. Some of the most relevant systems are:

- a) **Gold nanoparticles.** Their low cytotoxicity (CONNOR ET AL., 2005; PAN ET AL., 2007) as well as their ease of surface functionalization (TIWARI ET AL., 2011) and unique photophysical properties make them suitable for imaging, sensing and photothermal therapies (LI ET AL., 2009; ALKILANY & MURPHY, 2010). Due to their versatility as dual imaging and therapeutic agents, GNPs are nowadays considered a very promising tool for cancer treatment (KENNEDY ET AL., 2011; JAIN ET AL., 2012).
- b) **Mesoporous silicon micro- and nanoparticles.** Silicon biocompatibility and tuneable porous size through electrochemical synthesis (ANGLIN

ET AL., 2008) makes them excellent candidates for controlled drug delivery. Different drugs (SALONEN ET AL., 2005) and siRNA (TANAKA ET AL., 2010; MA ET AL., 2013; MENG ET AL., 2013) can be encapsulated inside the particle pores in order to improve their efficacy through an efficient and sustained delivery to the target cells and/or tissues. Moreover, the silicon surface can be easily functionalised to incorporate extra functions such as targeting or stimuli-responsive drug release (YANG ET AL., 2012).

- c) **Super paramagnetic iron nanoparticles.** Their magnetic properties make them remarkable agents for both diagnostics (magnetic resonance imaging) and treatment (magnetic heat treatment) of cancer cells (MAHMOUDI ET AL., 2011; HAYASHI ET AL., 2013). In addition, super paramagnetic iron nanoparticles have shown low cytotoxicity and their surface can be functionalized with molecules of interest to achieve targeting or drug delivery (HUANG ET AL., 2011; YOFFE ET AL., 2013).
- d) **Quantum dots.** Quantum dots are nanocrystals made of fluorescent semiconductor materials. They have unique optical properties such as a narrow and tunable emission spectrum, a broad excitation spectrum and they do not photobleach. These properties as well as their bioconjugation with targeting molecules give new avenues for *in vitro* and *in vivo* imaging applications (MEDINTZ ET AL., 2005; J. PARK ET AL., 2011; MONTON ET AL., 2012, 2015).
- e) **Carbon nanotubes.** Carbon nanotubes can be considered as a single layer of graphite rolled up into a cylinder, as they are made up of hexagonal networks of carbon atoms of 1 nm in diameter and 1-100 nm in length. Carbon nanotubes present unique physical, mechanical and electronic properties, which are of special interest for several biomedical applications, such as bone tissue engineering (VENKATESAN ET AL., 2014), stem cell research (RAMÓN-AZCÓN ET AL., 2014) or cancer theranostics (CHEN ET AL., 2015).
- f) **Liposomes.** Liposomes were the first nanoengineered drug delivery system used in clinics. They consist of enclosed lipid bilayers that can be

used for encapsulating drugs or nucleic acids. This protects the latter from degradation, thereby enhancing their cellular uptake and cytoplasmic delivery of the cargo (ALLEN & CULLIS, 2013). Furthermore, liposomes can be combined with different molecules such as polymers (ADLAKHA-HUTCHEON ET AL., 1999) or targeting molecules (WANG ET AL., 2014) and this may control and improve the efficiency of the drug delivery system.

- g) Polymer micro- and nanoparticles.** The use of biodegradable polymers with controllable physicochemical properties, such as polyethyleneglycol, chitosan or Poly(DL-lactic-co-glycolic acid), among others, has yielded remarkable results for drug delivery. Polymer particles offer many advantages such as lower clearance by immune system, intracellular delivery and stimuli-responsive drug delivery (LIECHTY ET AL., 2010).
- h) Dendrimers.** Dendrimers are repetitively branched molecules, generally described as a new class of polymeric materials which have a symmetric structure around a core, often acquiring spherical three-dimensional conformations (BOSMAN ET AL., 1999). Their uniform size, high branching degree, high solubility, well-defined molecular weight and available internal cavities have attracted interest for drug delivery applications (NANJWADE ET AL., 2009).

Properties and applications of the different types of micro- nanodevices for biomedicine are summarized in FIGURE 3.

The outlook for micro- and nanoplatforms use in nanomedicine is fascinating and promising, especially in the case of cancer diagnostics and treatment. However, while nanomedicine has reached encouraging outcomes at an experimental level so far, it still remains a young discipline and there is a long way to go from its current experimental stages to actual clinical applications. A recent study identified 247 nanomedicine products that were either approved or under various clinical stages, of which 100 have reached a commercial stage (TABLE 1) (ETHERIDGE ET AL., 2013).








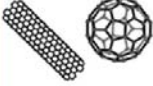
	Particle type	Composition/Structure	Applications
ORGANIC		Polymer e.g., PLGA, glycerol, chitosan, DNA; monomers, copolymers, hydrogels	Drug delivery; passive release (diffusion), controlled release (triggered)
		Dendrimer PAMAM, etc.	Drug delivery
		Lipid Liposomes, micelles	Drug delivery
INORGANIC		Quantum dots CdSe, CuInSe, CdTe, etc.	Optical imaging
		Gold Spheres, rods, or shells	Hyperthermia therapy, drug delivery
		Silica Spheres, shells, mesoporous	Contrast agents, drug delivery (encapsulation)
		Magnetic Iron oxide or cobalt-based; spheres, aggregates in dextran or silica	Contrast agents (MRI), hyperthermia therapy
		Carbon-based Carbon nanotubes, buckyballs, graphene	Drug delivery

FIGURE 3. Summarized classification of the most relevant types of micro- and nanodevices used for biomedical applications. Adapted from DAWIDCZYK ET AL., 2014.

The translation of nanomedicine research into real clinical applications is still at an early stage. For instance, in the case of cancer nanomedicine, clinical trials represent only a 2% of the total number of publications in the field over the last 10 years (WICKI ET AL., 2015). Furthermore, and in spite of all research efforts, there are only 12 currently approved nanomedicines, which are listed in TABLE 2.

This context warrants further discussion about the limitations of applying nanomedicine into clinical practice. This can be attributed to several issues, as outlined below.

Nanocomponent	Investigational			Commercial		
	Therapeutic	Device	Total	Therapeutic	Device	Total
Hard NP	3	12	15	0	28	28
Nanodispersion	5	0	5	1	1	2
Polymeric NP	23	0	23	9	0	9
Protein NP	4	0	4	2	0	2
Liposome	53	0	53	7	1	8
Emulsion	18	1	19	9	0	9
Micelle	8	0	8	3	1	4
Dendrimer/Fleximer	2	2	4	0	3	3
Virosome	6	0	6	2	0	2
Nanocomposite	0	0	0	0	18	18
NP Coating	0	2	2	0	6	6
Nanoporous material	0	3	3	0	2	2
Nanopatterned	0	2	2	0	2	2
Quantum dot	0	1	1	0	4	4
Fullerene	0	1	1	0	0	0
Hydrogel	0	0	0	0	1	1
Carbon nanotube	0	1	1	0	0	0
Total	122	25	147	33	67	100

TABLE 1. Classification of the different types of identified nanoproducts, according to their developmental stage. Adapted from ETHERIDGE ET AL., 2013.

First, the lack of uniformity in the experimental conditions, often followed by inconsistent reports of various parameters such as tumour characteristics, dose, or physico-chemical properties of nanomaterials, makes it difficult to compare the obtained results among reports and to draw solid conclusions about the outcomes (ETHERIDGE ET AL., 2013; DAWIDCZYK ET AL., 2014).

Second, research efforts in nanotechnology have largely been focused upon the design and fabrication of new nanomaterials and have mainly involved proof-of-concept studies. This has incurred in a high number of publications about new and varied nanomaterials at the expense of more fundamental approaches studying the interactions of nanomaterials with the biological systems.

Product [company]	Drug	Nanomaterial	Application	Approval
Abraxane® [Abraxis/Celgene]	Paclitaxel	Nanoparticle albumin-bound	Breast, pancreatic, non- small-cell lung cancer	2005
DaunoXome® [Galen]	Daunorubicin	Liposome	Kaposi's sarcoma	1996
DepoCyt® [Pacira]	Cytosine Arabinoside	Liposome	Neoplastic meningitis	1999
Doxil®/Caelyx® [Johnson & Johnson]	Doxorubicin	Liposome	Kaposi's sarcoma Ovarian and breast cancer Multiple myeloma	1995, 1999, 2003, 2007 (Europe, Canada)
Genexol-PM® [Samyang Biopharm]	Paclitaxel	PEG-PLA polymeric micelle	Breast, lung and ovarian cancer	2007 (South Korea)
Lipo-Dox® [Taiwan Liposome]	Doxorubicin	Liposome	Kaposi's sarcoma, breast and ovarian cancer	1998 (Taiwan)
Marqibo® [Talon]	Vincristine	Liposome	Acute lymphoid leukaemia	2012 (USA)
Mepact® [Takeda]	Mifamurtide MTP-PE	Liposome	Osteosarcoma	2009 (Europe)
Myocet® [Cephalon]	Doxorubicin	Liposome	Breast cancer (cyclophosphamide)	2000 (Europe)
NanoTherm® [Magforce Nanotechnologies]		Iron oxide nanoparticle	Thermal ablation glioblastoma	2010 (Europe)
Oncaspar® [Enzon/Sigma-tau]	L-asparaginase	PEG protein conjugate	Leukaemia	2006
Zinostatin stimalamer® (Zinostatin) [Yamanouchi]	Styrene maleic anhy- dride neocarzinostatin (SMANCS)	Polymer protein conjugate	Liver and renal cancer	1994 (Japan)

TABLE 2. Approved nanomedicines for cancer therapy in 2015. Adapted from WICKI ET AL., 2015.

For example, a major concern that limits the application of nanomedicine-based therapies is the safety of nanomaterials. While most of the studied nanomaterials have shown to render a high biocompatibility, others, such as carbon nanotubes (KESHARWANI ET AL., 2015), metal oxide particles (FRÖHLICH, 2013; SARKAR ET AL. 2014; VALDIGLESIAS ET AL., 2015) or quantum dots (DERFUS ET AL., 2004; KING-HEIDEN ET AL. 2009; BRADBURNE ET AL., 2013) may trigger toxic effects. In this regard, it is worth mentioning that harmful effects induced by nanoparticles rely upon certain physicochemical properties of nanomaterials such as their size, surface properties and functional groups. Further discussion on how particle design influences cytotoxicity is given in Section 1.3.3.

In conclusion, a complete characterization of the nanomaterial properties, as well as a deeper knowledge of the behaviour of micro- and nanoparticles within physiological environments, have become increasingly important for the design of efficient and safe micro- and nanosystems (STARK, 2011).

1.3. Understanding particle interactions at the bio-interface

Micro- and nanoparticulate systems can be administered into the organism through several ways: orally (O'HAGAN ET AL., 1993; ROY ET AL., 1999; UL-AIN ET AL., 2003; URBANSKA ET AL., 2012), inhaled (MARETTI ET AL., 2014; PARIKH ET AL., 2014), intravenously (PERACCHIA ET AL., 1999; LIOPO ET AL., 2012; HAYASHI ET AL., 2013) and topically (CAVALLI ET AL., 2002; MÜLLER-GOYMANN, 2004; KIM ET AL., 2009). Once inside the organism, they will encounter several biological barriers (FIG. 4).

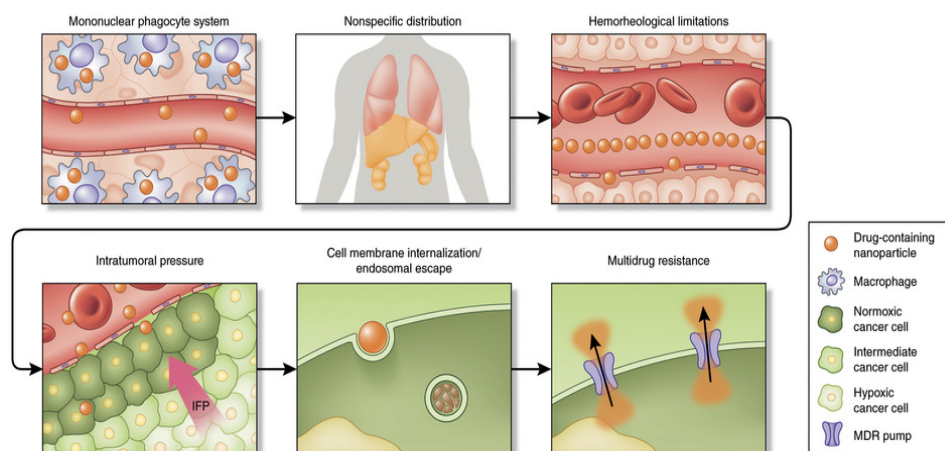


FIGURE 4. Biological barriers encountered by nanoengineered drug delivery systems (BLANCO ET AL., 2015). Reproduced with permission from the copyright owner.

First, micro- and nanoparticles will interact with different biomolecules present in the biological fluids. For example, when micro- and nanoplatforms reach the bloodstream, molecules present in the serum (mainly proteins) will adsorb on the particle surface forming the so-called **protein corona** (CED-ERVAL ET AL., 2007; NEL ET AL., 2009; WALCZYK ET AL., 2010; SAKULKHU

ET AL., 2014). The study of protein corona formation around nanoparticles is currently a growing focus of interest regarding nanomedicine research, as it has been shown to play an important role in modulating nanomaterials biodistribution (AGGARWAL ET AL., 2009; MONOPOLI ET AL., 2011; BARGHEER ET AL., 2015), circulation time (SAKULKHU ET AL., 2014) and cellular uptake (LESNIAK ET AL., 2012; YAN ET AL., 2013; RITZ ET AL., 2015). Moreover, protein corona has shown to mask targeting ligands, resulting in a significant reduction of specificity (SALVATI ET AL., 2013).

Second, opsonised micro- and nanomaterials will interact with the immune system, since they will be detected as “foreign” particles and cleared out of the circulation immediately by the mononuclear phagocyte system (PATEL ET AL., 1998; ZOLNIK ET AL., 2010).

Third, micro- and nanosystems will access the bloodstream, where their circulation time, pharmacokinetics and capability of extravasation through the vascular walls will depend not only on their opsonisation and sequestration by the mononuclear phagocyte system, but also on the particle design (DECUZZI ET AL., 2005; GENTILE ET AL., 2008; TASCIOTTI ET AL., 2008; DECUZZI ET AL., 2009; ARVIZO ET AL., 2011; TAN ET AL., 2013). In the case of tumour tissues, although the enhanced permeation effect allows the accumulation of nanoparticles, this accumulation can be severely compromised by high interstitial fluid pressures in certain tumour microenvironments (HELDIN ET AL., 2004).

Finally, micro- and nanoplatfoms able to reach target tissues need to be internalised by cells, where they will need to overcome several barriers such as the cellular membrane (See section 1.3.1) and their entrapment in endolyosomal compartments (See section 1.3.2).

In order to design innovative micro- and nanoengineered materials able to overcome the biological barriers, a deeper understanding about the behaviour of nanomaterials within the biological systems is required. For this reason, in this thesis we have focused on the study of particle interactions at cellular level.

1.3.1. Portals of particle entry into cells

Plasma membrane is crucial to maintain the intracellular environment. It is selectively permeable, so that whereas some small and non-polar molecules can easily diffuse through the lipid bilayer, ions and other large molecules are not capable of crossing the hydrophobic membrane by themselves (VERMA & STELLACCI, 2010). Some of these molecules can be transported across the cell membrane by specialized mechanisms (COOPER & HAUSMAN, 2013; ALBERTS ET AL., 2014) .

In the case of bigger molecules such as proteins, macromolecules, large complexes and micro- and nanoparticles, their transport across the cell membrane is actively carried out through an energy-dependent process called **endocytosis** (CONNER & SCHMID, 2003). Generally, endocytosis can be divided in two major groups: **phagocytosis** (“cell eating”, involves the uptake of large particles) and **pinocytosis** (“cell drinking”, involves uptake of smaller molecules, fluids and solutes). FIGURE 5 shows a schematic representation of the different endocytic pathways, which will be explained in detail below.

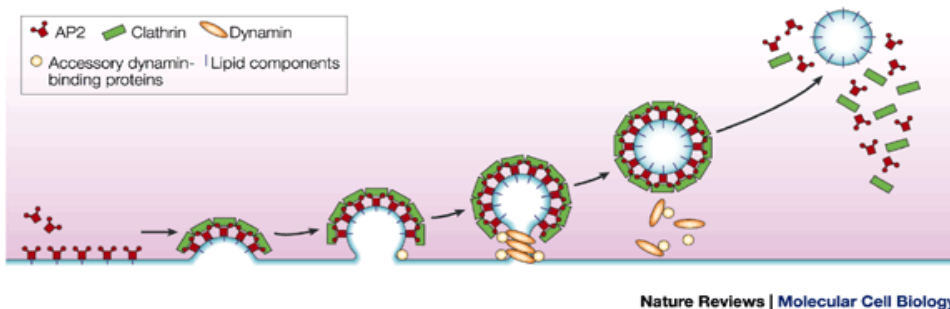


FIGURE 5. Schematic representation of the different endocytic pathways. Adapted from MAYOR & PAGANO, 2007.

The process of phagocytosis occurs only in specialized cells, such as macrophages, dendritic cells or polymorphonuclear neutrophils (UNDERHILL & GOODRIDGE, 2012), whereas pinocytosis occurs in all cell types. Several mechanisms of pinocytosis have been described, which mainly differ in the size of the formed vesicle, the nature of the cargo and the machinery involved in the

vesicle formation. Depending on the endocytic mechanism, vesicles can be directed to different cell compartments, where the content of vesicles is degraded or recycled (COOPER & HAUSMAN, 2013; ALBERTS ET AL., 2014). Thus, a better knowledge about internalization mechanisms of nanomedicines is crucial for an efficient delivery and minimized toxic effects.

Phagocytosis

Specialized cells of the immune system such as polymorphonuclear neutrophils and macrophages have a special mechanism, which allows them to endocytose big particles such as foreign materials, pathogens or dead cells, in order to clear them out of the organism. Phagocytosis is triggered by the formation of cell surface-protrusions through the polymerization of actin, one of the structural proteins of the cell cytoskeleton. These protrusions surround the particle until it is engulfed by the cell, forming an intracellular vesicle, the phagosome, which is normally directed to the endo-lysosomal system for the degradation of its contents (ADEREM & UNDERHILL, 1999; CHIMINI & CHAVRIER, 2000). Macrophages have shown to be able to phagocytose particles with diameters above 20 μm (CANNON & SWANSON, 1992).

Pinocytosis

a) **Clathrin-mediated endocytosis (CME).** This mechanism involves the concentration of transmembrane receptors and their bound ligands into a coated membrane invaginations or “pits”, a consequence of the recruitment and assembly of cytosolic proteins such as adaptors and clathrin. Vesicle scission from the plasma membrane is driven by the recruitment of dynamin, a multidomain GTPase protein that assembles into a spiral or “collar”. This constricts the invaginated pits at their necks, leads to membrane fission and ultimately results in the release of the endocytic vesicles. After vesicles are completely formed, the coating components are recycled for their re-use (CONNER & SCHMID, 2003). FIGURE 6 shows a schematic representation of vesicle formation by CME.

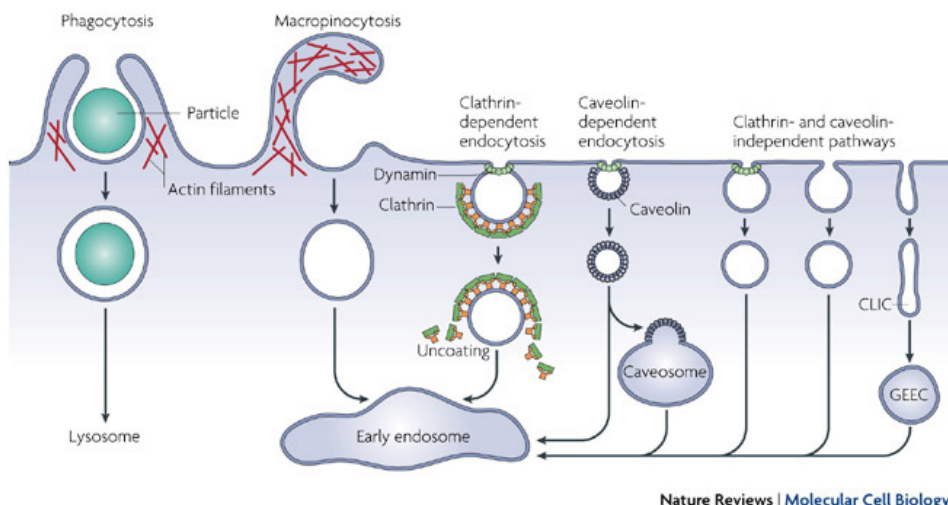


FIGURE 6. Schematic representation of the clathrin coated vesicle formation (GUNDELFINGER ET AL., 2003). Reproduced with permission from the copyright owner.

Vesicles formed by CME are often about 120 nm in diameter and their content is normally directed to the lysosomal degradation pathway. However, the final destination of a vesicle not only depends on the mechanism of internalization, but also on the ligand-receptor signalling. For this reason, when uptaken by CME, particles conjugated with a targeted ligand might not follow the same intracellular pathway than the free ligand itself (WANG ET AL., 2010; TEKLE ET AL., 2008).

- b) Caveolin-mediated endocytosis.** Caveolin is a dimeric protein located in cholesterol- and sphingolipid-enriched membrane domains (**lipid rafts**), leading to the formation of small flask-shaped membrane invaginations called **caveolae** (CONNER & SCHMID, 2003). As CME, caveolin-mediated endocytosis is normally triggered by ligand-receptor signalling. In addition, dynamin has also shown an important role on the formation of vesicles. But in this case, vesicle fate is not always the endo-lysosomal compartment. It has been described that caveolin-mediated endocytosis can bypass the endo-lysosomal compartment in some cases. Then, the cargo accumulates in vesicle-like structures called caveosomes and are

later processed through non-degradative pathways to different cell compartments such as the endoplasmic reticulum and/or the nucleus, as it is the case of SV40 virus (PELKMANS ET AL., 2002).

- c) **Clathrin- and caveolin- independent endocytosis.** This type of endocytosis has been relatively recently described and its mechanisms and properties still remain poorly understood (SANDVIG ET AL., 2008). It has been observed that some features are shared with caveolin-dependent endocytosis, such as cholesterol sensitivity and lipid rafts, but in this case it is regulated by non-caveolar intermediates, being this type of endocytosis caveolin- and dynamin- independent (KIRKHAM & PARTON, 2005).
- d) **Macropinocytosis.** Macropinocytosis is another special type of clathrin- and caveolin- independent endocytosis. It is an actin-triggered process that allows the internalization of large volumes of extracellular fluid (SWANSON & WATTS, 1995).

Understanding the mechanism of internalization and intracellular pathways of nanomedicines is essential to improve their design and efficacy. On the one hand, nanomedicines need to interact with the cell membrane in order to trigger any of the endocytic mechanisms. The capability of micro- and nanoparticles to bind to the cell membrane has been shown to strongly rely upon the physicochemical properties of nanomaterials such as their size, shape, surface charge, and functionalization (ALBANESE ET AL., 2012; ZHANG ET AL., 2012; DEL BURGO ET AL., 2014). The more affinity a particle has to the cell membrane, the more possibilities to be internalized. The effect of particle design on particle-cell interactions will be further discussed in Section 1.3.3. On the other hand, it is crucial to characterize the endocytic mechanism by which a specific nanomaterial is internalized, as this strongly influences the post-internalization fate and intracellular location of nanoparticles (YAMEEN ET AL., 2014). Furthermore, some mechanisms of endocytosis are unspecific, so that particles uptaken by these pathways are, in principle, able to enter all cell types. By contrast, particles internalized via ligand-receptor signalling can

be directed to a specific target cell type, since some receptors are differentially expressed in specific types of cells (EL-SAYED ET AL., 2006; BAREFORD & SWAAN, 2007; ZHONG ET AL., 2014). In this regard, it is worth noting that some polarized cell types may also show a spatial distribution of endocytic mechanisms. For example, it has been described that CME is preferentially regulated and expressed in the apical side of polarized epithelial cells, whereas the predominant mechanism in the basolateral side of the cell is caveolin-mediated endocytosis (SANDVIG & VAN DEURS, 2005; IVERSEN ET AL., 2011). Endothelial cells are also expected to show this differential distribution of endocytic properties.

In order to identify the mechanisms of nanomaterials internalisation by cells, the different endocytic pathways can be inhibited with either chemical or pharmacological agents (TABLE 3). Another approach that is becoming increasingly popular for the study of endocytosis pathways is the use of mutants, such as knock-out cell lines, which lack the protein involved in a specific endocytic pathway (DUTTA & DONALDSON, 2012).

1.3.2. Intracellular transport: endolysosomal network entrapment and cytosol delivery strategies

In a classical endocytic process, primary formed vesicles deliver their contents and membrane into early endosomes (EE), a vesicular compartment often located in the peripheral cytoplasm. This compartment provides the adequate environment for molecular sorting, to either recycling or degradation pathways (MELLMAN, 1996). Recycling of molecules is carried out by vesicle formation for transport to the plasma membrane and is regulated by several proteins (BONIFACINO & ROJAS, 2006; PFEFFER, 2009). For 8-15 min, EEs accumulate cargo and after that period, they mature into late endosomes (LE) by inheriting newly synthesized lysosomal hydrolases and membrane components from the secretory pathway (HUOTARI & HELENIUS, 2011). LEs have a round or oval morphology, with a diameter of 250-1000 nm and pH 6-5, and their limiting membrane contains lysosomal proteins, such as lysosome as-

Chemical inhibitors

Endocytosis inhibitor	Pathway targeted	Mode of action
Hypertonic sucrose	CME	Traps clathrin in microcages
Potassium depletion	CME	Aggregates clathrin
Cytosol acidification	CME	Inhibits the scission of the clathrin pits from the membrane
Chlorpromazine	CME	Translocates clathrin and AP2 from the cell surface to intracellular endosomes
Monodansylcadaverine	CME	Stabilizes CCVs
Phenylarsine oxide	CME	Not clearly known
Chloroquine	CME	Affects the function of CCVs
Monensin	CME	Affects proton gradient
Phenothiazines	CME; phagocytosis	Affects the formation of CCVs
Methyl- β -Cyclodextrin	Lipid raft	Removes cholesterol out of the plasma membrane
Filipin	CIE	Binds to cholesterol in the membrane
Cytochalasin D, latrunculin	Phagocytosis; macropinocytosis	Depolymerizes F-actin
Amiloride	Macropinocytosis	Inhibits Na ⁺ /H ⁺ exchange

Pharmacological inhibitors

Endocytosis inhibitor	Pathway targeted	Mode of action
Dynasore	CME	Blocks GTPase activity of Dynamin
Dynoles, dyngoies	CME	Blocks GTPase activity of Dynamin I
Pitstop	CME	Interferes with binding of proteins to the N-terminal domain of clathrin

TABLE 3. Chemical and pharmacological inhibitors of endocytosis (adapted from DUTTA & DONALDSON, 2012). CME, Clathrin-mediated endocytosis; CIE, Clathrin-independent endocytosis; CCV, clathrin coated vesicles

sociate membrane protein (LAMP-1) (HUOTARI & HELENIUS, 2011). During their maturation, LEs move towards the perinuclear area of the cell, where they fuse with each other, thereby leading to the formation of larger bodies or undergoing “kiss-and-run” fusions. These larger bodies fuse with lysosomes and generate a hybrid organelle called endolysosome, where the hydrolysis of most of the endocytosed cargos takes place (LUZIO ET AL., 2007). Finally, endolysosomes mature into lysosomes, which are heterogeneously shaped vesicular compartments, with an electron-dense lumen, irregular content and often various membrane sheets (SAFTIG & KLUMPERMAN, 2009). Lysosomes contain about 50 different degradative enzymes that are only active at an acidic pH (pH range in lysosomes=4.5-5) and are highly specialised in the hydrolysis of several molecules such as lipids, proteins, DNA, RNA and polysaccharides (COOPER, 2000). The maturation and recycling pathways of EE, LE, endolysosomes and lysosomes is a continuous and dynamic process (FIG. 7).

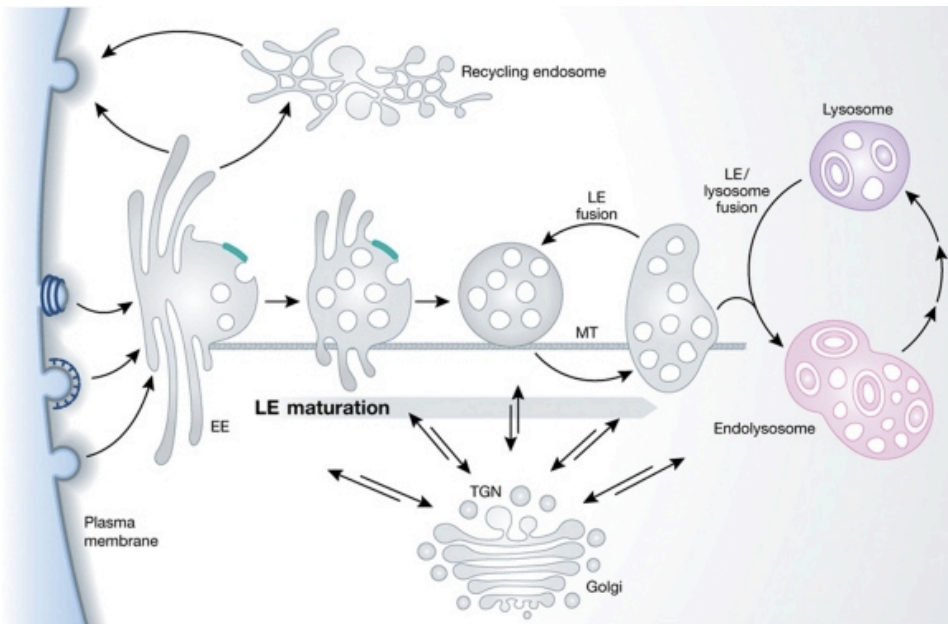


FIGURE 7. Schematic representation of endosome maturation into lysosomes (HUOTARI & HELENIUS, 2011). EE=Early endosome; LE=Late endosome; MT=Microtubule; TGN=Trans Golgi network. Reproduced with permission from the copyright owner.

One of the major bottlenecks of nanomedicines efficacy in therapeutic applications is their accumulation and possible degradation in the endolysosomal network (SHETE ET AL., 2014). For this reason, evaluating the intracellular localisation of micro- and nanomaterials is crucial. This can be assessed by either fluorescence detection of specific markers for endosomes/lysosomes, or by electron microscopy, as shown in FIGURE 8.

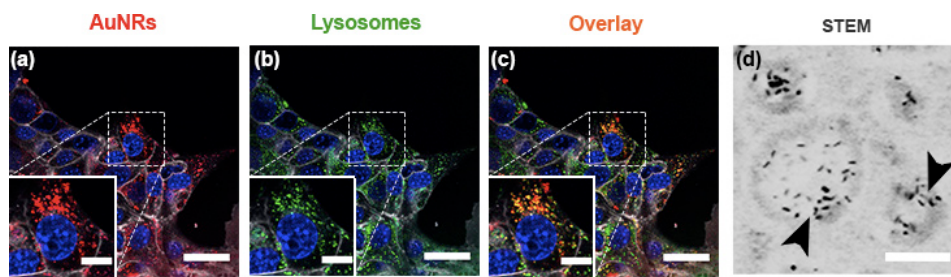


FIGURE 8. CSLM live cell and STEM imaging of intracellular location of gold nanorods (AuNRs) in 6606 pancreatic ductal adenocarcinoma cells (PATIÑO ET AL., 2015). Cells were incubated with AuNRs for 4 h and were either observed under a confocal microscope (a-c) or fixed for their examination under a STEM (d). AuNRs, functionalized with Texas Red[®] streptavidin appear in red. Lysosomes were stained with LysoTracker[®] Green DND-26 (green) plasma membrane was stained with CellMask[™] Deep-Red stain (gray), and cell nuclei were stained with Hoechst 33342 (blue). Overlay of the different channels is shown in (c). Magnified STEM image of internalized AuNRs is shown in (d), where black arrowheads indicate AuNRs located inside a vesicle-like structure. Scale bar corresponds to 250 nm. Scale bars in (a-c) correspond to 30 μm. Insets show a magnification of the selected area, the scale bars corresponding to 10 μm. STEM=Scanning transmission electron microscopy. Reproduced with permission from the copyright owner.

In those cases where the purpose of nanomaterials is to target the endolysosomal network, such as the treatment of certain lysosomal storage disorders, endocytosis provides a direct accessibility to the target (BAREFORD & SWAAN, 2007). By contrast, when endosomes or lysosomes are not the ultimate target of nanomaterials, their accumulation in those compartments may constitute a major limitation for their therapeutic efficacy. This is due to the fact that maturation of endocytic vesicles leads to rapid acidification, from pH 6 to pH 4, and the recruitment of degradative enzymes, which can lead to destruction of

vesicle cargo (CHOU ET AL., 2011). In order to circumvent this issue, several approaches have been attempted, which could be classified into **physical** and **biochemical** delivery strategies.

Amongst the physical delivery strategies, microinjection and electroporation have been the most commonly used. Microinjection has been widely used in the production of transgenic animals, oocyte intracytoplasmic sperm injection and non-permeable cell studies, where nucleic acids, peptides, proteins and drugs, or even nuclei and cells, can be mechanically transferred into a single cell. However, microinjection is a labour-intensive and time-consuming technique, which represents a limitation for studying a large number of cells (ZHANG & YU, 2008). On the other hand, electroporation consists of applying a high-voltage electric field impulse, which leads to the formation of transient hydrophilic pores in the plasma membrane, allowing the passive transport of nanoparticles into the cell (TSONG, 1991). The disadvantages of electroporation are the requirement for specialized equipment, the limitation of only working with cells in suspension and the possible cytotoxic effects caused by the electrical impulse (STEPHENS & PEPPERKOK, 2001). Thus, although the application of these two approaches for research can be useful, their use in commercial or clinical approaches is limited.

To overcome the limitations of the aforementioned physical approaches, micro- and nanoparticles can be further engineered with **biochemical**-based approaches as an alternative (CHOU ET AL., 2011). In general, cationic particles have shown better internalization and delivery to the cytosol. In order to achieve positively charged particles, they can be coated with cell penetrating peptides, cationic lipids (LI ET AL., 2008; PAN ET AL., 2008; DONKURU ET AL., 2010; KOYNOVA & TENCHOV, 2011) or cationic polymers (CALVO ET AL., 1997; ELIYAHU ET AL., 2005; KASTURI, SACHAPHIBULKIJ & ROY, 2005; SUN & ZHANG, 2010; BOLHASSANI ET AL., 2014). The effect of surface modifications of micro- and nanoparticles on endosomal escape and other interactions with cells will be further detailed in section 1.3.3. about surface properties.

Effect of particle design on their interactions with cells: Size, Shape and Surface Properties

1.3.3.

Due to the high diversity of physico-chemical properties of the newly developed nanomaterials, as well as the high variability on the experimental conditions, it is very difficult to predict the interactions between nano-engineered materials and cells within the physiological environment. Several intrinsic properties of micro- and nanoparticles such as their **size**, **shape** and **surface properties**, have demonstrated to play a key role on the modulation of cell-particle interactions (FIG. 9). Thus, the effect of each particle property should be taken into account when designing a nanomaterial for biomedical applications. In this section, the effect of the different particle features on their interactions with cells, such as efficiency of uptake, intracellular fate and cytotoxicity, will be discussed.

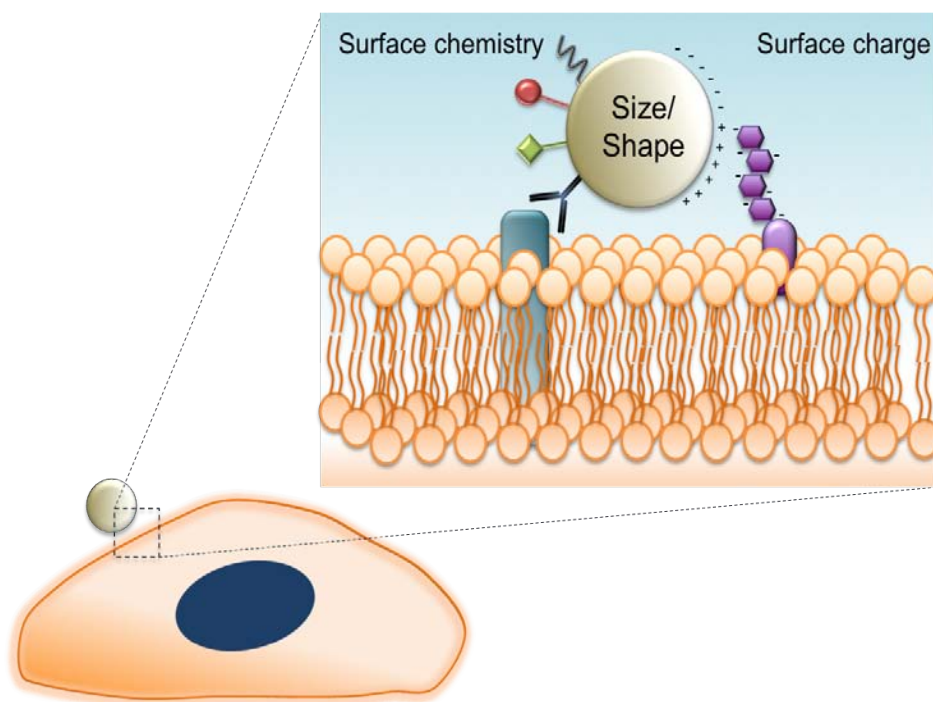


FIGURE 9. Schematic representation of the key factors of particle design for the interaction of particles with the cell membrane.

Size

Particle size is one of the most relevant factors that determines cellular uptake (MAILÄNDER & LANDFESTER, 2009; NEL ET AL., 2009; PACHECO ET AL., 2013; SHANG ET AL., 2014). Size-dependent uptake efficiency of diverse types of particles, such as Au (CHITHRANI ET AL., 2006; CORADEGHINI ET AL., 2013; TOMIC ET AL., 2014; WANG ET AL., 2015), mesoporous silica (LU ET AL., 2009), polystyrene (ZAUNER ET AL., 2001; VARELA ET AL., 2012; BLANK ET AL., 2013) and iron oxide (THOREK & TSOUREKAS, 2008; LARSEN ET AL., 2009) particles, has been reported to occur in different cell lines. Furthermore, particle size has been shown to not only affect uptake efficiency but also the kinetics (CHITHRANI ET AL., 2006) and mechanisms of endocytosis (REJMAN ET AL., 2004; GRATTON ET AL., 2008).

Different studies concur that the optimal uptake efficiency occurs when nanoparticle size ranges between 30-50 nm (Shang et al. 2014). However, it is worth mentioning that while achieving an optimal uptake by cells may be of interest for some applications, particles with a high non-specific uptake are not desirable for those drug delivery applications with targeting purposes since those particles may enter all cell types with a high efficiency. In this regard, Barua and co-workers observed a higher targeting capability of micron-sized particles when compared to their nano-sized counterparts. In their study, whereas cell-uptake of nano-sized rods increased by six-fold once coated with a specific targeting antibody, larger, micron-sized rods exhibited a 15-fold increased uptake once coated with the same antibody (BARUA ET AL., 2013). In addition to this, it is noteworthy to highlight that smaller nanoparticles have shown to correlate positively with cytotoxicity in some cases (PAN ET AL., 2007; KARLSSON ET AL., 2009; PARK M. V. D. Z. ET AL., 2011; CORADEGHINI ET AL., 2013). However, cytotoxicity of particles has been shown to depend not only on the size of nanoparticles but also on the material and surface reactivity. For example, Karlsson and co-workers observed that CuO nanoparticles showed a higher level of cytotoxicity, attributed to their ability to damage mitochondria, with respect to their micron-sized counterparts. However, in the case of TiO₂ particles, micron-sized particles caused more DNA damage than nanoparticles (KARLSSON ET AL., 2009).

Shape

In spite of having received less attention in the literature, micro- and nanoparticles shape has been shown to have a substantial impact on particle-cell interactions. Rod-shaped polymer particles (>100 nm) have been demonstrated to be more efficiently uptaken than their spherical counterparts, followed by cylinders and squares (GRATTON ET AL., 2008). Paradoxically, in other studies where particles had a size below 100 nm, the contrary was observed, the spheres being more efficiently internalized than their rod-shaped counterparts (CHITHRANI ET AL., 2006; QIU ET AL., 2010). Interestingly, particle shape has also been proven to modulate the interaction of ligand-functionalized particles with the target cell receptors, where the targeting is enhanced by rod-shaped particles with respect to spherical ones (BARUA ET AL., 2013). This is believed to be due to a higher availability of contact surface between cell and particle, with more antibodies able to reach their target receptors.

Lastly, a recent study has shown that sharp-shaped nanoparticles are able to escape from endosomal compartments once endocytosed, whereas spherical particles either remain entrapped in the lysosomal compartment or are exocytosed (CHU ET AL., 2014).

Surface properties

In addition to size and shape, surface properties are a strong determinant for the uptake of nano- and microparticles. Generally, cationic particles have rendered better results regarding cellular uptake than anionic ones (SINGH ET AL., 2000; HAUCK ET AL., 2008; THOREK & TSOURKAS, 2008; ZHANG ET AL., 2013). This can be attributed to an increased electrostatic-mediated interaction of the positively charged particles with the negatively charged molecules present in the cell membrane surface, such as certain phospholipids or glycoproteins (COOPER & HAUSMAN, 2013; ALBERTS ET AL., 2014). In addition, cationic molecules have shown to induce membrane permeability through the creation of nanoscale holes, this effect being strongly dependent upon the charge density of polycations (CHEN ET AL., 2009). In an attempt to

increase the net surface charge of particles for an enhanced cell uptake, several approaches have been explored, such as their coating with cationic lipids (LI ET AL., 2008; PAN ET AL., 2008), cationic polymers (CALVO ET AL., 1997; THIELE ET AL., 2003; LI ET AL., 2014; LABALA ET AL., 2015) or cell penetrating peptides rich in positively charged aminoacids (BROCK, 2014; COPOLOVICI ET AL., 2014).

The use of cationic coatings has gained an additional interest, as highly positive-charged molecules have shown to surpass the endo-lysosomal entrapment and thus enhance the cytosolic delivery of their cargo. This could be attributed to either electrostatic interactions that destabilize the endo/lysosomal membrane (XU & SZOKA, 1996), a pH buffering-effect by the protonation of amine groups, known as **proton-sponge effect** (BOUSIFF ET AL., 1995), or a combination of both (ELSABAHY ET AL., 2009; SHRESTHA ET AL., 2012). Particularly, the proton-sponge effect was proposed by Bousiff and co-workers to explain the high efficiency of polyethyleneimine (PEI), a cationic polymer rich in amino groups and available in linear or branched forms, on the intracellular delivery of DNA (BOUSIFF ET AL., 1995). This hypothesis suggests that endosome disruption is caused by pH buffering due to the protonation of PEI amine groups, the PEI acting as a “sponge” for protons. The capability of PEI to sequester protons leads to the continuous action of proton pumps present in the endo/lysosome membrane. To avoid the formation of a membrane potential, the increase of positive charges is compensated by the influx of Cl⁻ ions. This raises the endo/lysosomal osmolarity, leading to subsequent endo/lysosomal swelling and disruption, due to an excessive water influx (FIG. 10). However, since a recent study carried out by Benjaminsen and coworkers demonstrated that the proton-sponge effect mediated by PEI is not caused by a change in lysosomal pH (BENJAMINSEN ET AL., 2013), more research is required to fully elucidate the mechanism of endo/lysosomal disruption. On the other hand, while endosomal escape has been successful for delivering DNA, siRNA, small drugs or small nanoparticles, it remains controversial in the case of larger particles (IVERSEN ET AL., 2011).

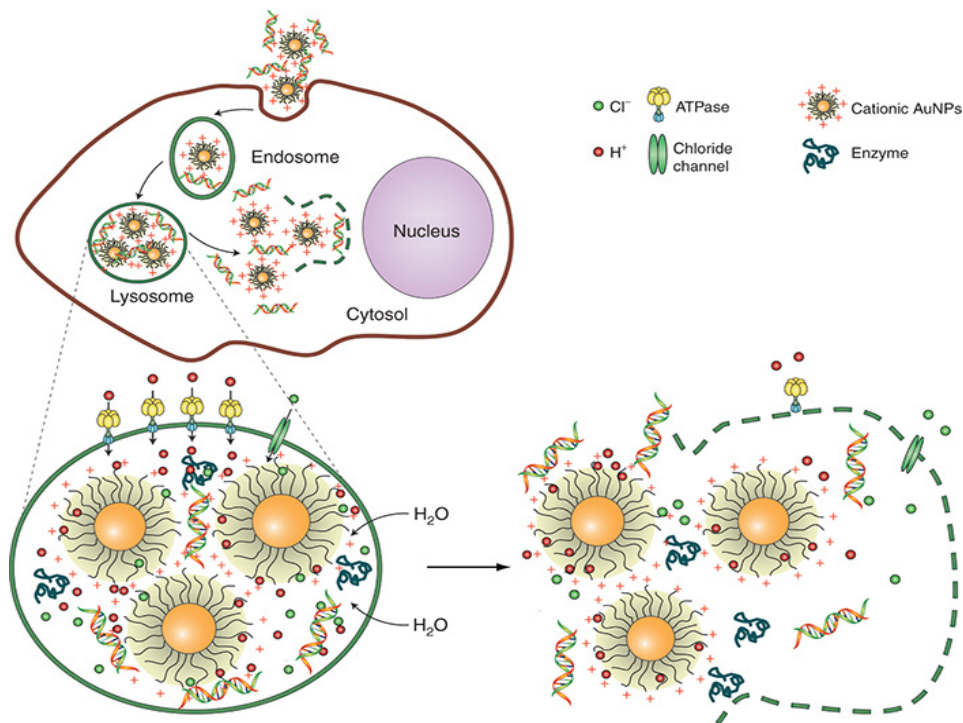


FIGURE 10. Schematic representation of the endosomal escape of cationic nanoparticles mediated by the proton sponge effect (DING ET AL., 2009).

Despite cationic particles being an interesting approach for an enhanced uptake as well as cytosolic delivery, they have shown to promote cytotoxic effects, when compared to their anionic or neutral counterparts (FRÖHLICH, 2012; KIM ET AL., 2013; ANGUISSOLA ET AL., 2014). In this regard, induction of apoptosis by some types of cationic particles, such as amino-functionalized (ANGUISSOLA ET AL., 2014) or Poly(amidoamine) dendrimer coated particles (THOMAS ET AL., 2009), has shown to be the main cause for their cytotoxicity. In the case of cationic lipids and polymers, their cytotoxicity has been attributed to an excessive cationic charge density, since higher densities and molecular weights have been shown to yield higher cytotoxicity (FISCHER ET AL., 2003; LV ET AL., 2006). The cytotoxic effect in this case is attributed to the strong electrostatic-mediated interactions between polycations and the cell membrane, which can alter its integrity and lead to cell death (FISCHER ET AL., 2003).

1.4. Impact of cell type on particle-cell interactions

Although particle design unequivocally plays an important role on cell interactions, several studies have shown inconsistent results when using different cell lines. Thus, it appears that cell type is also a critical factor for cell-particle interactions.

With regard to particle **size**, and as aforementioned, it is understood that particles within the 30-50 nm range are more easily uptaken by the majority of cells. However, some particular cell types have shown a clear preference for larger particles internalization. For example, the enterocyte-like Caco2 cell line showed a clear preference for the uptake of particles between the range of 100-200 nm, when compared to 50 nm, 500 nm and 1000 nm particles (YIN WIN & FENG, 2005). Another example is the case of phagocytic cells, which have demonstrated a great capability for internalizing micron-sized particles (GONZÁLEZ ET AL., 1996; CHAMPION ET AL., 2008) or aggregates (LANKOFF ET AL., 2012) with high efficiency.

On the other hand, functionalized GNPs have shown different uptake efficiencies and mechanisms of internalization in human cervix epithelial cancer cells and human breast epithelial non-cancer cells (SAHA ET AL., 2013). These results are in agreement with those obtained by Kuhn and coworkers, who also observed differences in the uptake mechanism of 40-nm polystyrene particles in epithelial cells and macrophages (KUHN ET AL., 2014).

Regarding cytotoxicity, the cell line has also been proven to play an important role, as Xia and colleagues demonstrated that whereas 60-nm amino-functionalized polystyrene particles induced highly toxic effects on macrophages and epithelial cells, human microvascular endothelial, hepatoma and pheochromocytoma cells were relatively resistant to cytotoxicity induced by these particles (XIA ET AL., 2008).

Therefore, understanding and characterizing the response of a particular cell type to a specific nanomaterial may significantly improve its therapeutic efficacy.

Polystyrene is one of the most extensively used plastic, its structure being based on an aromatic polymer obtained from the polymerization of styrene monomers (LOOS ET AL., 2014). Polystyrene surface is highly hydrophobic and it can be easily modified, making it worthy for a number of applications, such as cell culture growth (VAN MIDWOUD ET AL., 2012). For this reasons, polystyrene has shown to be suitable for the fabrication of micro- and nanoparticles with a high homogeneity, low polydispersity index and able to form stable colloids within the biological environment (LOOS ET AL., 2014).

Polystyrene nanoparticles have been used for a number of applications, such as biosensing (VELEV & KALER, 1999), photonics (ROGACH ET AL., 2000) and self-assembly structures (BOAL ET AL., 2000). This is due to the fact that their size and surface properties can be easily controlled and modified, respectively. In addition, the inertness and biocompatibility of the material offers an advantage for their application in the study of biological systems. Thus, micro- and nanoparticles with different sizes or surface modifications can be used for analysing cell-particle interactions, without additional material-triggered effects. Whereas several groups have proven the suitability of a polystyrene based micro- or nanopatform for the study of phagocytosis (THIELE ET AL., 2003; SEYRANTEPE ET AL., 2010; MAGENAU ET AL., 2011), endocytosis and the effect of size (ZAUNER ET AL., 2001; VARELA ET AL., 2012; PACHECO ET AL., 2013), shape (BARUA ET AL., 2013) and surface properties (DAUSEND ET AL., 2008; LUNOV ET AL., 2011; KIM ET AL., 2013; ANGUISSOLA ET AL., 2014) on particle-cell interactions, the present thesis has tackled the study of cell-particle interactions by using these microparticles as a model.



2

Objectives

According with the literature background, the objectives of this thesis were set in order to tackle the current needs on the field of biological applications of micro- and nanoengineered systems, and can be defined as follows:

- I.** To evaluate the impact of microparticle coating with different transfection reagents on their uptake by non-phagocytic cells.
- II.** To determine the cell type effect on microparticle uptake responses.
- III.** To investigate the interactions of multi-material intracellular chips with cells in order to explore their potential as multi-functional systems for biological applications.



3

Results

3.1

**Enhancing microparticle
internalization by nonphagocytic cells
through the use of noncovalently
conjugated polyethyleneimine**

Enhancing microparticle internalization by nonphagocytic cells through the use of noncovalently conjugated polyethyleneimine

This article was published in the following Dove Press journal:
International Journal of Nanomedicine
7 November 2012
[Number of times this article has been viewed](#)

Tania Patiño
Carme Nogués
Elena Ibáñez
Leonardo Barrios

Unitat de Biologia Cel·lular,
Departament de Biologia Cel·lular,
Fisiologia i Immunologia, Facultat
de Biociències, Universitat Autònoma
de Barcelona, Bellaterra, Spain

Abstract: Development of micro- and nanotechnology for the study of living cells, especially in the field of drug delivery, has gained interest in recent years. Although several studies have reported successful results in the internalization of micro- and nanoparticles in phagocytic cells, when nonphagocytic cells are used, the low internalization efficiency represents a limitation that needs to be overcome. It has been reported that covalent surface modification of micro- and nanoparticles increases their internalization rate. However, this surface modification represents an obstacle for their use as drug-delivery carriers. For this reason, the aim of the present study was to increase the capability for microparticle internalization of HeLa cells through the use of noncovalently bound transfection reagents: polyethyleneimine (PEI) Lipofectamine™2000 and FuGENE 6®. Both confocal microscopy and flow cytometry techniques allowed us to precisely quantify the efficiency of microparticle internalization by HeLa cells, yielding similar results. In addition, intracellular location of microparticles was analyzed through transmission electron microscopy and confocal microscopy procedures. Our results showed that free PEI at a concentration of 0.05 mM significantly increased microparticle uptake by cells, with a low cytotoxic effect. As determined by transmission electron and confocal microscopy analyses, microparticles were engulfed by plasma-membrane projections during internalization, and 24 hours later they were trapped in a lysosomal compartment. These results show the potential use of noncovalently conjugated PEI in microparticle internalization assays.

Keywords: HeLa cells, internalization efficiency, endocytosis, drug delivery

Introduction

In the past decade, the fabrication of microelectromechanical systems with controlled physical and chemical properties in the micron and submicron scales has been of great interest in the biomedical field due to the high number of potential applications that they offer, such as the creation of biosensor systems, drug delivery systems, or therapeutic implants.¹ In fact, fabrication of biological microelectromechanical systems for a wide range of applications, such as cell tracking,² embryo tagging³ or drug delivery,⁴⁻⁶ has been achieved.

The application of biological microelectromechanical systems has acquired special importance due to their potential use in creating systems able to deliver a drug, in a controlled manner, to a specific target cell.⁷ The aforementioned studies have been successful with use of phagocytic cells, but when nonphagocytic cells are used, their low capacity of internalization is still a limitation that has to be overcome. Moreover, it has been shown that several features of microparticle design play an important role in their uptake by cells: their size,^{8,9} shape,^{10,11} and surface properties.¹² Several molecules have

Correspondence: Leonardo Barrios
Unitat de Biologia Cel·lular, Facultat
de Biociències, Universitat Autònoma
de Barcelona, E-08193 Bellaterra,
Cerdanyola del Vallès, Spain
Tel +34 93 581 2776
Fax +34 93 581 2295
Email lleonard.barrios@uab.cat

been used to increase the capacity for microparticle uptake in nonphagocytic cells, in order to study the internalization process. In all cases, the microparticles were covalently modified with a selected molecule¹³⁻¹⁵ or coated with a bacterial membrane.¹⁶

Since it has been reported that positive-charged microparticles are more easily internalized by cells,¹¹ the use of transfection procedures in microparticle internalization experiments could be considered as a possible approach to increase microparticle uptake when working with nonphagocytic cells. These procedures are based on the interaction between the positive charges of cationic polymers, like polyethyleneimine (PEI) or cationic lipids, like Lipofectamine™ 2000 (LF2000), FuGENE®, or DOTAP, and the negative charges of DNA.¹⁷ The positive charges of the transfection reagents can also interact with the negatively charged oligosaccharides of the plasma membrane surface, facilitating the internalization of the complex by endocytosis. Once inside the cell, these reagents can disrupt the endocytic pathway, releasing the contents of the endosomes to the cytosol.^{18,19} In fact, the covalent binding of PEI to the microparticle surface facilitates their incorporation into HeLa cells.^{14,20} However, the modification of microparticles with covalently bound PEI would render difficult or even impede their functionalization with other molecules, such as the drug to be delivered. Thus, a new strategy is necessary to improve microparticle uptake by nonphagocytic cells. In this sense, cationic lipids have been recently used as fusogenic agents to improve the internalization of polystyrene particles.²¹

Against this background, the aim of this study was to improve the efficiency of internalization of polystyrene microparticles by nonphagocytic (HeLa) cells through the use of the cationic polymer PEI and the cationic lipids LF2000 and FuGENE 6 added to the culture medium as transfection agents. The internalization efficiency was evaluated using two completely different methods, confocal scanning laser microscopy (CSLM) and flow cytometry (FC), and took into account first, the cytotoxic effect of the transfection agent at one (LF2000) or three different concentrations (PEI), and second, the number of live, adhered cells with an internalized microparticle. Finally, the intracellular fate of microparticles was determined by immunogold labeling transmission electron microscopy (TEM) and by CSLM.

Materials and methods

Reagents

Unless otherwise stated, reagents were purchased from Life Technologies (Carlsbad, CA).

Polystyrene microparticles

Two types of polystyrene microparticles of 3µm diameter were used: fluorescent microparticles (Fluoresbrite® YG Microsphere 3 µm; Polysciences, Inc, Warrington, PA) and nonfluorescent carboxylated microparticles (Polybead® Carboxylate Microspheres 3 µm; Polysciences). Nonfluorescent carboxylated microparticles were functionalized with an Alexa Fluor® 594 conjugated goat anti-rabbit IgG antibody (H + L) (Life Technologies) using the PolyLink Protein Coupling kit (Polysciences), following the manufacturer's recommendations.

Cell culture

HeLa cells were cultured at 37°C in a 5% CO₂ atmosphere, using minimum essential medium (MEM) with Earle's salts and L-Glutamine supplemented with 10% fetal bovine serum (FBS).

PEI, LF2000, and FuGENE 6 cytotoxicity assay

The cytotoxicity of PEI 25 KDa (Sigma-Aldrich, St Louis, MO) used at three different concentrations (0.05, 0.10, and 0.15 mM), of LF2000 (Life Technologies), and of FuGENE 6 (Promega Corporation, Fitchburg, WI), used at the concentrations recommended by the manufacturers, was evaluated after the transfection procedure by assessing two different parameters: the percentage of cells that remained attached to the dish (normalized to the control group), and the viability of the attached cells. The global effect of the treatment was calculated by multiplying the normalized percentage of attached cells by the percentage of viable attached cells.

For the first parameter tested, ie, the percentage of cells that remained attached after the transfection procedure, 1.5 × 10⁵ HeLa cells were seeded in 35 mm diameter dishes (Nalge Nunc Int, Roskilde, Denmark). The next day, the transfection reagents at their respective concentrations were prepared and added to the cell cultures. Briefly, PEI 10 mM was initially diluted with NaCl 150 mM, incubated at room temperature for 40 minutes, and then diluted to the three working concentrations (0.05, 0.10, and 0.15 mM) in MEM without serum. LF2000 and FuGENE 6 were prepared according to the manufacturer's instructions, also in MEM without serum. The culture medium of HeLa cells was then replaced with the corresponding transfection solution, and the cells were incubated for 4 hours at 37°C and 5% CO₂. After that, the transfection solutions were replaced with fresh culture medium. In the control culture, a 4-hour incubation with MEM without serum was performed. To determine the

number of cells that remained attached, cells were harvested 24 hours later using 0.05% Trypsin-EDTA, centrifuged at 500 g for 5 minutes, and resuspended in fresh culture medium. Then, 50 μ L of cell suspension was mixed with 50 μ L of Perfect-Count Microspheres™ CYT-PCM50 (Cytognos SL, Salamanca, Spain) and counted in a Becton Dickinson FACSCanto II flow cytometer (BD Biosciences, Franklin Lakes, NJ) equipped with BD Biosciences FACSDiva™ software, the beads and the cells being counted together. The cell concentration was obtained taking into account the concentration of Perfect-Count microspheres.

On the other hand, to evaluate cell viability after the transfection procedures, cells were seeded and incubated with the transfection reagents, at the indicated concentrations. At 24 hours, attached cells were harvested as described, and their viability was determined by FC after applying the LIVE/DEAD® Viability/Cytotoxicity Kit for mammalian cells (L3224; Life Technologies), according to the manufacturer's instructions. The calcein acetomethoxy (AM) derivative of the kit diffuses through the cell membrane and, once inside the cell, it is converted to highly green fluorescent calcein by the intracellular esterases of living cells. The ethidium homodimer-1 of the kit can only enter cells with damaged membranes, being able to reach the nucleus and bind to DNA, which emits red fluorescence. Therefore, living cells are labeled with green fluorescence, whereas dead cells are labeled with red fluorescence.

Analysis of Zeta potential of polystyrene microparticles

The Zeta potential of microparticles in culture media before and after PEI, LF2000, and FuGENE 6 treatments, was measured using a Zetasizer Nano ZS (Malvern Instruments Malvern, UK).

Internalization of polystyrene microparticles in HeLa cells

To analyze the internalization of microparticles in HeLa cells, two approaches were carried out: CSLM (Fluoview® FV1000; Olympus Corp, Tokyo, Japan) and FC (previously described). For confocal microscope analysis, cells were seeded at a density of 1.5×10^5 cells/dish on 35 mm-diameter gridded glass-bottom coverslip dishes (MatTek Corp, Ashland, MA). For FC analysis, cells were seeded at a density of 1.2×10^6 cells/flask on 75 cm² flasks (Nunc). After 24 hours of incubation, transfection was performed as described in the previous section. But, in this case, transfection solutions were mixed with 3 μ m diameter polystyrene fluorescent microparticles at a final concentration of 10^6 microspheres/mL. The efficiency

of internalization of microparticles by HeLa cells was determined 24 hours later.

For FC analyses, cells were harvested as mentioned above and microparticle–cell association was analyzed measuring the forward scatter and the fluorescent intensity.

For CSLM analyses, cells were washed twice with phosphate-buffered saline (PBS) for 5 minutes, and fixed with 4% paraformaldehyde (Sigma-Aldrich). Then, cells were washed thrice with PBS, blocked with 1% bovine serum albumin ([BSA] Sigma-Aldrich) in PBS, and finally stored at 4°C until their analysis. Samples were first examined under a phase contrast inverted microscope (Olympus IX71, Olympus, Hamburg, Germany) to determine the percentage of cells that were in contact with one or more microparticles. Thus, several fields were captured and then analyzed using image analysis software (ImageJ version 1.43r; National Institutes of Health, Bethesda, MD). Two hundred cells per sample were evaluated for each treatment, and 484 cells in the case of the control group. Following this preliminary assessment, the location of microparticles (ie, inside the cells or attached to their plasma membrane) was determined using CSLM. With this aim, cells were stained with wheat germ agglutinin conjugated to Texas Red (10 μ g/mL; Life Technologies) and counterstained with Hoescht 33258 (1 μ g/mL; Sigma-Aldrich), to visualize the plasma membrane and the nucleus, respectively. Samples were then examined under the CSLM using a 63 \times oil immersion objective, where x-y-z sequential acquisition was performed and orthogonal projections of the stacks were analyzed to determine the location of the microparticles within the cell. For the image analyses, the FV10-ASW Application Software (Ver. 01.07c; Olympus) was used.

The use of gridded dishes allowed us to examine the same fields in both microscopic evaluations (ie, inverted microscope and CSLM).

Electron microscopy

To analyze the intracellular location of microparticles, transfected cells (as described in above) were fixed with 2.5% glutaraldehyde in phosphate buffer (PB). After 1 hour of incubation with the fixative at 4°C, they were washed with PB and postfixed with 1% osmium tetroxide in PB containing 0.8% potassium ferricyanide at 4°C. Next, samples were dehydrated in acetone, infiltrated with Epon™ (Electron Microscopy Sciences, Hatfield, PA) resin over 2 days, embedded in the same resin, and polymerized at 60°C over 48 hours. Ultrathin sections were obtained using a Leica Ultracut UC6 ultramicrotome (Leica Microsystems, Wetzlar, Germany) and mounted

on Formvar-coated copper grids. They were stained with 2% uranyl acetate in water and lead citrate. Finally, sections were observed in an electron microscope (J1010; Jeol Ltd, Tokyo, Japan) equipped with a CCD camera SIS Megaview III.

Lysosome associated membrane protein I (LAMP-I) immunogold

After microparticle internalization using PEI 0.05 mM treatment, HeLa cells were chemically fixed at 4°C with a mixture of 4% paraformaldehyde and 0.1% glutaraldehyde in PB. After washing with PB containing 50 mM glycine, cells were embedded in 12% gelatine and infused in 2.3 M sucrose. Mounted gelatine blocks were frozen in liquid nitrogen. Thin sections were prepared in an EM Ultracut UC6/FC6 ultracyromicrotome (Leica Microsystems, Wetzlar, Germany). Ultrathin cryosections were collected with 2% methylcellulose in 2.3 M sucrose.

Cryosections were incubated at room temperature on drops of 2% gelatine in PBS for 20 minutes at 37°C, followed by 50 mM glycine in PBS for 15 minutes, 10% FBS in PBS for 10 minutes, and 5% FBS in PBS for 5 minutes. Then they were incubated with 5 µL of rabbit anti-LAMP-1 polyclonal antibody (Abcam, Cambridge, UK) for 30 minutes. After three washes on drops of PBS for 10 minutes, sections were incubated for 20 minutes using colloidal gold conjugated goat anti-rabbit IgG (cat. 111-205-144) Jackson ImmunoResearch Laboratories Inc, West Grove, PA) using a 1:30 dilution in 5% FBS/PBS. This was followed by three washes on drops of PBS for 10 minutes, and two washes with distilled water. As a control for nonspecific binding of the colloidal gold conjugated antibody, the primary antibody was omitted.

The observations were done in an electron microscope (Jeol) with a CCD camera SIS Megaview III.

Early endosome antigen I protein (EEA-I) and LAMP-I immunolabeling

To visualize the location of the microparticles 24 hours after the transfection procedure, cells were seeded at a density of 1.5×10^5 cells/dish on 35 mm-diameter gridded glass-bottom coverslip dishes (MatTek Corp). After 24 hours of incubation, transfection with PEI 0.05 M mixed with 3 µm diameter polystyrene functionalized microparticles (previously described) at a final concentration of 10^6 microspheres/mL was performed as described above. After 24 hours, cells were washed twice with PBS fixed in 4% paraformaldehyde/PBS, permeabilized with 0.25% Triton X-100 in PBS, and blocked with 5% PBS/BSA. Then, cells were incubated for 1 hour at 37°C with one of two primary antibodies, mouse anti-EEA-I

monoclonal antibody (cat. 610456 BD Biosciences) or mouse anti-LAMP-1 polyclonal antibody (cat. 555798 BD Biosciences), to label the endosomal or the lysosomal compartment, respectively. Finally, cells were incubated for 1 hour at room temperature with Alexa 488-conjugated chicken anti-mouse IgG antibody (Life Technologies), counterstained with Hoechst 33258, and analyzed by CSLM. For each marker, 40 cells with microparticles were analyzed.

Statistical analyses

Normal distribution of data was verified with the Kolmogorov–Smirnov test, and homoscedasticity was assessed with the Levene's test. When necessary, data (x) on percentages were transformed with arcsin square root transformation ($\arcsin\sqrt{x}$) for accomplishing the parametric assumptions. The comparison among the different treatments was done with a one-way analysis of variance (ANOVA), followed by a posthoc t -test with Bonferroni's correction for multiple comparisons. $P < 0.05$ was considered to be statistically significant.

Results

Cytotoxic effect of transfection reagents

The percentage of cells that remained attached to the dish after the transfection procedures can be seen in Figure 1A, showing that all treatments resulted in a significant decrease in the percentage of attached cells. Normalized to the control group, PEI 0.05 mM was the less aggressive treatment (77.4% of cells remaining attached) when compared with the rest of the treatments (47.5%, 36.5%, 20.8%, and 20.1% for PEI 0.10 mM, FuGENE 6, LF2000, and PEI 0.15 mM, respectively).

The viability of the attached cells was determined by calcein AM/ethidium homodimer-1 staining. Figure 1B shows that after PEI 0.10 mM and 0.15 mM treatments, the percentages of living cells were significantly lower (65.6% and 62.5%, respectively) than those observed following the other treatments (94.7% [control], 94.1% [FuGENE 6], 90.4% [PEI 0.05 mM], and 87.6% [LF2000]). Moreover, the difference between control and LF2000 was also significant.

When both parameters are considered (Figure 1C), PEI 0.05 mM appears as the least cytotoxic treatment, with 70% of cells remaining viable; whereas in the other treatments, less than 35% of the cells remained alive (34.3% FuGENE 6; 31.2% PEI 0.10 mM; 12.6% PEI 0.15 mM; and 18.2% LF2000).

Effect of transfection reagents on microparticle surface charge

To evaluate the electrochemical changes at the microparticle surface due to the treatment with the transfection reagents,

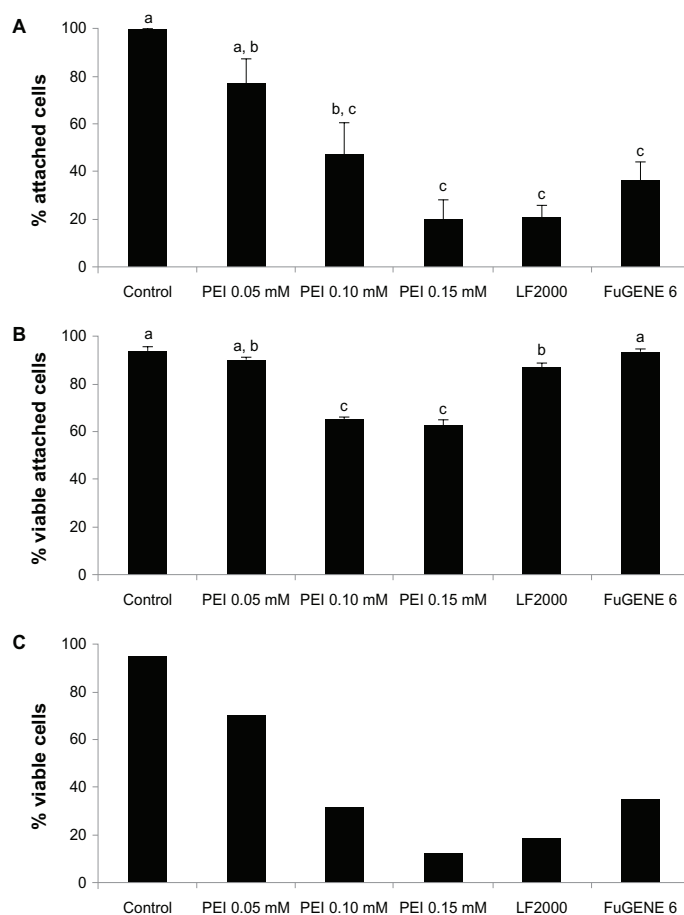


Figure 1 Cytotoxicity of transfection treatments. (A) Percentage of cells that remained attached to the dish after treatments, normalized to the control. (B) Percentage of viable attached cells after treatments. (C) Percentage of viable cells.

Note: a, b, c denote significant differences among groups.

Abbreviations: PEI, polyethylenimine; LF, Lipofectamine™.

their Z potential was analyzed. As can be seen in Figure 2, nontreated fluorescent microparticles showed a highly negative Z potential (-45.9), whereas treatment with the transfection reagents clearly changed the surface to positively charged. This change also occurred in functionalized microparticles after PEI 0.05 treatment.

Internalization of polystyrene microparticles by HeLa cells

Microparticle internalization by HeLa cells was evaluated by two approaches, FC and CSLM. By FC, it was observed

that for all treatments, the number of cells in contact with microparticles was clearly increased from twofold (PEI 0.15 mM) to fivefold (PEI 0.05 mM) when compared with the control (Figure 3). In addition, for all treatments, in the population of cells associated with microparticles, there were no differences among the percentages of cells with one, two, three, or more microparticles (Figure 4).

Confocal microscopy analyses were performed next to precisely determine whether microparticles were located inside or outside the cells (Figure 5A and B). As can be seen in Figure 5C, in the cells that remained attached to the dish,

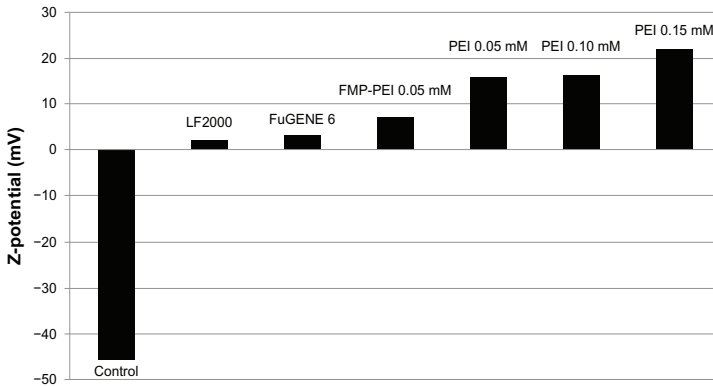


Figure 2 Z potential of control microparticles and of microparticles treated with PEI, LF2000 and FuGENE 6®.

Note: The Zeta potential of the functionalized microparticle is also shown.

Abbreviations: FMP, functionalized microparticle; PEI, polyethyleneimine; LF, Lipofectamine™.

a significant increase ($P < 0.05$) in the percentage of cells in contact with microparticles and in the percentage of cells with internalized microparticles was observed for all treatments compared with the control group, these results being consistent with those previously obtained by FC.

Finally, the results obtained from FC and CSLM analyses were compared taking into account the cytotoxic effect of the different treatments (see Figure 1C). Figure 6 shows that PEI 0.05 mM provided the highest microparticle internalization efficiency, doubling at least the efficiency of the other treatments.

Internalization of functionalized polystyrene microparticles by HeLa cells

To test whether PEI 0.05 mM could also enhance microparticle internalization when a cargo is covalently attached to

their surface, the internalization efficiency of antibody-functionalized microparticles was determined by CSLM. This analysis showed that 18.9% of the cells had internalized at least one functionalized microparticle, a percentage equivalent to that for non-functionalized microparticles (25.5%) and significantly higher than that for the control group (3.7%).

Intracellular location of microparticles

To investigate the intracellular fate of microparticles, TEM analyses were carried out in Epon-embedded samples. According to the previous results, only the PEI 0.05 mM treatment was selected for these analyses. A plasma membrane evagination was clearly observed around microparticles whilst they were being engulfed by HeLa cells (Figure 7A). Once internalized, microparticles appeared to be tightly surrounded

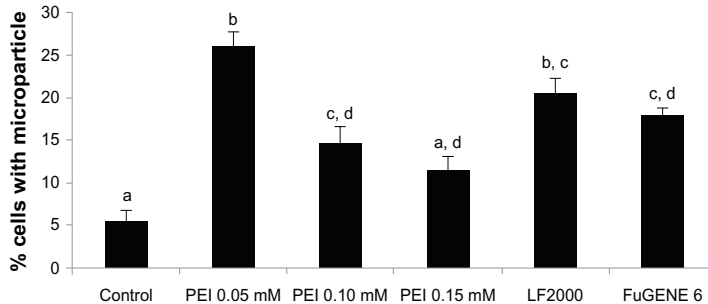


Figure 3 Flow cytometry analysis. Percentage of cells in contact with at least one microparticle.

Notes: a, b, c, d denote significant differences among groups.

Abbreviations: PEI, Polyethyleneimine; LF, Lipofectamine™.

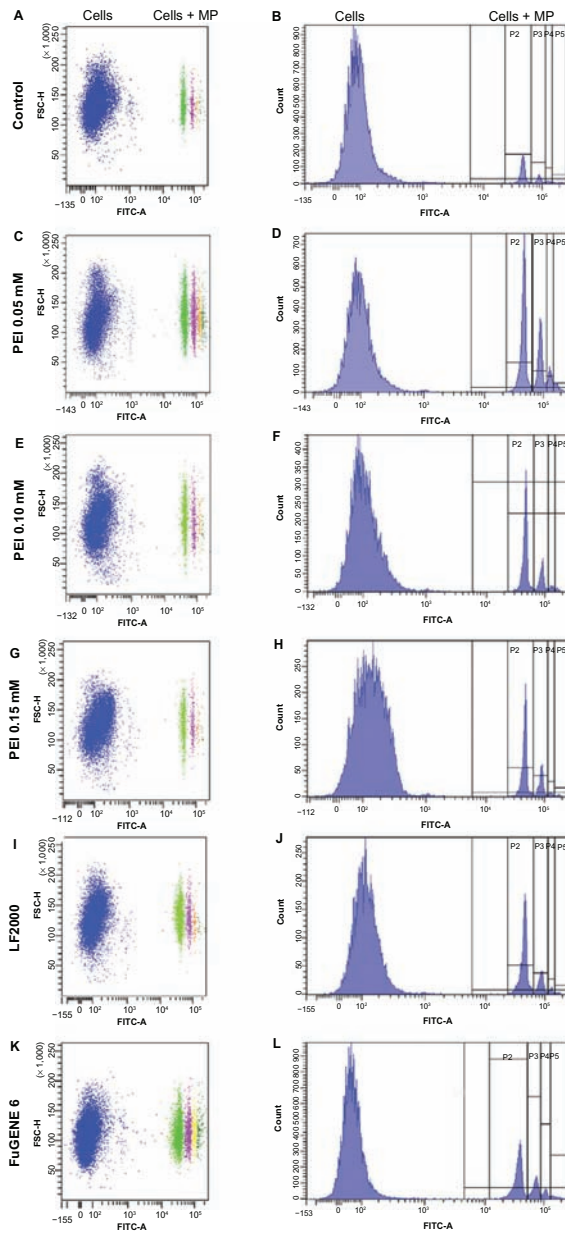


Figure 4 Flow cytometry analysis. Transfection agents' effect on the internalization of fluorescent microparticles by HeLa cells. (A), (C), (E), (G), (I) and (K) Dot plots showing two populations of cells: associated (cells + MP) or not associated (cells) with green fluorescent microparticles. (B), (D), (F), (H), (J) and (L) Histograms showing the fluorescence intensity of the different populations of cells.

Notes: Cells = cell population not associated with microparticles. Cells + MP = cell population associated with at least one microparticle. P2, P3, P4, P5 = cell population associated with one, two, three, or more than three microparticles, respectively.

Abbreviations: MP, microparticle; PEI, polyethylenimine; LF, Lipofectamine™.

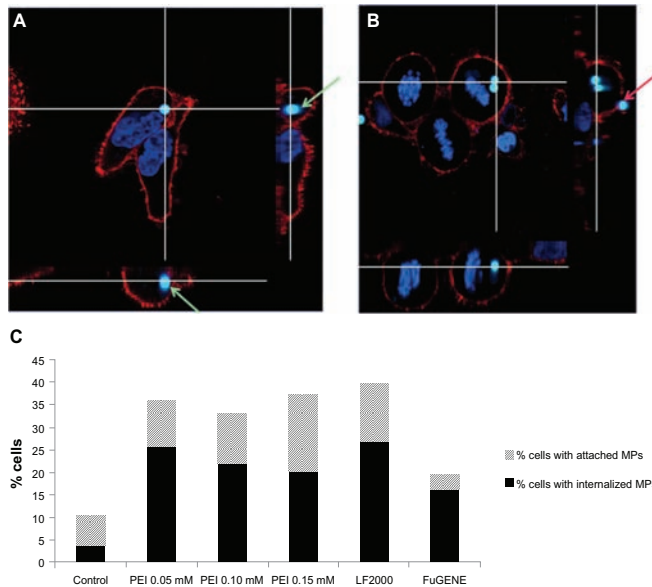


Figure 5 CSLM analyses of microparticle location. (A and B) CSLM-obtained images (middle) and their orthogonal projections of the z-stack reconstructions (right and bottom) of consecutive focal planes (0.5 μm each). (C) Percentage of cells in contact with microparticles, either attached or internalized, analyzed by CSLM. **Notes:** Green arrows indicate a microparticle located inside the cell, clearly surrounded by the plasma membrane. The red arrow points to a microparticle attached to the plasma membrane but outside the cell. Plasma membrane appears in red (WGA-Texas Red® Staining) and chromatin in blue (Hoescht 33258). **Abbreviations:** CSLM, confocal scanning laser microscopy; PEI, polyethyleneimine; LF, Lipofectamine™.

by a single membrane in the majority of cases (Figure 7B), and occasionally, they were additionally surrounded by a two-membrane complex (Figure 7C and D).

The immunolocalization of LAMP-1 showed that in the majority of cells analyzed, the membrane surrounding the microparticles was positive for LAMP-1, indicating that microparticles were trapped in a lysosomal compartment (Figure 8).

To quantify the number of internalized microparticles located inside lysosomes, CSLM analysis using two cell compartment markers (EEA-1 for endosomes and LAMP-1 for lysosomes) was carried out. In this case, antibody-functionalized microparticles were used because their lower fluorescence intensity in relation to fluorescent microparticles allowed us to observe the colocalization of the internalized microparticles and the endosomal/lysosomal compartments.

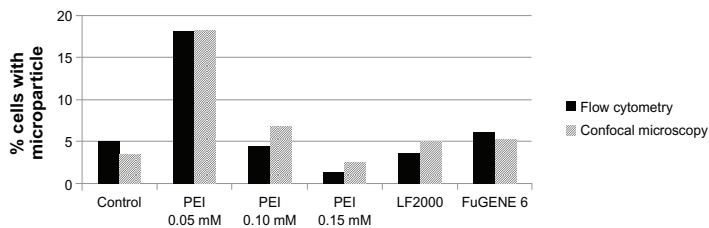


Figure 6 Microparticle internalization efficiency. Percentage of viable cells with one or more internalized microparticles after the different transfection treatments. **Notes:** Results were obtained from internalization analyses by both CSLM and FC, taking into account the number of cells that remained attached to the dish after treatments and their viability. **Abbreviations:** CSLM, confocal scanning laser microscopy; FC, flow cytometry; PEI, polyethyleneimine; LF, Lipofectamine™.

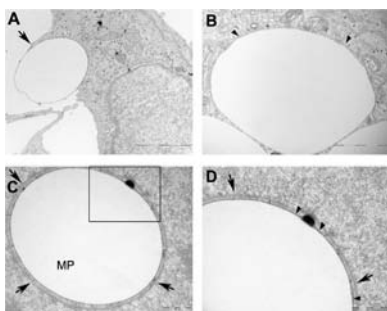


Figure 7 Microparticle localization by transmission electron microscopy. Micrographs of HeLa cells with internalized microparticles. (A) Illustration of the internalization of microparticles; arrow indicates a cell membrane evagination, typical of macropinocytosis. (B) A single membrane surrounding an internalized microparticle. (C) Microparticle surrounded by a double membrane. (D) Enlarged view of the microparticle shown in C.

Notes: Arrow heads point to a single membrane tightly associated to microparticle. Arrows indicate the two membrane complex. Scale bars: (A) 2 μm (B) 1 μm (C) and (D) 500 nm.

Abbreviation: MP, microparticle.

It was observed that 24 hours after treatment, none of the microparticles colocalized with endosomes and 83.4% colocalized with lysosomes, confirming the results previously obtained by TEM.

Discussion

The use of micro- and nanoparticles as carriers for drug delivery applications has gained interest in recent years.⁷ It has been shown that their uptake by cells is highly dependent on their physical and chemical properties, especially their

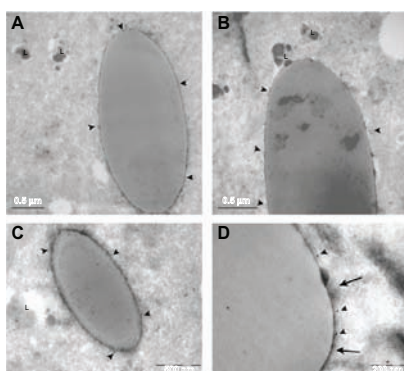


Figure 8 LAMP-1 immunogold detection. Cryotransmission electron micrographs of LAMP-1 immunogold performed in HeLa cells. (A–C) Arrow heads indicate positive LAMP-1 marks. (D) Arrow heads indicate positive LAMP-1 marks whereas arrows point to the lysosome membrane.

Abbreviation: LAMP-1, lysosome associated membrane protein 1; L, lysosome.

size and surface charge (being that cationic particles are more easily uptaken by cells).¹¹ However, the low capacity of nonphagocytic cells for the internalization of micron-sized particles is a handicap that needs to be improved.

In order to increase microparticle uptake by nonphagocytic cells, PEI, LF2000, and FuGENE 6 were chosen because of their efficiency in DNA transfection procedures. Moreover, PEI and LF2000 have also been used in microparticle-^{14,20,21} and nanoparticle-internalization²² experiments.

In our study, we analyzed the effect of free PEI (ie, noncovalently bound to microparticle surface) on the microparticle-internalization efficiency. Considering that these microparticles are expected to be drug-delivery carriers in the future and that the cargo will need to be attached to their surface, we considered the use of free PEI as a more appropriate approach to avoid competition for the same substrate. To the best of our knowledge, this is the first time that free PEI has been used for internalizing microparticles. In this regard, although PEI, LF2000, and FuGENE 6 have been widely used in DNA transfection procedures with positive results, it has been described that they produce a considerable cytotoxic effect, which has to be taken into account.^{18,23} Thus, with the aim of finding the best balance between efficiency of microparticle internalization and cytotoxicity, three different concentrations of PEI were tested in the present study. The highest concentration was set at 0.15 mM since it has been reported that an intense cytotoxic effect is observed at higher concentrations.²⁴ In the case of LF2000 and FuGENE 6, the concentrations used were those recommended by the manufacturers, which provided good results when used for internalizing 1 or 3 μm -sized beads in the case of LF2000.²¹

In our study, the number of cells remaining attached to the culture plates after their exposure to the transfection reagents was determined, together with the viability of these attached cells. This combined analysis allowed us to more accurately determine the cytotoxic effect of the treatments. We observed that compared with the control culture, the percentage of viable cells among those attached was high in all treatments (more than 60% viable cells), but a reduction in the percentage of attached cells was observed for all treatments. These data demonstrate the usefulness of taking into account not only the viability of the cells but also the percentage of remaining cells after treatments in the cytotoxicity assays and moreover, showed that PEI at 0.05 mM was the least cytotoxic treatment. On the other hand, our viability results are in agreement with previous reports in that free PEI treatments produced a dose-dependent cytotoxic effect.²⁵ None of the

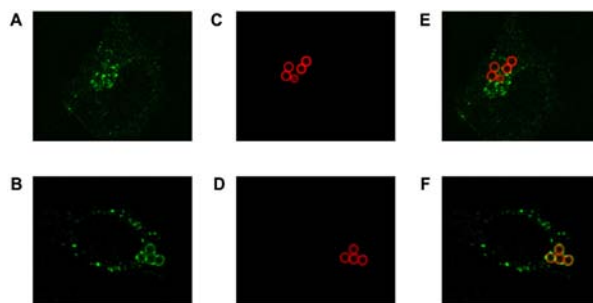


Figure 9 Intracellular location analysis of functionalized microparticles by CSLM. (A) Endosomal labeling with EEA-1. (B) Lysosomal labeling with LAMP-1. (C and D) Microparticles functionalized with an Alexa Fluor®-594 conjugated antibody. (E and F) Merged images of compartment and microparticles.

Abbreviations: CSLM, confocal scanning laser microscopy; EEA-1, early endosome antigen 1 protein; LAMP-1, lysosome associated membrane protein 1.

reported studies that used LF2000 to improve microparticle uptake^{21,26} analyzed the cytotoxic effect of this agent.

To calculate the efficiency of microparticle uptake, two different strategies were used. FC studies allowed us to clearly identify the population of cells associated with microparticles but also to discriminate among cells associated with one or more microparticles. The results obtained by FC showed that all treatments increased the percentage of cells associated with microparticles, especially PEI 0.05 mM (25.9%) and LF2000 (20.4%). Furthermore, no significant differences were found between these two treatments, indicating that both would be equally efficient in terms of microparticle internalization. In the case of PEI, a decrease in the percentage of cells in contact with microparticles was observed as PEI concentration was increased. However, FC did not allow us to distinguish between internalized microparticles and those only bound to the cell surface.

To complement the FC data and to determine the location of microparticles, confocal analyses of cells were performed. By confocal microscopy, it was possible to discriminate and quantify the number of microparticles that had been internalized or that were only in contact with the cell surface. With regards to the use of LF2000, our results are in agreement with those of Kobayashi et al,²¹ who reported an increase in the rate of internalization of 1 μm -sized microparticles by HeLa cells when using this reagent. On the other hand, and concerning the use of PEI, the data obtained in the present study agree with previous studies, such as that of Thiele et al,¹⁴ who demonstrated that microparticles covalently bound to PEI are more efficiently internalized by macrophages and dendritic cells than are microparticles alone. In the present study, we demonstrated that PEI could also increase microparticle internalization in nonphagocytic

cells, and that this could be accomplished without its covalent attachment to the microparticle surface. In addition, we observed a dose-dependent, inverse relationship between PEI concentration and internalization efficiency. In agreement with FC, quantification by CSLM indicated that increasing concentrations of PEI not only resulted in an increase in the number of microparticles in contact with cells, but also in a decreased internalization. Our results suggest that the lower internalization rates at higher PEI concentrations could be related to its higher cytotoxic effect, especially membrane damage,^{27,28} which would lead to an incapability of the affected cells for microparticle internalization.

The higher efficiency of microparticle internalization after their treatment with a transfection reagent seems to be related to the changes in surface charges, as determined by the results of the Z potential analysis. Our results also showed that although surface properties of the microparticles were modified after the antibody conjugation, PEI could still interact with them, increasing their uptake by cells without affecting the fluorescence emission of the functionalizing molecule.

Both FC and CSLM analyses showed that, when the cytotoxic effect of the transfection reagents is considered, PEI 0.05 mM turns out to have been the most effective treatment, since it led to at least a twofold increased microparticle internalization rate. The advantage of FC was the high number of cells that could be analyzed in a short period of time, whereas the advantage of CSLM was its ability to ascertain internalization.

Considering that microparticles are expected to deliver their cargo inside the cell, it is necessary to determine their exact location inside the cell. Our results, using TEM analyses, showed that they were engulfed by a cell membrane

evagination and no discernible coat was visible. We also observed that once inside the cell, they appeared to be tightly surrounded by a single membrane, positive for the LAMP-1 lysosome marker, indicating that after 24 hours, the majority of microparticles were entrapped in lysosomes. These results have been confirmed by the use of nonfluorescent microparticles functionalized with an Alexa 594-conjugated secondary antibody, as the majority of internalized microparticles were also localized in the lysosomal compartment. We anticipated that using PEI, microparticles would be found in the cytosol, because it has been previously reported that the capability of protonation of PEI results in the disruption of endosomes.²⁹⁻³¹ Authors that have covalently attached PEI to microparticles²⁰ have reported that these particles can be found free in the cytosol as early as 4–6 hours posttransfection when using PEI 70 kDa but not when using PEI 25 kDa. Kobayashi et al²¹ demonstrated that the use of free cationic lipids increases the internalization of microparticles and that once in the endosomes compartment, they escape in a few minutes. According to this author, the rupture of the endosome membrane induces the formation of an autophagosome. In our study by TEM, we found that a few microparticles were surrounded by a double membrane, which could correspond to endoplasmic reticulum, indicating that an autophagic process was taking place. Our results regarding the intracellular location of microparticles by CSLM confirmed the results of the TEM studies, indicating that in the majority (83.4%) of cells, the internalized microparticles were located in the lysosomal compartment. As no endosomal association with microparticles was observed, the microparticles that were not located in lysosomes could be either free in the cytosol, or part of an autophagic process. Further studies will be necessary to analyze whether, when microparticles are functionalized with a specific cargo, the cargo can be released into the cytosol even if the microparticle remains trapped inside an organelle.

Conclusion

To sum up, our results show that PEI 25 kDa at a concentration of 0.05 mM significantly increases microparticle internalization by nonphagocytic HeLa cells with a low cytotoxic effect, and that this can be achieved without the covalent binding of PEI to the microparticle surface. Both CSLM and FC can be used for the quantification of internalization efficiency, yielding similar results, but FC allows a fast analysis of high numbers of cells whereas CSLM allows distinction between cells with internalized microparticles and cells with microparticles attached to their surface. Finally, our results show that 0.05 mM PEI 25 kDa does not induce

endosomal disruption, as internalized microparticles remain surrounded by a lysosomal membrane. With a view to drug delivery, further studies will be necessary to evaluate whether functionalized microparticles entrapped in lysosomes are still able to release their cargo into the cytosol.

Acknowledgments

This work was supported by the Spanish Ministerio de Ciencia e Innovación (MINAHE 3; TEC2008-06883-C03-03 y MINAHE 4; TEC2011-29140-C03-03), the Generalitat de Catalunya (2009 SGR-282), and the AGAUR FI-DGR 2011 and FI-DGR 2012 grants. The authors wish to thank the staff at the Servei de Microscòpia and the Unitat de Citometria de Flux of the Universitat Autònoma de Barcelona, and the staff at the Unitat de Microscòpia Electrònica i Reconeixement Molecular in Situ, especially Carmen López at the Universitat de Barcelona.

Disclosure

The authors report no conflicts of interest in this work.

References

- Grayson ACR, Shawgo RS, Johnson AM, et al. A BioMEMS review: MEMS technology for physiologically integrated devices. *Proc IEEE*. 2004;92(1):6–21.
- Fernandez-Rosas E, Gómez R, Ibañez E, et al. Intracellular polysilicon barcodes for cell tracking. *Small*. 2009;5(21):2433–2439.
- Novo S, Barrios L, Santaló J, et al. A novel embryo identification system by direct tagging of mouse embryos using silicon-based barcodes. *Hum Reprod*. 2011;26(1):96–105.
- Tao Z, Toms B, Goodisman J, Asefa T. Mesoporous silica microparticles enhance the cytotoxicity of anticancer platinum drugs. *ACS Nano*. 2010;4(2):789–794.
- Tasciotti E, Liu X, Bhavane R, et al. Mesoporous silicon particles as a multistage delivery system for imaging and therapeutic applications. *Nat Nanotechnol*. 2008;3(3):151–157.
- Serda RE, Gu J, Bhavane RC, et al. The association of silicon microparticles with endothelial cells in drug delivery to the vasculature. *Biomaterials*. 2009;30(13):2440–2448.
- Caldorera-Moore M, Peppas NA. Micro- and nanotechnologies for intelligent and responsive biomaterial-based medical systems. *Adv Drug Deliv Rev*. 2009;61(15):1391–1401.
- Zauner W, Farrow NA, Haines AM. In vitro uptake of polystyrene microspheres: effect of particle size, cell line and cell density. *J Control Release*. 2001;71(1):39–51.
- Rejman J, Oberle V, Zuhorn IS, Hoekstra D. Size-dependent internalization of particles via the pathways of clathrin- and caveolae-mediated endocytosis. *Biochem J*. 2004;377(Pt 1):159–169.
- Geng Y, Dalhaimer P, Cai S, et al. Shape effects of filaments versus spherical particles in flow and drug delivery. *Nat Nanotechnol*. 2007;2(4):249–255.
- Gratton SE, Ropp PA, Pohlhaus PD, et al. The effect of particle design on cellular internalization pathways. *Proc Natl Acad Sci U S A*. 2008;105(33):11613–11618.
- Makino K, Yamamoto N, Higuchi K, Harada N, Ohshima H, Terada H. Phagocytic uptake of polystyrene microspheres by alveolar macrophages: effects of the size and surface properties of the microspheres. *Colloid Surf B*. 2003;27(1):33–39.

13. Foster KA, Yazdani M, Audus KL. Microparticulate uptake mechanisms of in-vitro cell culture models of the respiratory epithelium. *J Pharm Pharmacol*. 2001;53(1):57–66.
14. Thiele L, Merkle HP, Walter E. Phagocytosis and phagosomal fate of surface-modified microparticles in dendritic cells and macrophages. *Pharm Res*. 2003;20(2):221–228.
15. Bühler OT, Wiedig CA, Schmid Y, Grassl GA, Bohn E, Autenrieth IB. The *Yersinia enterocolitica* invasion protein promotes major histocompatibility complex class I- and class II-restricted T-cell responses. *Infect Immun*. 2006;74(7):4322–4329.
16. Tsuda K, Amano A, Umebayashi K, et al. Molecular dissection of internalization of *Porphyromonas gingivalis* by cells using fluorescent beads coated with bacterial membrane vesicle. *Cell Struct Funct*. 2005;30(2):81–91.
17. Tros de Ilarduya C, Sun Y, Düzgünes N. Gene delivery by lipoplexes and polyplexes. *Eur J Pharm Sci*. 2010;40(3):159–170.
18. Godbey WT, Wu KK, Mikos AG. Poly(ethyleneimine) and its role in gene delivery. *J Control Release*. 1999;60(2–3):149–160.
19. Pichon C, Billiet L, Midoux P. Chemical vectors for gene delivery: uptake and intracellular trafficking. *Curr Opin Biotechnol*. 2010;21(5):640–645.
20. Kasturi SP, Sachaphibulkij K, Roy K. Covalent conjugation of polyethyleneimine on biodegradable microparticles for delivery of plasmid DNA vaccines. *Biomaterials*. 2005;26(32):6375–6385.
21. Kobayashi S, Kojidani T, Osakada H, et al. Artificial induction of autophagy around polystyrene beads in nonphagocytic cells. *Autophagy*. 2010;6(1):36–45.
22. Hu C, Peng Q, Chen F, Zhong Z, Zhuo R. Low molecular weight polyethyleneimine conjugated gold nanoparticles as efficient gene vectors. *Bioconjug Chem*. 2010;21(5):836–843.
23. Duan Y, Zhang S, Wang B, Yang B, Zhi D. The biological routes of gene delivery mediated by lipid-based non-viral vectors. *Expert Opin Drug Deliv*. 2009;6(12):1351–1361.
24. Lambert RC, Maulet Y, Dupont JL, et al. Polyethyleneimine-mediated DNA transfection of peripheral and central neurons in primary culture: probing Ca²⁺ channel structure and function with antisense oligonucleotides. *Mol Cell Neurosci*. 1996;7(3):239–246.
25. Deng R, Yue Y, Jin F, et al. Revisit the complexation of PEI and DNA – how to make low cytotoxic and highly efficient PEI gene transfection non-viral vectors with a controllable chain length and structure? *J Control Release*. 2009;140(1):40–46.
26. Gómez-Martínez R, Vázquez P, Duch M, et al. Intracellular silicon chips in living cells. *Small*. 2010;6(4):499–502.
27. Helander IM, Alakomi HL, Latva-Kala K, Koski P. Polyethyleneimine is an effective permeabilizer of gram-negative bacteria. *Microbiology*. 1997;143(Pt 10):3193–3199.
28. Helander IM, Latva-Kala K, Lounatmaa K. Permeabilizing action of polyethyleneimine on *Salmonella typhimurium* involves disruption of the outer membrane and interactions with lipopolysaccharide. *Microbiology*. 1998;144(Pt 2):385–390.
29. Boussif O, Lezoualc'h F, Zanta MA, et al. A versatile vector for gene and oligonucleotide transfer into cells in culture and in vivo: polyethyleneimine. *Proc Natl Acad Sci U S A*. 1995;92(16):7297–7301.
30. Creusat G, Rinaldi AS, Weiss E, et al. Proton sponge trick for pH-sensitive disassembly of polyethyleneimine-based siRNA delivery systems. *Bioconjug Chem*. 2010;21(5):994–1002.
31. Sonawane ND, Szoka FC Jr, Verkman AS. Chloride accumulation and swelling in endosomes enhances DNA transfer by polyamine-DNA polyplexes. *J Biol Chem*. 2003;278(45):44826–44831.

International Journal of Nanomedicine

Publish your work in this journal

The International Journal of Nanomedicine is an international, peer-reviewed journal focusing on the application of nanotechnology in diagnostics, therapeutics, and drug delivery systems throughout the biomedical field. This journal is indexed on PubMed Central, MedLine, CAS, SciSearch®, Current Contents®/Clinical Medicine,

Submit your manuscript here: <http://www.dovepress.com/international-journal-of-nanomedicine-journal>

Dovepress

Journal Citation Reports/Science Edition, EMBASE, Scopus and the Elsevier Bibliographic databases. The manuscript management system is completely online and includes a very quick and fair peer-review system, which is all easy to use. Visit <http://www.dovepress.com/testimonials.php> to read real quotes from published authors.

3.2

**Surface modification of
microparticles causes differential
uptake responses in normal and
tumoral human breast epithelial cells**

SCIENTIFIC REPORTS

OPEN

Surface modification of microparticles causes differential uptake responses in normal and tumoral human breast epithelial cells

Received: 16 December 2014

Accepted: 26 May 2015

Published: 12 June 2015

Tania Patiño, Jorge Soriano, Lleonard Barrios, Elena Ibáñez & Carme Nogués

The use of micro- and nanodevices as multifunctional systems for biomedical applications has experienced an exponential growth during the past decades. Although a large number of studies have focused on the design and fabrication of new micro- and nanosystems capable of developing multiple functions, a deeper understanding of their interaction with cells is required. In the present study, we evaluated the effect of different microparticle surfaces on their interaction with normal and tumoral human breast epithelial cell lines. For this, AlexaFluor₄₈₈ IgG functionalized polystyrene microparticles (3 μm) were coated with Polyethyleneimine (PEI) at two different molecular weights, 25 and 750 kDa. The effect of microparticle surface properties on cytotoxicity, cellular uptake and endocytic pathways were assessed for both normal and tumoral cell lines. Results showed a differential response between the two cell lines regarding uptake efficiency and mechanisms of endocytosis, highlighting the potential role of microparticle surface tuning for specific cell targeting.

In recent years, the development of micro- and nanotechnology for biomedical applications has attracted a great deal of attention. This is due to the unique and controllable physicochemical properties of micro- and nanoparticles, which allow them to integrate multiple functions such as biosensing^{1–4}, targeting^{5–8} and drug delivery^{9–11}. Recently, a wide range of studies has focused on the fabrication and characterization of new micro- and nanoparticles for biomedical purposes. However, a deeper understanding of their interactions with biological systems at the cellular level is required for the design of new multifunctional micro and nanosystems with potentiated effects on target cells and diminished side effects on healthy ones.

Different studies have revealed that size^{12–15}, shape^{16,17} and surface functionalization of particles¹⁸ are key factors regarding their internalization by cells. Particularly, surface charge of micro- and nanoparticles has been described to play a critical role in their internalization by cells, the cationic particles being more efficiently internalized than the anionic ones^{19,20}, in the majority of cases. Thus, with the aim to obtain cationic particles, several approaches have been performed, including their coating with cationic lipids or polymers. Specifically, particle coating with Polyethyleneimine (PEI) has been of particular relevance^{21–23} due to the widely known proton sponge effect, which involves the protonation of PEI amine groups that leads to endo/lysosomal pH buffering, membrane disruption, and ultimate liberation of the content to the cytosol²⁴. Moreover, the proton sponge effect has been shown to be more efficiently achieved when a high molecular weight of PEI is used²⁵.

Unitat de Biologia Cel·lular, Departament de Biologia Cel·lular, Fisiologia i Immunologia. Facultat de Biociències. Universitat Autònoma de Barcelona, 08139 Bellaterra, Spain. Correspondence and requests for materials should be addressed to C.N. (email: carme.nogues@uab.cat)

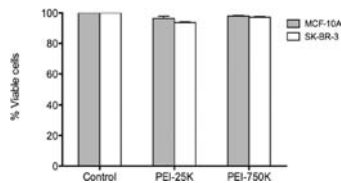


Figure 1. Effect of 0.05 mM PEI-25 K or PEI-750 K treatments on the viability of non-tumoral (MCF-10A) and tumoral (SKBR-3) human breast epithelial cells.

On the other hand, micro- and nanoparticles cellular uptake and the mechanism of internalization can differ among cell types^{12,13,18,26}. This, however, has received less attention in the literature.

Specific antibodies or peptides against certain cell surface markers are used to enhance particle internalization in target cells^{27–30}. However, other intrinsic properties of non-targeted particles can also have a differential effect upon different cell lines¹⁸. Moreover, whilst there is a wide range of particle-cell interaction studies conducted with nanoparticles, less is known about the interaction of larger particles with cells. More research is thus required to improve the strategies for biomedical applications of micron-sized delivery systems, as they have been proved to be a good approach for drug delivery^{31–35}.

Hence, the aim of the present work was to provide an integrated study about the impact of different non-specific surface modifications of microparticles upon their interaction with different cell types, in terms of cytotoxicity, uptake efficiency, mechanism of internalization and intracellular fate. With this purpose, 3- μ m polystyrene microparticles were functionalized with a fluorescently-labeled non-specific antibody. Then, two types of PEI, both differing on their structure and molecular weight, were used for microparticle coating. The cytotoxicity and internalization of those microparticles were studied in two human breast epithelial cell lines, one normal and another tumoral.

Results

Effect of 0.05 mM PEI on cell viability. The cytotoxic effect of PEI treatments was evaluated by flow cytometry 24 h after incubation of cells with PEI-25 K or PEI-750 K. Figure 1 shows that the percentage of viable cells, normalized to the control, was higher than 90% in all cases. Moreover, no significant differences ($P > 0.05$) were found between PEI treatments and control cells, indicating that 4 h incubation with either PEI-25 K or PEI-750 K 0.05 mM did not cause cytotoxicity in either SKBR-3 or MCF-10A cells.

Characterization of microparticles. Polystyrene microparticles were functionalized with Alexa Fluor[®]488 conjugated goat anti-Rabbit IgG (Alexa488-IgG) and then coated with different molecular weight Polyethyleneimine (PEI), 25 kDa or 750 kDa (PEI-25 K or PEI-750 K), as described in Fig. 2a. Surface charge of microparticles was evaluated by measuring their ζ -potential (Fig. 2b). Results showed that Alexa488-IgG microparticles were successfully coated with PEI, as their negatively charged surface changed to positively charged, being significantly higher when PEI-750 K was used. In order to qualitatively assess the dispersion status of microparticles, SEM images of microparticles were recorded (Fig. 2c). Although the majority of particles were in a monodispersed form, few aggregates were also observed. To quantify the amount of monodispersed particles, samples were analyzed using a Flow Cytometer, where the amount of fluorescence intensity allowed discriminating between single and aggregated particles (Fig. 2d). Figure 2e shows that in all cases the percentage of monodispersed microparticles was above 80%, which was considered as an acceptable value for our studies.

Microparticle internalization efficiency. Internalization of microparticles by both MCF-10A and SKBR-3 cells was measured by flow cytometry. In order to distinguish cells with membrane-attached microparticles from cells that had completely internalized them, trypan blue (TB) quenching of extracellular microparticles was performed (optimization of TB concentration to completely quench microparticle fluorescence is summarized in supplementary data, figures S1 and S2). Figure 3 shows how the TB quenching effect was used for distinguishing microparticles internalized from those attached to the cell membrane. Fluorescence of Alexa488-IgG-microparticles was analyzed before and after the addition of 2 mg/ml TB (Fig. 3a). We observed that fluorescence was completely eliminated after TB addition.

Figure 3b shows a schematic representation of the extracellular quenching effect by TB. As TB is not capable of penetrating live cells, the quenching effect only occurs in the extracellular space. Thus, the fluorescence of microparticles bound to the membrane can be quenched by TB, whereas the internalized ones remain intact. Figure 3c shows a typical flow cytometry analysis of cells incubated with microparticles (in this case MCF-10A cells incubated with PEI-25 K coated microparticles). Two different populations of cells were observed before TB addition: the population of cells without microparticles (no fluorescence emission) and the population of cells with microparticles, either internalized or bound to the cell membrane (green fluorescence emission). After the addition of TB, the fluorescence of

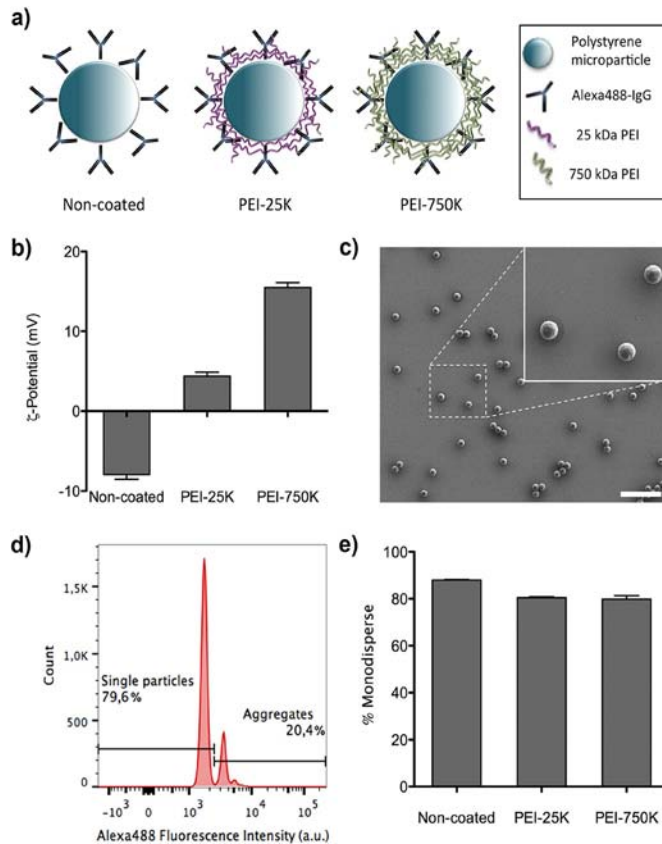


Figure 2. Characterization of Alexa488-IgG functionalized microparticles. a) Scheme of Alexa488-IgG microparticles (non-coated) and coated with different molecular weight PEI (PEI-25 K and PEI-750 K, respectively). b) ζ -Potential of non-coated and coated (PEI-25 K and PEI-750 K) Alexa488-IgG microparticles. c) Representative SEM image of Alexa488-IgG microparticles, in the example coated with PEI-25 K. Scale bar corresponds to 20 μ m. Inset shows a magnification of the selected area. d) Representative fluorescence intensity histogram of Alexa488-IgG microparticles (in the example coated with PEI-25 K), obtained by flow cytometry analysis. e) Percentage of monodisperse, non-coated, PEI-25 K and PEI-750 K Alexa488-IgG microparticles, calculated by flow cytometry analyzed as shown in d).

non-internalized microparticles was quenched, allowing us to discriminate between microparticles internalized (green fluorescence) and microparticles adhered to the cell membrane (no fluorescence emission). Moreover, the addition of TB to the cell suspension permitted to determine cell viability, since TB can only enter in cells with damaged plasma membranes. Thus, a third population was observed after the TB addition, corresponding to dead cells which emitted red fluorescence due to the presence of TB in their cytoplasm. In this study, we used the Q4 population, i.e. live cells with internalized microparticles. In order to compare the effect of the different surface modifications of microparticles on their uptake efficiency by SKBR-3 and MCF-10A cells.

Figure 4 shows the percentage of live cells with internalized microparticles for both cell lines. We observed that MCF-10A cells internalized non-coated microparticles (Alexa488-IgG-microparticles) with a 3-fold higher efficiency than SKBR-3 cells. By contrast, PEI coating of microparticles resulted in an opposed effect. When PEI coated microparticles (PEI-25 K and PEI-750 K) were used, a significant reduction in microparticle internalization was observed in MCF-10A cells, whereas the opposite effect

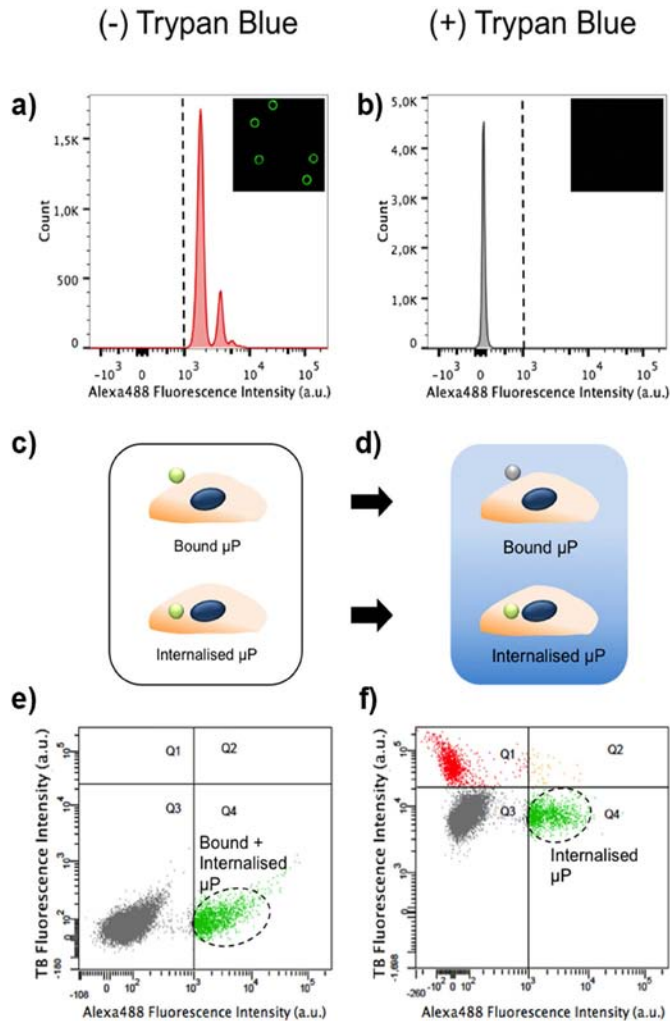


Figure 3. Quenching effect of Trypan Blue (TP) allowing discriminating internalized microparticles from those attached to the cell membrane. a,b) Fluorescence intensity of Alexa488-IgG microparticles before (a) and after (b) TB addition, analyzed by flow cytometry. Fluorescence boundary was established with Alexa488-IgG microparticles fluorescence emission (>103 a.u.). Inset shows an image of the same Alexa488-IgG microparticles before and after TB addition. c,d) Scheme of extracellular quenching effect by TB. After TB addition (d), only Alexa488-IgG microparticles attached to the cell membrane can be quenched, TB cannot quench internalized ones. e,f) Representative dot-plot of cells incubated with Alexa488-IgG microparticles, analyzed by flow cytometry after 4 h of incubation before (e) and after (f) TB addition. In the absence of TB, two populations of cells were observed: cells with Alexa488-IgG microparticles (Q4, green), either attached to the plasma membrane or internalized, and cells without microparticles (Q3, grey). TB can enter only in cells with damaged membrane (dead cells), thus the addition of TB induced the visualization of a new population of cells: those emitting in the red channel (Q1). Therefore, Q3 and Q4 constitute the population of live cells, being Q3 cells without microparticles or cells with microparticles attached to the membrane that have been quenched, whereas Q4 shows the population of cells that have internalized the microparticles.

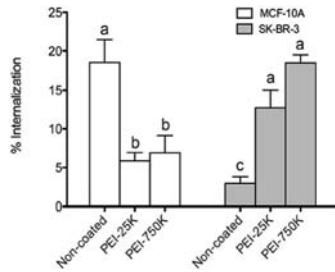


Figure 4. Internalization efficiency of non-coated and PEI-coated Alexa488-IgG microparticles by MCF-10A and SKBR-3 cell lines, analyzed by flow cytometry. Results are representative of three independent experiments and data is shown as the mean \pm SEM. Different superscripts (a–c) denote groups of significance ($P < 0.05$).

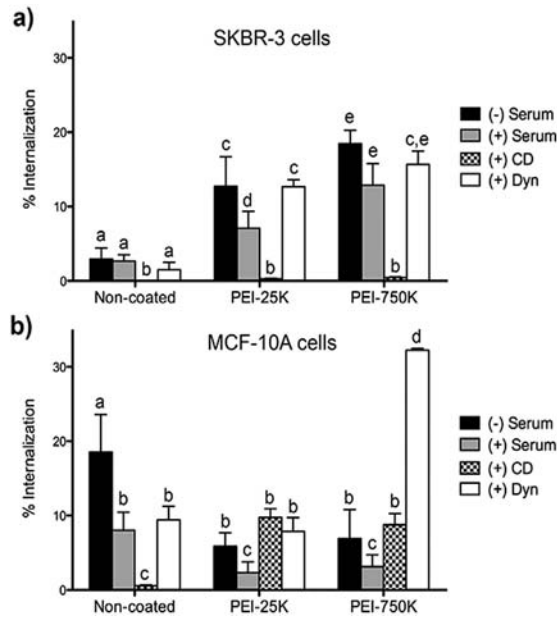


Figure 5. Internalization of Alexa488-IgG functionalized microparticles either coated or not with PEI (25K or 750K) by SKBR-3 (a) and MCF-10A (b) cells, when incubated with serum, Cytochalasin D (CD) or Dynasore (Dyn). Results are shown as the mean \pm SEM. Different superscripts (a–e) denote groups of significance ($P < 0.05$).

was observed in SKBR-3 cells. In addition, for both cell lines, although a higher percentage of internalization was observed in the case of PEI-750K, no significant differences were found when compared to PEI-25K. All experiments were conducted by incubating the microparticles in serum-free medium.

Effect of serum and endocytic inhibitors on microparticle internalization. The effect of serum and endocytic inhibitors on microparticle internalization was evaluated by flow cytometry, as previously

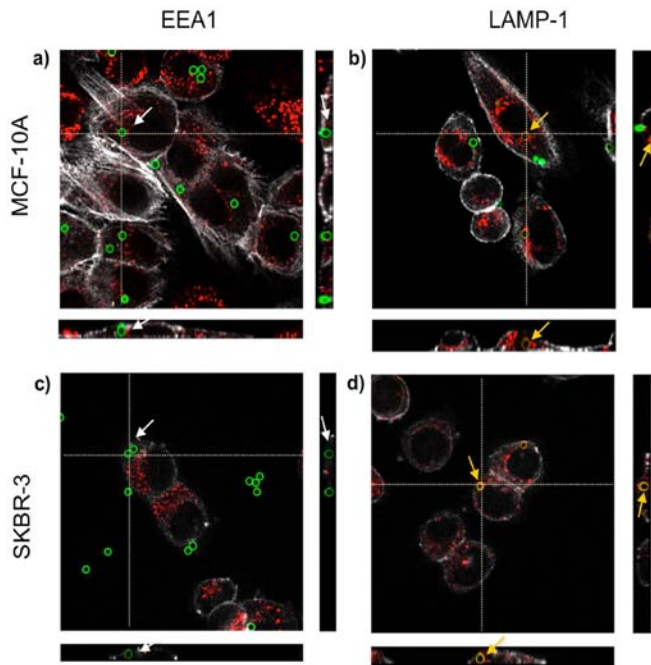


Figure 6. Intracellular location of microparticles, analyzed by Confocal Laser Scanning Microscope (CLSM). Orthogonal projections of z-stacks of MCF10A (a,b) or SKBR-3 (c,d) cells incubated with the endosome marker EEA1 (red) (a,c) or the lysosome marker LAMP-1 (red) (b,d). Microparticles could be only observed in lysosomes (orange arrows), but not in endosomes (white arrows). In all cases, cell cortex was stained using AlexaFluor® 594-conjugated Phalloidin.

described. Figure 5a,b show the percentages of internalization in SKBR-3 and MCF-10A cells, respectively. For both cell lines, the presence of serum during incubation with microparticles significantly reduced their internalization, except in the case of SKBR-3 in presence of non-coated microparticles and MCF-10A incubated with PEI-750K coated microparticles, where internalization was not affected.

Regarding endocytosis inhibition, we observed a cell line dependent effect of macropinocytosis inhibition by cytochalasin D (CD). Whereas in SKBR-3 cells the internalization of all types of microparticles was completely inhibited by CD, in MCF-10A cells the CD effect was only detected in the case of non-coated microparticles.

The addition of Dynasore (Dyn) also induced a differential cell response regarding internalization of microparticles. In SKBR-3 cells, Dyn did not affect the internalization of any type of microparticles. By contrast, the incubation with Dyn significantly reduced the uptake of non-coated microparticles by MCF-10A cells. This reduction was not observed in either PEI-25K or PEI 750K.

The cytotoxicity of all incubation conditions was determined by the use of TB in flow cytometry analyses. Results showed that none of the incubation conditions altered cell survival when compared to control cells (figure S3).

Intracellular location of microparticles. In order to determine the intracellular fate of non-coated, PEI-25K and PEI-750K microparticles in SKBR-3 and MCF-10A cells, immunolocalization of EEA-1 (endosomal compartment) and LAMP-1 (lysosomal compartment) proteins was carried out. Confocal Laser Scanning Microscope (CLSM) analyses showed that at 4h the majority of microparticles positively colocalized with LAMP-1 marker, indicating that microparticles were located inside the lysosomal compartment (Fig. 6). These results were found for both cell lines and for all microparticle treatments. Moreover, 24h later, the majority of microparticles (>80%) remained in the lysosomal compartment.

Discussion

Although the use of micro- and nanosystems for drug delivery has shown a strong potential for biomedical applications, a deeper understanding of their interaction with cells is required for more efficient design of drug delivery systems. Moreover, whereas a wide range of studies have focused on the study of nanoparticles behavior in contact with cells, less is known about larger particles.

In the present study we compared the response of normal and tumoral breast epithelial cell lines to 3 μm microparticles with different surface properties. First, polystyrene microparticles were covalently conjugated to a fluorescently labelled secondary antibody. Then, the cationic polymer PEI at two different molecular weights was used to coat microparticles in order to 1) further modify their surface properties and, 2) evaluate how this could impact on their interaction with cells. Although PEI has been successfully used for gene delivery and/or functionalization of micro- and nanoparticles^{36–39}, it has been proved to yield cytotoxic effects, depending on its form (linear or branched) and molecular weight⁴⁰.

Thus, the first step in this work was to assess the cytotoxicity of free PEI-25k and PEI-750K at a 0.05 mM concentration. Given that PEI at that concentration did not trigger cytotoxic effects in either MCF-10A or SKBR-3 cells, microparticles were coated with PEI-25k and PEI-750 K (0.05 mM). PEI coating clearly changed the surface of microparticles from negatively to positively charged. This change was significantly higher for PEI-750 K than for PEI-25K, almost certainly due to the former having a higher molecular weight and a higher number of protonable amine groups than the latter.

To evaluate the surface charge effect of the PEI coating of microparticles on cellular uptake, flow cytometry was used to determine the internalization efficiency. Results showed that microparticle internalization was dependent on surface charge in both cell lines, as it has been previously described by other authors^{17,20,41}. However, although it has been widely reported that positively charged microparticles are preferentially uptaken by cells, we observed that MCF-10A cells were more able to internalize negatively charged non-coated microparticles than their PEI-coated counterparts. In contrast, in SKBR-3 cells the uptake increased with positively charged microparticles (PEI-coated), being nearly depreciable for non-coated ones (negatively charged). In fact, it has been reported that MCF-10A cells can internalize both positively¹⁸ and negatively⁴⁰ charged nanoparticles and the same seems to apply to microparticles. Taken together, our results indicate that surface charge clearly determines microparticle uptake by cells. However, the uptake can be either enhanced or inhibited, depending on the cell type, which suggests that targeting to certain cell types can benefit from the microparticle surface charge. Thus, to identify the behavior of a specific cell line in front of a specific particle is very important when designing new particles for drug delivery. Our results indicate that two human cell lines, both coming from the mammary epithelia showed completely different uptake capability depending on their tumorigenic or non-tumorigenic nature.

The presence of serum in the culture medium is also critical for microparticle internalization, as a protein corona can form around micro/nano particles, modifying their surface⁴². In this regard, it is shown that the presence of serum had an inhibitory internalization effect on both cell lines and for all types of microparticles, except for internalization of non-coated microparticles by SKBR-3 cells and PEI-750K coated microparticles by MCF-10A. This finding highlights the impact of cell type on microparticle-cell interactions, and is in agreement with Yan *et al.* (2013), who observed a differential impact of protein corona in THP-1 monocytic cells and macrophages⁴³.

In order to further investigate whether the mechanism of internalization was also dependent on the cell line and surface properties of microparticles, two endocytosis inhibitors, CD and Dyn, were used. CD has been reported to mainly inhibit macropinocytosis, whereas Dyn causes inhibition of dynamin-dependent endocytosis⁴⁴, i.e. clathrin- and caveolin-mediated endocytosis. In the case of the SKBR-3 line, microparticle internalization was inhibited almost completely by CD but not by Dyn, both for non-coated and PEI-coated microparticles, indicating that in these cells microparticle internalization occurs by macropinocytosis rather than by dynamin-dependent mechanisms. It has been reported that SKBR-3 cells internalize their overexpressed ErbB2 receptors in a clathrin- and caveolin- independent endocytic pathway⁴⁵. What is more, SKBR-3 cells lack caveolae, and ErbB2 internalization is sensitive to the depletion of cholesterol, which is necessary for most of the clathrin-independent pathways⁴⁶. In addition, an association between macropinocytosis and tumor progression/metastasis has been reported⁴⁷. Altogether, these studies could explain why SKBR-3 cells use the macropinocytosis pathway to internalize all types of microparticles, regardless of their surface properties.

By contrast, in MCF-10A cells, both CD and Dyn inhibited negatively charged microparticle uptake, suggesting that both macropinocytosis and dynamin-dependent endocytosis were involved. On the other hand, internalization of PEI-coated microparticles by MCF-10A cells was not affected by either CD or Dyn, suggesting that positively charged microparticles are internalized through alternative mechanisms in these cells. In addition, a higher percentage of PEI-750K microparticles were internalized in the presence of Dyn than in its absence. This fact could be attributed to a compensatory effect, as it has been previously described that clathrin and caveolae dependent endocytosis inhibition can cause stimulation of macropinocytosis of positively charged nanoparticles²². However, further studies are needed to better understand this particular result. Taken together, all these findings suggest that both the surface charge and the cell type have a strong impact not only on the uptake efficiency, but also on the mechanism of microparticle internalization (Fig. 7).

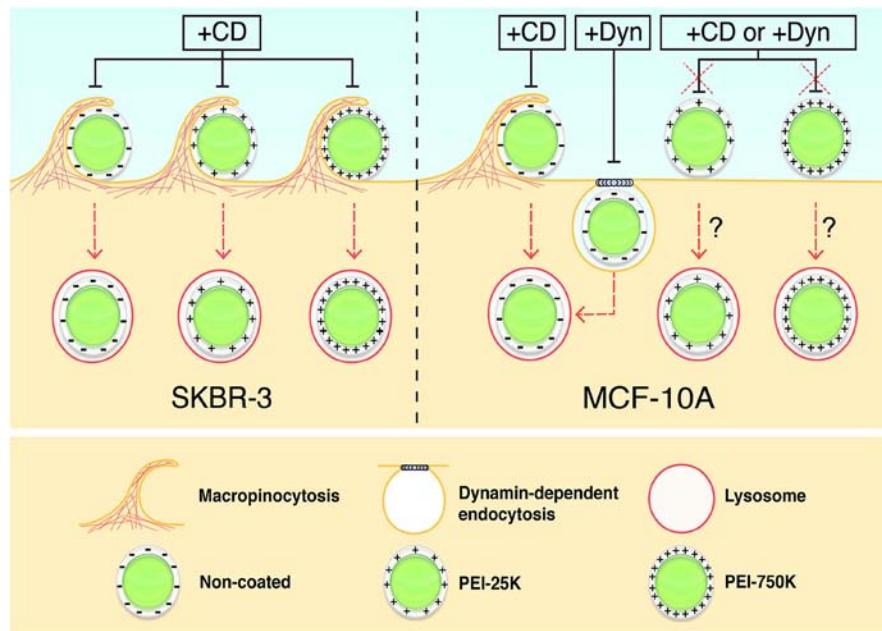


Figure 7. Scheme of the differential mechanisms of microparticle internalisation by SKBR-3 and MCF-10A cells. SKBR-3 cells internalized all types of microparticles by macropinocytosis, as their internalization was only inhibited by Cytochalasin D (CD). By contrast, MCF-10A cells showed different mechanisms of internalization, depending on the microparticle type. Non-coated Alexa488-IgG microparticles could be taken up by both macropinocytosis and dynamin-dependent endocytosis, as their internalization was inhibited by both CD and Dynasore (Dyn). By contrast, the uptake of PEI-25 K and PEI-750 K coated microparticles was not affected by either CD or Dyn, indicating that they are taken up by alternative mechanisms.

Finally, we assessed the intracellular location of microparticles in order to evaluate whether surface charge or cell type could affect the intracellular fate of the microparticles. Results showed that in all cases microparticles were located inside the lysosomal compartment, regardless of their surface properties and cell type. This suggests that despite the fact that PEI proton-sponge effect allows the delivery of DNA and small nanoparticles to the cytosol⁴⁸, it is not capable of releasing large microparticles into the cytosol. In this regard, future research should be focused on alternative approaches for the efficient delivery of desired microparticles or molecules into the cytosol.

In summary, we have demonstrated that normal and tumor cells use different endocytic pathways when internalizing different types of modified microparticles. The tumor cell line SKBR-3 internalizes, mainly, positively charged microparticles, using the macropinocytosis pathway. When this pathway is inhibited, internalization is interrupted. By contrast, the non-tumor cell line MCF-10A uses different pathways to predominantly internalize negative microparticles. It seems that there is not a predominant uptake mechanism, and that compensatory internalization pathways are used when one of the pathways is inhibited. Regardless of the cell line and microparticle surface, the fate of the microparticles is always the lysosome compartment, even in presence of PEI-750 K. Thus new strategies, as pH sensitive cargo-link or esterase sensitive cargo-link, among others, must be envisaged to allow the liberation of the cargo to the cytoplasm. Consequently, the design of microcarriers against specific tissues must be done taken into account i) the surface of the microparticle and ii) the characteristics of the target cell, i.e., the uptake pathway and the final fate.

Methods

Functionalization of microparticles. Carboxylated microparticles (Polybead[®] Carboxylate Microspheres 3 μ m; Polysciences, Inc, Warrington, PA) were functionalized with an Alexa Fluor[®]

488 conjugated goat anti-Rabbit IgG H&L antibody (Life Technologies, Carlsbad, CA) using the PolyLink Protein Coupling kit (Polysciences, Inc.), following the manufacturer's instructions (Alexa488-IgG-microparticles, from now on).

PEI coating and characterization of microparticles. To coat Alexa488-IgG microparticles with PEI, 5 μ L of PEI-25 K or PEI-750 K (10 mM) were diluted in 135 μ L of NaCl. In parallel, 3 μ L of microparticle solution (3×10^6 microparticles) was diluted in 137 μ L of NaCl. Then, the PEI solution was added to the microparticle solution, mixed slowly and left at room temperature (RT) for 40 min in order to form the PEI-Alexa488-IgG-microparticles complexes. After incubation, 720 μ L of serum-free culture medium was added to the solution to obtain a final 0.05 mM concentration of PEI. Non-coated functionalized (Alexa488-IgG-microparticles) and non-functionalized (-COOH microparticles) microparticles, were treated in the same way, but without PEI addition. ζ -Potential of microparticles was measured using a Zetasizer Nano ZS (Malvern Instruments, Malvern, UK). Images of microparticles were recorded using a Scanning Electron Microscope (Zeiss Merlin, Jena, Germany). Fluorescence intensity of microparticles was analyzed using a Becton Dickinson FACSCanto II flow cytometer (BD Biosciences, Franklin Lakes, NJ) equipped with BD Biosciences FACSDiva™ software, in order to quantitatively determine the dispersion state of microparticles.

Cell culture. Experiments were conducted with two different human mammary epithelial cell lines, a non-tumorigenic (MCF-10A) and a metastatic one (SKBR-3). The MCF-10A cell line (ATCC) was cultured in DMEM/F12 (Gibco, Paisley, United Kingdom) supplemented with 5% horse serum (Gibco), 20 ng/ml epidermal growth factor (Gibco), 0.5 mg/ml hydrocortisone (Sigma-Aldrich, St Louis, MO, USA), 100 ng/ml cholera toxin (Sigma) and 10 μ g/ml insulin (Gibco). The SKBR-3 adenocarcinoma cell line (ATCC) was cultured in McCoy's 5A modified medium (Gibco) supplemented with 10% fetal bovine serum (Gibco). Both cell lines were maintained at 37 °C and 5% CO₂ (standard conditions).

Polyethylenimine cytotoxicity analysis. PEI with a molecular weight of 25 kDa (PEI-25K) and 750 kDa (PEI-750K) were purchased from Sigma and a 10 mM stock solution was prepared as previously described⁴⁸.

MCF-10A and SKBR-3 cells were seeded in 35 mm Petri dishes (Nalge Nunc Int, Roskilde, Denmark) at a density of 1.5×10^5 cells/dish. After 48 h, culture medium was replaced with serum-free culture medium containing 0.05 mM of PEI-25 K or PEI-750 K and cells were maintained in standard conditions. Control cells were treated in the same way but in absence of PEI. After 4 h of incubation, the medium was replaced by fresh supplemented culture medium and the cells were incubated again for 24 h. Finally, cells were harvested by trypsinization and cytotoxicity was evaluated using the "LIVE/DEAD® Viability/Cytotoxicity Kit for mammalian cells" (Life Technologies, Carlsbad, CA), following the manufacturer's instructions. Cells were analyzed under a Becton Dickinson FACSCanto II flow cytometer (BD Biosciences, Franklin Lakes, NJ) equipped with BD Biosciences FACSDiva™ software. For each treatment, four independent experiments were performed, where 20,000 cells were analyzed.

Microparticle internalization. MCF-10A and SKBR-3 cells were seeded in 35 mm petri dishes at a density of 1.5×10^5 cells/dish. After 48 h, the medium was removed and cells were incubated with Alexa488-IgG-microparticles either non-coated, or coated with PEI-25 K or PEI-750 K at a 5:1 ratio (microparticle:cell), in serum-free medium for 4 h in standard conditions. Microparticle internalization was evaluated at 4 h, when cells were harvested by trypsinization and analyzed under a flow cytometer. In order to distinguish internalized microparticles from those attached to the cell membrane, 2 mg/ml Trypan Blue (TB, Sigma) was used to quench the extracellular fluorescence^{13,21}. Cells were analyzed under a Becton Dickinson FACSCanto II flow cytometer both prior and after TB addition. This method allowed obtaining integrated information about cell viability and microparticle internalization efficiency (% of cells with internalized microparticles). For each PEI treatment and time of incubation, three independent experiments were performed analyzing 20,000 cells each.

Endocytosis inhibition. To elucidate the mechanism of microparticles internalization, two endocytosis inhibitors were used: Cytochalasin D (CD; macropinocytosis inhibition) and Dynasore (Dyn; Dynamin-dependent endocytosis inhibition). MCF-10A and SKBR-3 cells were seeded in 35 mm petri dishes at a density of 1.5×10^5 cells/dish. At 48 h, prior to the addition of microparticles, cells were pre-incubated for 1 h with 10 μ g/ml CD (Sigma-Aldrich), or 80 μ g/ml Dyn (Sigma-Aldrich) in serum-free medium. After that, pre-incubation medium was removed and cells were exposed to non-coated Alexa488-IgG-microparticles, PEI-25 K or PEI-750 K coated Alexa488-IgG-microparticles at a 5:1 ratio (microparticle:cell) in presence of the endocytosis inhibitors (10 μ g/ml CD, or 80 μ g/ml Dyn) for 4 h. Finally, cells were recovered by trypsinization and analyzed under a Becton Dickinson FACSCanto II flow cytometer.

In addition, the effect of serum on microparticle internalization was tested by incubating the microparticles (non-coated and PEI-coated) in culture medium containing serum. After 4 h of incubation, the cells were trypsinized and microparticle internalization was evaluated by flow cytometry.

Immunofluorescence detection of endosomal and lysosomal compartments. Cells were seeded on coverslips in 4-well culture dishes at a density of 30,000 cells/well. After 48 h, they were exposed to functionalized microparticles, either non-coated or coated with PEI-25 K or PEI-750 K, at a 5:1 ratio (microparticle:cell) and incubated for 4 h. Then, cells were washed twice with PBS, fixed with 4% paraformaldehyde/PBS (Sigma-Aldrich), permeabilized with 0.1% Triton X-100 (Sigma-Aldrich) in PBS, and blocked with 5% PBS-BSA (Sigma-Aldrich) for 40 min. Cells were incubated for 1 h at 37 °C with either mouse anti-EEA-1 monoclonal antibody (BD Biosciences, Franklin Lakes, NJ) or mouse anti-LAMP-1 polyclonal antibody (BD Biosciences), in order to label endosomal or lysosomal compartments, respectively. After that, cells were washed thrice with PBS and incubated at RT for 1 h with Cy5-conjugated chicken anti-mouse IgG antibody (Life technologies). Finally, cells were washed twice with PBS and incubated with Alexa 594-Conjugated Phalloidin (5 µg/ml, Life Technologies) and Hoechst 33258 (0.5 µg/ml, Life Technologies) to stain actin and DNA, respectively, prior to their analysis under a Confocal Laser Scanning Microscope (CLSM, Olympus XT7). For each labelling, treatment, and time of incubation with microparticles, at least 20 cells were analyzed.

Statistical analyses. Statistical analyses were conducted using a statistical package (IBM SPSS® for Windows, version 20.0; SPSS Inc., Chicago, IL, USA). Data were first tested for normality (Shapiro-Wilk test) and homogeneity of variances (Levene test). When necessary, data (x) in percentages were arcsine-transformed ($\arcsin \sqrt{x}$) to accomplish the parametric assumptions (i.e. normal distribution and variance homogeneity).

A series of separate general linear models (analysis of variance, ANOVA) were run to test the effects of non-coated microparticles and/or PEI concentrations on ζ -potential, cell viability and percentage of internalization. Briefly, the effects of PEI treatments on SKBR-3 and MCF-10A viability and internalization were determined through a two-way ANOVA (factors: PEI treatment and cell line, SKBR-3 and MCF-10A; variables: % cell viability or % internalization), followed by a post-hoc Sidak test, whereas ζ -Potential of carboxylated microparticles non functionalized (-COOH), Alexa 488-IgG functionalized microparticles (488IgG), Alexa488-IgG-microparticles coated with PEI25K (PEI25K) or PEI750K (PEI750K) was compared by a one-way ANOVA followed by a post-hoc Sidak test. Finally, the effects on non-coated, PEI-25kDa-, PEI750kDa-coated microparticles intake of incubation with or without serum, or with endocytosis inhibitors (CD or Dyn) were tested in MCF-10A and SKBR-3 cells through a three-way ANOVA (factors: medium composition, PEI treatment, and cell line; variable: % internalization), again followed by a post-hoc Sidak test.

In all cases, the level of significance was set at $P < 0.05$. Data are presented as mean \pm standard error of the mean (SEM).

References

- Carregal-Romero, S. *et al.* Multiplexed sensing and imaging with colloidal nano- and microparticles. *Annu. Rev. Anal. Chem. (Palo Alto, Calif.)* **6**, 53–81 (2013).
- Cederquist, K. B., Dean, S. L. & Keating, C. D. Encoded anisotropic particles for multiplexed bioanalysis. *Wiley Interdiscip. Rev. Nanomed. Nanobiotechnol.* **2**, 578–600 (2010).
- Sen, T. & Bruce, I. J. Surface engineering of nanoparticles in suspension for particle based bio-sensing. *Sci. Rep.* **2**, 564 (2012).
- Anker, J. N. *et al.* Biosensing with plasmonic nanosensors. *Nat. Mater.* **7**, 442–53 (2008).
- Yu, M. K., Park, J. & Jon, S. Targeting strategies for multifunctional nanoparticles in cancer imaging and therapy. *Theranostics* **2**, 3–44 (2012).
- Sanna, V., Pala, N. & Sechi, M. Targeted therapy using nanotechnology: focus on cancer. *Int. J. Nanomedicine* **9**, 467–483 (2014).
- Gu, F. X. *et al.* Targeted nanoparticles for cancer therapy. *Nano Today* **2**, 14–21 (2007).
- Jain, N. K., Mishra, V. & Mehra, N. K. Targeted drug delivery to macrophages. *Expert Opin. Drug Deliv.* **10**, 353–67 (2013).
- Caldorera-Moore, M. & Peppas, N. a. Micro- and nanotechnologies for intelligent and responsive biomaterial-based medical systems. *Adv. Drug Deliv. Rev.* **61**, 1391–401 (2009).
- Cai, Y., Chen, Y., Hong, X., Liu, Z. & Yuan, W. Porous microsphere and its applications. *Int. J. Nanomedicine* **8**, 1111–20 (2013).
- Mura, S., Nicolas, J. & Couvreur, P. Stimuli-responsive nanocarriers for drug delivery. *Nat. Mater.* **12**, 991–1003 (2013).
- Zauner, W., Farrow, N. a. & Haines, a. M. *In vitro* uptake of polystyrene microspheres: effect of particle size, cell line and cell density. *J. Control. Release* **71**, 39–51 (2001).
- Rejman, J., Oberle, V., Zuhorn, I. S. & Hoekstra, D. Size-dependent internalization of particles via the pathways of clathrin- and caveolae-mediated endocytosis. *Biochem. J.* **377**, 159–69 (2004).
- Pacheco, P., White, D. & Sulchek, T. Effects of microparticle size and Fc density on macrophage phagocytosis. *PLoS One* **8**, e60989 (2013).
- Shang, L., Nienhaus, K. & Nienhaus, G. U. Engineered nanoparticles interacting with cells: size matters. *J. Nanobiotechnology* **12**, 5 (2014).
- Barua, S. *et al.* Particle shape enhances specificity of antibody-displaying nanoparticles. *Proc. Natl. Acad. Sci. USA* **110**, 3270–5 (2013).
- Gratton, S. E. a. *et al.* The effect of particle design on cellular internalization pathways. *Proc. Natl. Acad. Sci. USA* **105**, 11613–8 (2008).
- Saha, K. *et al.* Surface functionality of nanoparticles determines cellular uptake mechanisms in mammalian cells. *Small* **9**, 300–5 (2013).

19. Dausend, J. *et al.* Uptake mechanism of oppositely charged fluorescent nanoparticles in HeLa cells. *Macromol. Biosci.* **8**, 1135–43 (2008).
20. Fröhlich, E. The role of surface charge in cellular uptake and cytotoxicity of medical nanoparticles. *Int. J. Nanomedicine* **7**, 5577–91 (2012).
21. Thiele, L., Merkle, H. P. & Walter, E. Phagocytosis and phagosomal fate of surface-modified microparticles in dendritic cells and macrophages. *Pharm. Res.* **20**, 221–8 (2003).
22. Harush-Frenkel, O., Debotton, N., Benita, S. & Altschuler, Y. Targeting of nanoparticles to the clathrin-mediated endocytic pathway. *Biochem. Biophys. Res. Commun.* **353**, 26–32 (2007).
23. Patiño, T., Nogués, C., Ibañez, E. & Barrios, L. Enhancing microparticle internalization by nonphagocytic cells through the use of noncovalently conjugated polyethyleneimine. *Int. J. Nanomedicine* **7**, 5671–5682 (2012).
24. Bousif, O. *et al.* A versatile vector for gene and oligonucleotide transfer into cells in culture and *in vivo*: polyethyleneimine. *Proc. Natl. Acad. Sci.* **92**, 7297–7301 (1995).
25. Yu, J.-H., Quan, J.-S., Huang, J., Nah, J.-W. & Cho, C.-S. Degradable poly(amino ester) based on poly(ethylene glycol) dimethacrylate and polyethyleneimine as a gene carrier: molecular weight of PEI affects transfection efficiency. *J. Mater. Sci. Mater. Med.* **20**, 2501–10 (2009).
26. Xiao, Y. *et al.* Dynamics and mechanisms of quantum dot nanoparticle cellular uptake. *J. Nanobiotechnology* **8**, 13 (2010).
27. Oliveira, S., Heukers, R., Sornkom, J., Kok, R. J. & van Bergen En Henegouwen, P. M. P. Targeting tumors with nanobodies for cancer imaging and therapy. *J. Control. Release* **172**, 607–617 (2013).
28. Patino, T. *et al.* Multifunctional gold nanorods for selective plasmonic photothermal therapy in pancreatic cancer cells using ultra-short pulse near-infrared laser irradiation. *Nanoscale* **7**, 5328–5337 (2015).
29. Connot, J. *et al.* Cancer immunotherapy: nanodelivery approaches for immune cell targeting and tracking. *Front. Chem.* **2**, 105 (2014).
30. Loureiro, J. A., Gomes, B., Coelho, M. A. N., do Carmo Pereira, M. & Rocha, S. Targeting nanoparticles across the blood-brain barrier with monoclonal antibodies. *Nanomedicine (Lond)* **9**, 709–722 (2014).
31. Ferrati, S. *et al.* Inter-endothelial transport of microvectors using cellular shuttles and tunneling nanotubes. *Small* **8**, 3151–60 (2012).
32. Palankar, R. *et al.* Controlled intracellular release of peptides from microcapsules enhances antigen presentation on MHC class I molecules. *Small* **5**, 2168–76 (2009).
33. Sukhorukov, G. B. *et al.* Multifunctionalized polymer microcapsules: novel tools for biological and pharmacological applications. *Small* **3**, 944–955 (2007).
34. Delcea, M. *et al.* Multicompartmental Micro- and Nanocapsules: Hierarchy and Applications in Biosciences. *Macromol. Biosci.* **10**, 465–474 (2010).
35. Salonen, J. *et al.* Mesoporous silicon microparticles for oral drug delivery: Loading and release of five model drugs. *J. Control. Release* **108**, 362–374 (2005).
36. Skandrani, N. *et al.* Lipid nanocapsules functionalized with polyethyleneimine for plasmid DNA and drug co-delivery and cell imaging. *Nanoscale* **6**, 7379–90 (2014).
37. Kasturi, S. P., Sachaphibulkij, K. & Roy, K. Covalent conjugation of polyethyleneimine on biodegradable microparticles for delivery of plasmid DNA vaccines. *Biomaterials* **26**, 6375–6385 (2005).
38. Ateh, D. D. *et al.* The intracellular uptake of CD95 modified paclitaxel-loaded poly(lactic-co-glycolic acid) microparticles. *Biomaterials* **32**, 8538–47 (2011).
39. McBain, S. C., Yiu, H. H. P., El Haj, a. & Dobson, J. Polyethyleneimine functionalized iron oxide nanoparticles as agents for DNA delivery and transfection. *J. Mater. Chem.* **17**, 2561 (2007).
40. Neu, M., Fischer, D. & Kissel, T. Recent advances in rational gene transfer vector design based on poly(ethylene imine) and its derivatives. *J. Gene Med.* **7**, 992–1009 (2005).
41. Qiu, Y. *et al.* Surface chemistry and aspect ratio mediated cellular uptake of Au nanorods. *Biomaterials* **31**, 7606–19 (2010).
42. Wang, F. *et al.* The biomolecular corona is retained during nanoparticle uptake and protects the cells from the damage induced by cationic nanoparticles until degraded in the lysosomes. *Nanomedicine* **9**, 1159–68 (2013).
43. Yan, Y. *et al.* Differential roles of the protein corona in the cellular uptake of nanoporous polymer particles by monocyte and macrophage cell lines. *ACS Nano* **7**, 10960–70 (2013).
44. Macia, E. *et al.* Dynasore, a cell-permeable inhibitor of dynamin. *Dev. Cell* **10**, 839–50 (2006).
45. Barr, D. J., Ostermeyer-Fay, A. G., Matundan, R. A. & Brown, D. A. Clathrin-independent endocytosis of ErbB2 in geldanamycin-treated human breast cancer cells. *J. Cell Sci.* **121**, 3155–3166 (2008).
46. Vaidyanath, A. *et al.* Enhanced internalization of ErbB2 in SK-BR-3 cells with multivalent forms of an artificial ligand. *J. Cell. Mol. Med.* **15**, 2525–2538 (2011).
47. Lim, J. P. & Gleeson, P. A. Macropinocytosis: an endocytic pathway for internalising large gulps. *Immunol. Cell Biol.* **89**, 836–843 (2011).
48. Bousif, O. *et al.* A versatile vector for gene and oligonucleotide transfer into cells in culture and *in vivo*: Polyethyleneimine. **92**, 7297–7301 (1995).

Acknowledgements

This study was supported by grants from the *Ministerio de Ciencia e Innovación* (TEC2011-29140-C03), and the *Generalitat de Catalunya* (2014SGR-524) and the AGAUR FI-DGR 2013. The authors wish to thank the *Unitat de Citometria de Flux* and the *Servei de Microscòpia* at the *Universitat Autònoma de Barcelona* and Antonio Aranda for the help in drawing schematics.

Author Contributions

T.P., J.S., L.B., E.I. and C.N. designed the experiments. T.P. and J.S. performed the experiments. T.P. and L.B. performed the statistical analyses. C.N., L.B. and E.I. supervised the experiments. T.P. and C.N. wrote the manuscript. All authors critically revised the manuscript and approved the final version.

Additional Information

Supplementary information accompanies this paper at <http://www.nature.com/srep>

Competing financial interests: The authors declare no competing financial interests.

How to cite this article: Patiño, T. *et al.* Surface modification of microparticles causes differential uptake responses in normal and tumoral human breast epithelial cells. *Sci. Rep.* **5**, 11371; doi: 10.1038/srep11371 (2015).



This work is licensed under a Creative Commons Attribution 4.0 International License. The images or other third party material in this article are included in the article's Creative Commons license, unless indicated otherwise in the credit line; if the material is not included under the Creative Commons license, users will need to obtain permission from the license holder to reproduce the material. To view a copy of this license, visit <http://creativecommons.org/licenses/by/4.0/>

3.3

**Polysilicon-chromium-gold
intracellular chips for
multi-functional applications**

Title

Polysilicon-chromium-gold intracellular chips for multi-functional applications

Authors

Tania Patiño¹, Jorge Soriano¹, Ezhil², Sara Durán³, Oriol Penon², Marta Duch³, Elena Ibañez¹, Leonardo Barrios¹, Jose Antonio Plaza³, Luisa Pérez-García², Carme Nogués^{1*}.

Affiliation

1. Unitat de Biologia Cel·lular, Departament de Biologia Cel·lular, de Fisiologia i d'Immunologia. Facultat de Biociències. Universitat Autònoma de Barcelona, 08139 Bellaterra, Spain.
2. Departament de Farmacologia i Química Terapèutica and Institut de Nanociència i Nanotecnologia (IN2UB), Universitat de Barcelona, Avda. Joan XXIII s/n, 08028, Barcelona, Spain.
3. Instituto de Microelectrónica de Barcelona, IMB-CNM (CSIC), Campus UAB, 08193, Cerdanyola, Barcelona, Spain.

Correspondence

*Carme Nogués Sanmiquel

Unitat de Biologia Cel·lular, Departament de Biologia Cel·lular, de Fisiologia i d'Immunologia, Facultat de Biociències.

Edifici C, Campus de Bellaterra

Universitat Autònoma de Barcelona

08193 Bellaterra, Spain

Phone: +34 93 581 2667

E-mail: carme.nogues@uab.cat

Abstract

Micro- and nanotechnology is a continuously growing field, which has allowed the creation of a wide number of micro- and nanosystems for their use in biomedical applications. One of the major goals of such platforms is to combine multiple functions in a single entity. However, achieving the design of an efficient and safe micro- or nanoplatform has shown to be strongly influenced by its interaction with the biological systems, where particle features or cell type play a critical role. In this work, we explored the feasibility of using multi-material pSi-Cr-Au intracellular chips (MMICCs) for multifunctional applications by characterizing their interactions with two different cell lines, one tumorigenic (SKBR-3) and one non-tumorigenic (MCF-10A), in terms of biocompatibility, internalization and intracellular fate. Moreover, we analysed the impact of MMICCs on the induction of an inflammatory response by evaluating $\text{TNF}\alpha$, $\text{IL1}\beta$, IL6, and IL10 human inflammatory cytokines secretion by macrophages. Results showed that MMICCs were biocompatible and their internalization efficiency was strongly dependent on the cell type. Moreover, no cytokine secretion was observed. Finally as a proof-of-concept, MMICCs were dually functionalized with transferrin and pHrodo® to target cancer cells and detect intracellular pH, respectively. In conclusion, MMICCs showed promising results for their use as multi-functional devices, as they showed high biocompatible and non-inflammatory properties, as well as the ability of developing multiple functions.

Introduction

The fast development of micro- and nanotechnologies in recent years has opened new and promising avenues to overcome some of the limitations of classical diagnostics and therapeutic medical approaches¹⁻³. Fabrication of micro- and nanoplatforms for biomedical applications can be achieved by either “bottom-up” or “top-down” synthetic strategies⁴. In “bottom-up” approaches, drug delivery tools are assembled from the molecular scale, by manipulating their chemical and physical properties, whereas “top-down” approaches are based on the adaptation of semiconductor industry microfabrication techniques such as lithography⁵.

Despite having received less attention in the biomedical field, the use of “top-down” based microfabrication techniques for the development of micro-electromechanical systems (MEMs) have shown a great potential for several applications such as drug delivery⁶⁻⁹, controlled-release¹⁰⁻¹² and diagnostics¹³. Moreover, the miniaturization of biological microelectromechanical system (BioMEMs) through combining microfabrication and nanotechnology techniques has allowed the creation of small silicon-based chips, which may be internalized by cells^{14,15} and are able to detect intracellular parameters such as pH¹⁶ or pressure¹⁷. In this regard, “top-down” microfabrication techniques offer some advantages over “bottom-up” approaches, such as a highly precise control upon the size, shape and monodispersity of the particles¹. This is of special relevance, as particle shape and size have been proven to play a key role in the interaction of micro- and nanodevices with biological systems¹⁸⁻²³. One step forward in the biomedical application of such devices would consist of combining diagnostic and therapeutic functions, since this is a main challenge for nanomedicine²⁴⁻²⁶. In this regard, we have recently demonstrated that the use of multi-material devices is an interesting approach for multifunctional purposes, as it provides a precise control over functionalized molecules location by using orthogonal chemistry²⁷. In contrast, other techniques such as the self-assembly approach, result in a disordered mixture of monolayers due to the coadsorption of the different components²⁸.

On the other hand, despite the encouraging outcomes from the use of micro- and nanoengineered platforms for intracellular applications, a deeper understanding of particle-cell interactions has become increasingly important in order to develop efficient and safe micro- and nanoplatfoms²⁹. In this sense, it has been shown that several features of particle design, such as size^{19,20,30-32}, shape^{22,33} and surface properties³⁴⁻³⁶, play a critical role in several biological parameters, such as uptake efficiency, internalisation or cytotoxicity. In addition, the biological responses to a specific type of particle are closely related to the cell type, as different cell types have shown to respond differently to a certain particle feature³⁷⁻³⁹.

In the present work, we aimed to investigate the feasibility of multi-material silicon chips for their use as multi-functional intracellular devices. With this purpose, we first characterized the biological interactions between multi-material polysilicon-Cr-Au intracellular chips (MMICCs) and two human breast epithelial cell types, the adenocarcinoma derived SKBR-3 and non-tumorigenic MCF-10A cells, in terms of biocompatibility, uptake and intracellular location. Second, we evaluated whether MMICCs induced an inflammatory response in THP-1 cell-derived macrophages. Finally, we used two different functionalization approaches, taking advantage of the multi-material nature of the chips, in order to render the MMICCs multifunctional. On the one hand, we functionalized the polysilicon layer with fluorescein-conjugated transferrin (Tf-FITC) in order to target the tumor-derived SKBR-3 cells, as transferrin receptor has shown to be overexpressed in most types of cancer cells⁴⁰⁻⁴². On the other hand, we functionalized the Au layer with pHrodo[®] in order to detect intracellular pH.

Material and methods

Fabrication and characterization of MMICCs

MMICCs were synthesized through photolithographic techniques combined with silicon microelectronic and micromachining technologies, as previously described²⁷. Once collected, MMICCs were stored at room temperature (RT) until used in further experiments.

In order to characterize size, shape and material composition, MMICCs were evaluated under a scanning electron microscope (SEM) (Carl Zeiss Merlin-Microscope GmbH) equipped with an Energy Dispersive-X-ray spectroscope (EDX).

Cell culture

Cell uptake and cytotoxicity studies were conducted using two different non-phagocytic human mammary epithelial cell lines. One of these cell lines was non-tumorigenic (MCF-10A), whereas the other had a tumoral origin (SKBR-3). MCF-10A cells were cultured in DMEM/F12 (Gibco) supplemented with 5% horse serum (Gibco), 20 ng·mL⁻¹ epidermal growth factor (Gibco), 0.5 mg·mL⁻¹ hydrocortisone (Sigma-Aldrich), 100 ng·mL⁻¹ cholera toxin (Sigma-Aldrich) and 10 µg/mL⁻¹ insulin (Gibco). Adenocarcinoma SKBR-3 cells were cultured in McCoy's 5A modified medium (Gibco) supplemented with 10% fetal bovine serum (FBS, Gibco).

Analysis of inflammatory cytokines secretion was conducted using macrophages derived from the human leukemia monocyte THP-1 cell line. THP-1 cells were cultured in RPMI 1640 medium (Gibco) supplemented with 20% FBS (Gibco). To differentiate THP-1 monocytes into macrophages, cells were seeded in 96-multiwell plates at a density of 60,000 cells/well and treated with 0.16 µM phorbol-12-myristate-13-acetate (Sigma) for 72 h.

All cell lines were purchased from ATCC and maintained at 37°C and 5% CO₂ (standard conditions). Culture medium was refreshed every 72 h.

Analysis of MMICCs uptake by scanning electron and confocal microscopy

Evaluation of MMICCs uptake was first carried out by SEM. Cells were seeded in 3.5-mm diameter glass bottom dishes (MatTEK) at a density of 1.5×10^5 cells/dish. At 24 h, MMICCs were added to culture medium at a particle:cell ratio of 5:1. Cells were incubated with MMICCs for either 4 or 24 h. Then, cells were fixed in 2.5% glutaraldehyde in cacodylate buffer, dehydrated in an ethanol series, dried with hexamethyl disilazane (Electron Microscopy Sciences) for 15 min and observed under a SEM (Carl Zeiss Merlin).

To further study and quantify MMICCs uptake, cells were seeded on glass coverslips in 24-well plates, at a density of 50,000 cells/well. After 24 h, MMICCs were added to the cell culture at a particle:cell ratio of 5:1. At 24 h of incubation, cells were fixed with 4% paraformaldehyde (PFA) in phosphate buffered saline (PBS) for 20 min and blocked for 40 min with 1% bovine serum albumin (BSA, Sigma-Aldrich) in PBS. Cells were subsequently stained with Texas Red[®]-conjugated phalloidin (TR-Phal; $10 \mu\text{g}\cdot\text{mL}^{-1}$; Life Technologies) and counterstained with Hoescht 33258 ($1 \mu\text{g}\cdot\text{mL}^{-1}$; Sigma-Aldrich) to visualize the cell cortex and the nucleus, respectively. Then, samples were washed thrice in PBS for 5 min, air dried and mounted using Fluoroprep solution (Biomerieux). Mounted samples were observed under a confocal laser scanning microscope (CLSM, Olympus XT7) using a 60X oil immersion objective.

For the detection of TR-Phal, excitation and emission wavelengths of 559 nm and 590 nm, respectively, were used. Excitation and emission wavelengths for Hoescht 33258 were 405 nm and 461 nm, respectively. MMICCs were visualized by detecting the reflected light using an excitation wavelength of 488 nm. Z-stacks were obtained by x-y-z sequential acquisition and orthogonal projections of the stacks were analysed to determine the location of MMICCs within the cell. For image analysis, the FV10-ASW Application Software (Ver. 01.07c; Olympus) was used. For each experiment, 200 cells per cell type were analysed and three independent experiments were performed.

Cytotoxicity analyses

Cells were seeded in 24-well dishes at a density of 50,000 cells/well and were allowed to grow for 24 hours. Then, MMICCs were added to cell culture at a particle:cell ratio of 5:1. After 24 and 72 hours of incubation, the viability of cells was evaluated using the Vybrant MTT Cell Proliferation Assay Kit (Molecular Probes), according to the manufacturer's instructions. Briefly, culture medium was replaced by 200 μ L of fresh culture medium containing 20 μ L of MTT stock solution (12 mM). After incubation at 37°C and 5% CO₂ for 2 hours, the medium was removed and formazan crystals were dissolved by adding 200 μ L of dimethyl sulfoxide (Sigma-Aldrich). Cells were incubated for 10 min at 37°C and 5% CO₂ for the complete solubilisation of formazan crystals. Then, the measurement of absorbance was conducted at 570 nm using a Victor 3 Multilabel counter (PerkinElmer). For each treatment, viability was calculated as the absorbance of cells exposed to MMICCs divided by the absorbance of non-exposed, control cells. Three independent experiments were performed.

Immunodetection of actin cytoskeleton and focal adhesions

Cells were seeded on glass coverslips in 4-well dishes at a density of 50,000 cells/well. After 24 hours, MMICCs at a particle:cell ratio of 5:1 were added to cell culture. At 4 and 24 hours of co-incubation, cells were fixed with 4% PFA in PBS for 20 minutes, subsequently permeabilised with 0.1% Triton X-100 (Sigma) in PBS for 15 minutes, and blocked with 5% BSA in PBS for 40 min. To visualize focal adhesions, samples were incubated with a mouse anti-vinculin antibody (Chemicon) for 60 minutes at RT. Next, samples were rinsed in PBS and incubated with a mixture of Alexa Fluor®594-conjugated Phalloidin (Invitrogen), Alexa Fluor®488 goat anti-mouse IgG secondary antibody (Invitrogen) and Hoechst 33258 (Sigma-Aldrich) at RT for 1 hour. Finally, samples were washed thrice in PBS for 5 minutes, air dried, and mounted using Fluoroprep solution (Biomerieux). Samples were imaged under a CLSM.

Immunodetection of endosomes and lysosomes

Cells were seeded on glass coverslips in 4-well dishes, at a density of 50,000 cells/well. After 24 h, MMICCs at a 5:1 particle:cell ratio were added to the culture, in serum free medium. At 24 h of incubation, cells were fixed with 4% PFA in PBS for 20 min, permeabilized with 0.1% Triton X-100 in PBS for 15 min and blocked for 40 min with 5% BSA in PBS. Endosomes and lysosomes were stained by incubating cells with a mouse anti-EEA-1 monoclonal antibody or a mouse anti-LAMP-1 polyclonal antibody (both from BD Biosciences), respectively. Following this, cells were washed thrice with PBS and incubated with an Alexa Fluor® 488-conjugated chicken anti-mouse IgG antibody (Life technologies). At the same time, cytocortex was labelled with TR-Phal at RT for 1 h. Cells were observed under a CLSM in order to determine the intracellular location of MMICCs.

Inflammatory cytokines secretion analysis

To study the possible induction of an inflammatory response by MMICCs, the human inflammatory cytokines (i.e. $\text{TNF}\alpha$, $\text{IL1}\beta$, IL6, IL10) profile released by macrophages was analysed using a flow cytometry bead array (CBA, Becton-Dickinson). Briefly, cells were seeded and differentiated as detailed in the cell culture section. After 72 h of differentiation, cells were exposed to MMICCs at a particle:cell ratio of 2:1. As a positive control, lipopolysaccharide (LPS; Sigma-Aldrich) was added to the culture medium at a final concentration of $1 \mu\text{g}\cdot\text{mL}^{-1}$. As a negative control, macrophages cultured in the absence of both MMICC and LPS. After 5 or 24 h of incubation, the supernatants of the cell cultures were collected and analyzed using a Becton-Dickinson FACSCanto II flow cytometer (BD Biosciences) equipped with BD Biosciences FACSDiva™ software. Three independent experiments were carried out.

Functionalisation of MMICCs with Tf-FITC and pHrodo®

MMICCs were orthogonally functionalized as previously described²⁷. Briefly, polysilicon was oxidized through piranha solution $\text{H}_2\text{SO}_4:\text{H}_2\text{O}_2$ (7:3) for 1 h. Then, MMICCs were washed thrice in MiliQ water by centrifugation (13,000

rpm, 5 min). Next, MMICCs were incubated with an ethanol solution of 8 mM mercaptoundecanoate-NHS for 3 h and washed thrice with ethanol by centrifugation. Then, a PBS solution of Tf-FITC (Invitrogen) was added to the MMICCs suspension and the mixture was maintained at RT overnight. Next, MMICCs were washed by centrifugation as aforementioned, and a mixture of 135 mM 11-(Triethoxysilyl)undecanal in ethanol and acetic buffer (pH 5.2) was added to the MMICCs suspension and incubated for 3 h at RT. MMICCs were then washed by centrifugation and air-dried. Following this, a PBS solution containing pHrodo® (Invitrogen) and 5 mM sodium cyanoborohydride was added to the MMICCs suspension. The mixture was kept at 4°C overnight. Finally, bi-functionalised MMICCs were washed by centrifugation and kept in water until their use.

Statistical analyses

All statistical analyses were conducted using a statistical package (IBM® SPSS® for Windows, Ver. 21.0; IBM Corp.). In all cases, data were first tested for normality (Shapiro-Wilk test) and homogeneity of variances (Levene test) and, when required, transformed through arcsine square-root transformation.

On the one hand, the cytotoxic effects of exposing SKBR-3 and MCF-10A cells to MMICCs were evaluated through a repeated measures analysis of variance (ANOVA), where the MTT assay outcome was the variable, the treatment (presence or absence of MMICCS) was the between-subjects factor and the incubation time (24 or 72 h) was the within-subjects factor.

On the other hand, percentages of MMICCs uptaken by SKBR-3 and MCF-10A cells were compared through a *t*-test for independent samples.

Finally, the effects of co-incubating MMICCs with macrophages derived from THP-1 monocytes on the cytokine profile were evaluated with repeated measures ANOVA, followed by a Sidak post-hoc test. In each case, the individual cytokine was the variable, the treatment (with MMICCs, negative control and positive control, with LPS) was the between-subjects factor and the incubation time (5 or 24 h) was the within-subjects factor.

In all cases, the minimal significance level was set at $P \leq 0.05$. Data are shown as mean \pm standard error of the mean (SEM).

Results

Characterization of MMICCs

FIGURE 1A shows the MMICCs design. MMICCs have a square shape of $3\ \mu\text{m}$ x $3\ \mu\text{m}$ in length and width and $0.5\ \mu\text{m}$ of thickness, being 0.1 , 0.03 and $0.4\ \mu\text{m}$ -thick the gold, chromium and polysilicon layers, respectively. SEM images showed that MMICCs were successfully synthesized, as the three different layers were observed (FIG. 1B). The different layers could be easily distinguished by the variation of surface roughness, being the gold layer rougher than the polysilicon one. The internal Cr layer was not visible under SEM due to its internal location as well as its extremely low thickness. However, EDX analyses demonstrated that the three materials, Si, Au and Cr, were present in the MMICCs, since the corresponding peaks for these elements were observed (FIG. 1C).

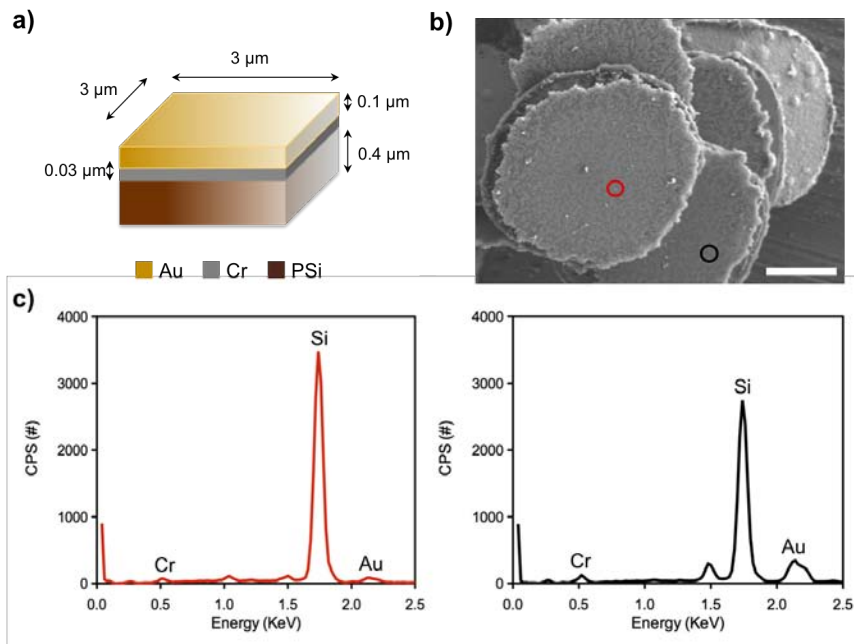


FIGURE 1. Design and characterisation of MMICCs. a) Schematic representation of the design of MMICCs, where the dimensions and thickness of the different material layers are specified. b) SEM image of MMICCs, where the actual size and material composition can be observed. Red and black circles indicate the areas where the EDX analysis was performed. Scale bar = $1\ \mu\text{m}$. c) EDX spectrum confirming the presence of Si, Au and Cr.

Uptake of MMICCs by SKBR-3 and MCF-10A cells

A qualitative assessment of MMICCs uptake was carried out by SEM imaging, after 4 and 24 h of co-incubation. Both in SKBR-3 and MCF-10A lines, cells showed an active uptake of MMICCs, as a membrane evagination surrounding MMICCs was observed (FIG. 2). In addition, in some cases, a cell protrusion was observed, indicating that chips were completely internalized (FIG. 2, arrow).

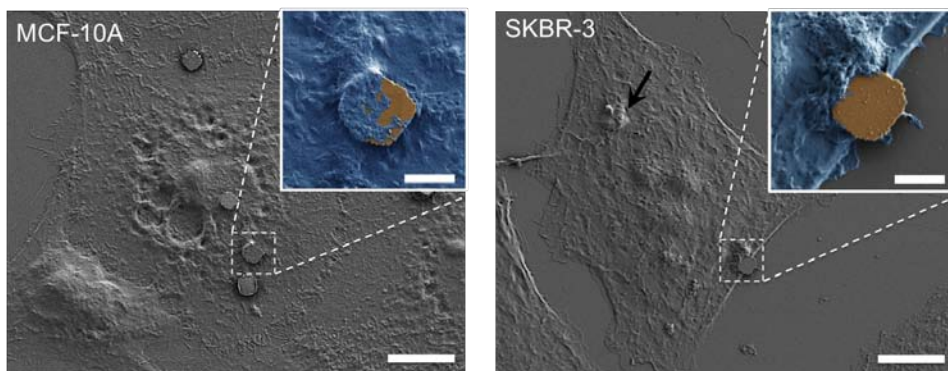


FIGURE 2. Evaluation of MMICCs internalization by SEM. Images show that MMICCs were actively uptaken by cells, as the plasma membrane was observed in the process of surrounding MMICCs in both cell lines. Arrow points a completely internalized MMICCs. Scale bar=10 μm . Insets show a magnification of the selected area, artificially coloured for a better visualization of the plasma membrane. Scale bar=2 μm .

In order to further confirm that chips had been completely internalized and to quantify MMICCs uptake, CLSM imaging was also performed (FIG. 3). Confocal analysis showed that the number of MMICCs associated with cells was higher in MCF-10A than in SKBR-3 cells (FIG. 3A-B). In order to determine whether MMICCs had been internalized by cells, orthogonal projections of z-stack reconstruction of consecutive focal planes (0.4- μm each) were analysed (FIG. 3C-D). Two hundred cells were analysed for each cell line in three independent experiments. Results showed that MMICCs internalization efficiency was significantly ($P<0.001$) higher in MCF-10A cells than in SKBR-3 cells (FIG. 3E). Moreover, confocal imaging allowed to precisely determine the number of particles internalized per cell, in both cell lines (FIG. 3F).

In this regard, it was shown that the majority of MCF-10A cells internalized more than one MMICCs, whereas in the case of SKBR-3 the majority of cells internalized only one MMICC.

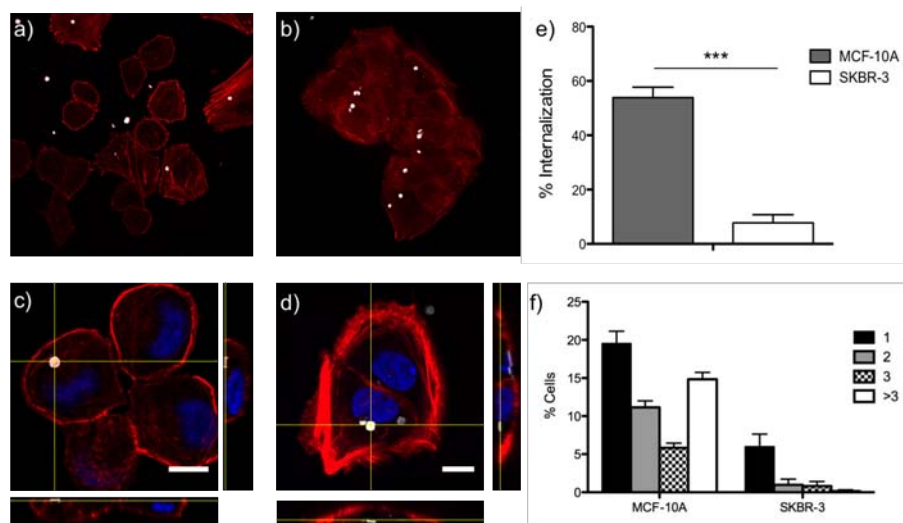


FIGURE 3. Quantitative analysis of MMICCs uptake by CLSM. a)-d) Images show SKBR-3 and MCF-10A cells, respectively, after 24 h incubation with MMICCs. Actin filaments were stained with Texas Red[®] Phalloidin (red) and cell nuclei were stained with Hoescht 33258 (blue). MMICCs were imaged by using the reflection mode. Scale bar=10 μ m. c),d) Orthogonal views of reconstructed z-stacks of SKBR-3 (c) and MCF-10A (d) cells. Scale bar=10 μ m. e) Percentage of cells that had internalized at least one MMICC. f) Distribution of cell populations according to the number of particles internalized per cell. Results are shown as the mean \pm SEM. Asterisks (***) indicate significant differences between both cell lines ($P=0.001$)

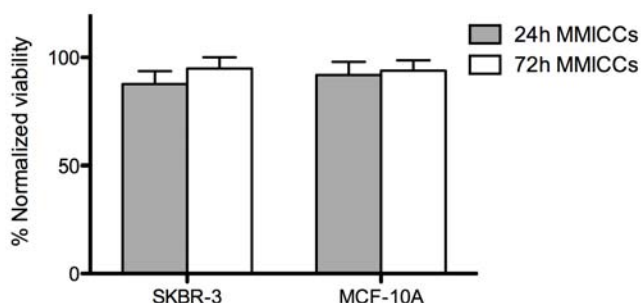


FIGURE 4. Effect of MMICCs on cell viability. The cytotoxic effect of MMICCs was evaluated by using the MTT cell proliferation assay at 24 and 72 h of cells incubation with MMICCs. Results were normalized to control cells and are shown as the mean \pm SEM of three independent experiments.

Cytotoxicity of MMICCs

The percentage of viable cells in three independent experiments was assessed at both 24 and 72 h after incubation with the MMICCs (FIG. 4). Results showed that MMICCs did not affect cell viability, as a high percentage of viable cells (>80%) was observed in both cell lines at both time points. Moreover, no significant differences were observed between cell lines, indicating that MMICCs were not cytotoxic for any of the cell types.

Effect of internalized MMICCs on cell morphology and adhesion

To verify whether internalization of MMICCs could affect cell morphology or focal contacts, actin cytoskeleton and vinculin were stained, respectively. The morphology and actin cytoskeleton structure of control MCF-10A and SKBR-3 cells was observed to be different. However, when cells with internalized MMICCs and cells without MMICCs were compared, no differences in the distribution of actin filaments and focal contacts were observed for any of the two cell lines (FIG. 5).

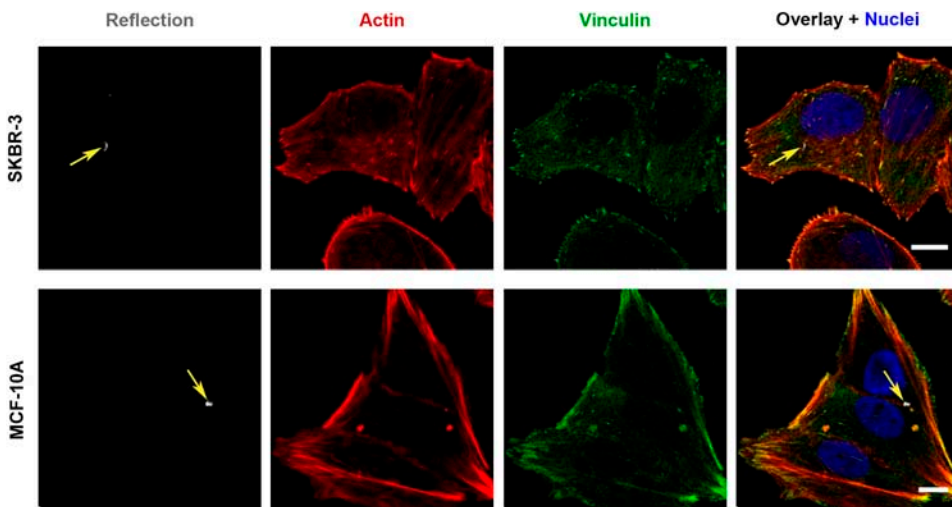


FIGURE 5. Actin cytoskeleton organization and focal contacts in cells with or without MMICCs. Images show a single slice from a z-stack, where the MMICCs are observed in gray, actin fibers are shown in red, focal contacts in green and nuclei in blue. Arrows indicate the internalized MMICC. Scale bar=10 μ m

Intracellular location of MMICCs

The evaluation of intracellular location of MMICCs was performed only in MCF-10A cells, as they showed a higher internalization rate than SKBR-3 cells. Immunolocalization of EEA-1 (endosomal compartment) and LAMP-1 (lysosomal compartment) proteins was carried out separately. After 24 h of incubation, MMICCs could be found in any of the two compartments (FIG. 6).

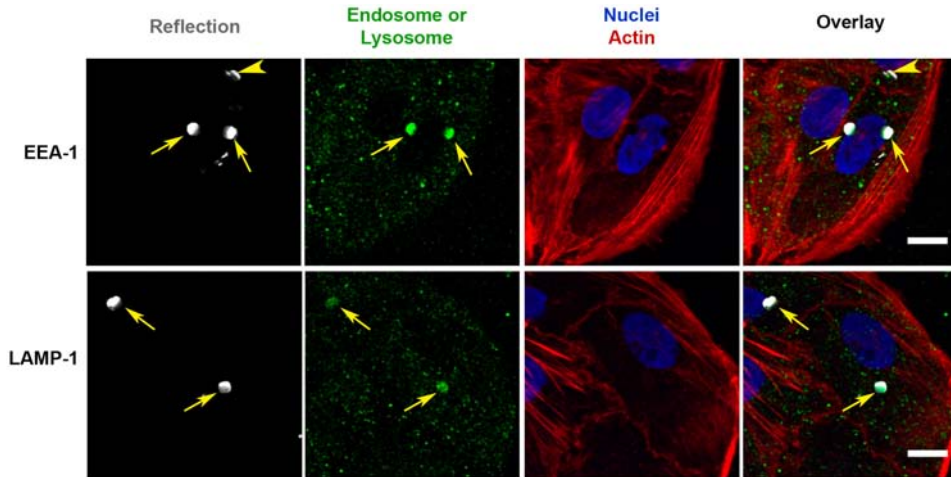


FIGURE 6. CLSM analyses of MMICCs intracellular location in MCF-10A cells. In order to label the endosomal and lysosomal compartments, immunofluorescence detection of EEA-1 and LAMP-1 markers, respectively, was performed (green). Cell nuclei were stained with Hoechst 33258 (blue) and actin cytoskeleton was stained with Texas Red[®] Phalloidin (red). MMICCs were visualized by reflection (gray). Arrows indicate MMICCs located inside the endosomal or lysosomal compartments. Arrowhead indicates one chip that is not located inside the endosomal compartment. Scale bar = 10 μ m.

Induction of inflammatory cytokine secretion

To assess whether MMICCs could trigger an inflammatory response, we analysed the release of four different human inflammatory cytokines, IL-1 β , IL-10, IL-6 and TNF- α by macrophages (FIG. 7). Macrophages incubated with LPS (positive control) showed a significant ($P < 0.05$) increase of cytokine release when compared with the negative control. By contrast, macrophages incubated with MMICCs did not trigger an increased release of any of the studied inflammatory cytokines with respect to the negative control cells.

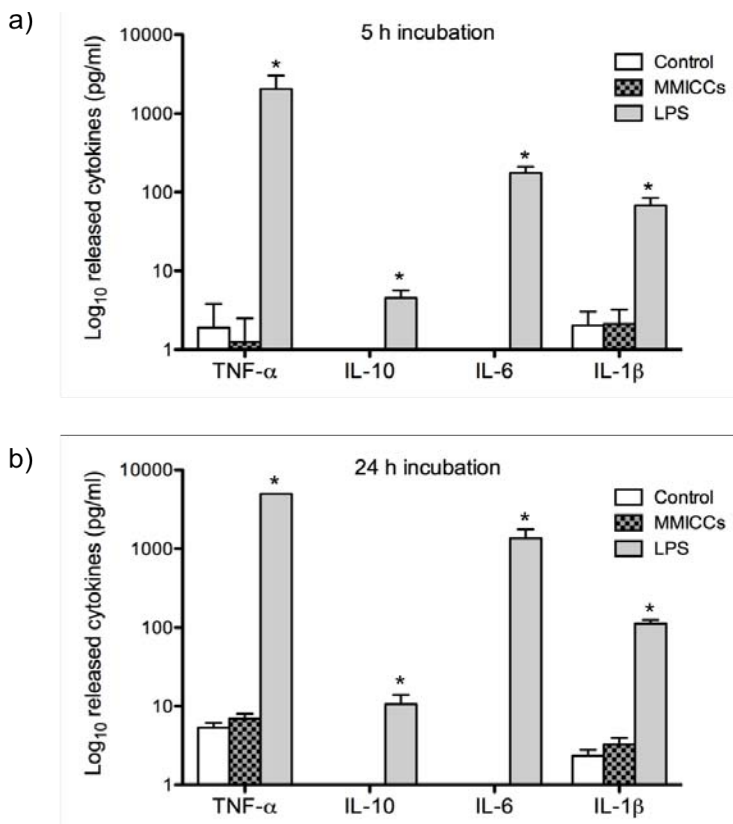


FIGURE 7. Evaluation of MMICCs induction of human inflammatory cytokines secretion by macrophages, analysed by flow cytometry. Quantification of human inflammatory cytokines was performed either 5 h (a) or 24 h (b) of MMICCs incubation with macrophages. Macrophages incubated in the absence of MMICCs (control) or in the presence of LPS acted as a negative and positive controls, respectively. Results are shown as the mean \pm SEM of three independent experiments. Asterisks indicate significant differences ($P < 0.05$) among groups (i.e. control, MMICCs or LPS).

Transferrin receptor targeting and pH detection with multi-functional MMICCs

In order to render MMICCs multifunctional, they were functionalized with both Tf-FITC and pHrodo[®] (FIG. 8A). The number of cells with internalized particles increased after functionalization of MMICCs with Tf-FITC in both SKBR-3 and MCF-10A cell lines, but the extent of the increase was higher in the former than in the latter (FIG. 8B).

In the case of pHrodo[®], red fluorescence indicated that MMICCs were located inside an acidic compartment, such as a lysosome or an endosome (FIG. 8C-E).

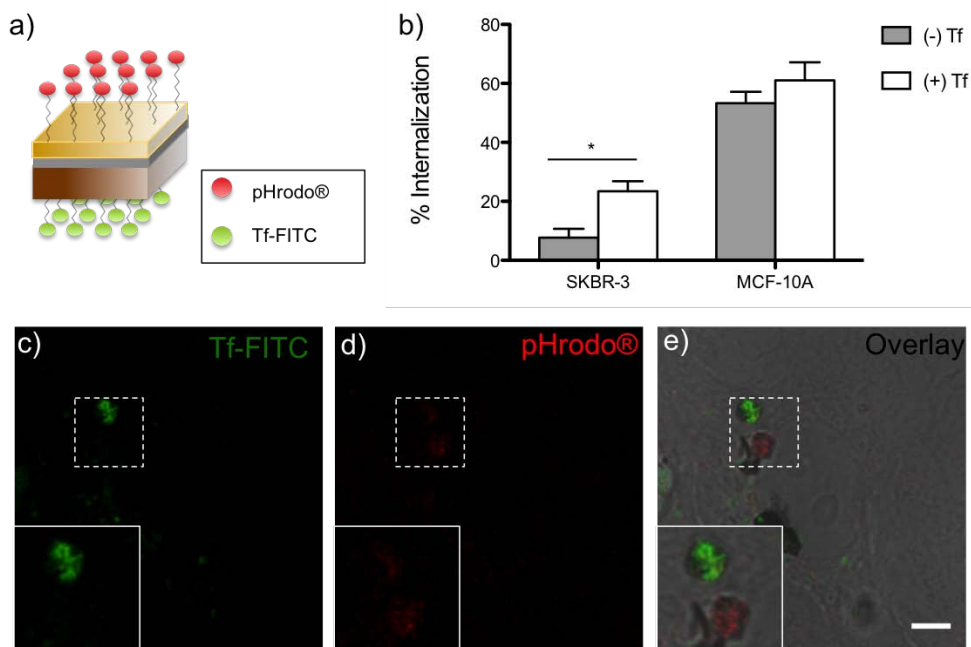


FIGURE 8. Evaluation of bi-functionalized Tf-FITC/pHrodo® MMICCs. a) Schematic representation of surface modifications of MMICCs. b) Percentage of cells with at least one internalized MMICC, either functionalized (+Tf) or not (-Tf). Results are shown as the mean \pm SEM. Asterisk indicates significant differences between groups. c)-e) CSLM images showing a MCF-10A cell with internalized Tf-FITC/pHrodo® MMICCs. Scale bar=10 μ m. Insets show a magnification of the selected area.

Discussion

The fast advances in micro- and nanotechnologies in recent years have led to exciting outcomes regarding their application in the biomedical field^{1,2,43}. However, despite BioMEMs having excellent and controllable physico-chemical properties for biomedical applications, a deeper understanding of their interaction with cells is required in order to improve their safety and effectiveness²⁹. In the present study, we assessed the biological interactions of 3- μm multi-material pSi-Cr-Au chips with tumorigenic SKBR-3 and non-tumorigenic MCF-10A human breast epithelial cells. First, we characterized the size and composition of MMICCs by SEM and EDX analyses, respectively. Results showed that top-down microfabrication approach is very efficient in terms of producing highly homogeneous size, shape and monodispersed MMICCs, as it was expected¹.

Although we previously reported that MMICCs could be internalized by macrophages²⁷, non-phagocytic cells have shown to internalize large particles with lower efficiency^{20,44}. In addition, we have demonstrated that the uptake of micron-sized polystyrene particles is cell line dependent⁴⁵. Thus, we investigated whether the MMICCs could be uptaken by two different types of non-phagocytic cell lines, one tumoral (SKBR-3) and another non-tumoral (MCF-10A). Although SEM analyses revealed that both cell lines could actively take up MMICCs, internalisation analysis using CLSM showed that SKBR-3 cells had a low capacity of internalizing MMICCs than MCF-10A cells. This finding matches with previous studies^{19,37,39,45} and highlights that the target cell line is a critical point to be considered when designing new micro- and nanoengineered materials for intracellular applications.

In addition to cellular uptake, the intracellular transport and fate of micro- and nanomaterials need to be well characterized. In this sense, micro- and nanoparticles have been shown to often remain trapped in endolysosomal compartments, which can be either desirable or not, depending on the purpose of the nanomaterial^{46,47}. In the present work, the study of the intracellular location of MMICCs using endosome and lysosome markers showed

that, after 24 h of co-incubation, they could be found in any of these two compartments. These results are in agreement with previous studies where micro- and nanoparticles have been found to remain trapped in the endo-lysosomal compartments⁴⁸.

Once the uptake and intracellular fate of MMICCs were evaluated, we studied their biocompatibility. In this regard, it is worth noting that in many cases micron-sized materials have been shown to render less cytotoxic effects when compared with their nano-sized counterparts^{49,50}, this being often correlated with a lower uptake⁴⁹. In spite of this, some authors have found significant cytotoxic effects for some types of microparticles, indicating that cytotoxicity not only depends on the size but also on material composition⁵¹ and surface properties³⁵. These findings suggest that cytotoxicity needs to be thoroughly evaluated in order to develop safe micro- and nanoengineered devices. For this reason, in the present study, we also assessed the viability, morphology and adhesion of cells incubated with MMICCs. First, we observed that the viability of both MCF-10A and SKBR-3 cells was not affected by the presence of MMICCs. Moreover, despite MMICCs being significantly more internalized in MCF-10A than in SKBR-3 cells, there were no significant differences in cell viability between these two cell lines. Second, the analyses of actin cytoskeleton and focal contacts showed no differences between cells with or without internalized MMICCs. Taken together, these results indicate that MMICCs do not affect cell viability regardless of the different uptake efficiency in both cell lines.

Apart from cytotoxicity, another possible undesirable effect of MMICCs could be the induction of an inflammatory response. In this regard, it has been shown that macrophages can be used as a model, since they trigger the release of inflammatory cytokines as a response to the presence of certain materials, such as titanium debris^{52,53}, silicon⁵⁴ and amorphous silica⁵⁵ particles, as well as metal ions, such as Au, Pd and Ni⁵⁶. Thus, we studied the inflammatory cytokines released by THP-1 derived macrophages after their incubation with MMICCs. We observed that the release of cytokines

was not significantly affected by incubation with MMICCs, at either 5 or 24 h, indicating that they do not trigger an immunogenic response in macrophages.

In the last series of experiments of this work, MMICCs were bi-functionalized as a proof-of-concept for their potential use as multi-modal devices. Due to their multi-material nature, MMICCs offer unique properties such as the precise spatial control over surface-conjugated molecules²⁷. Since the transferrin receptor (TfR) has been shown to be overexpressed in a wide number of malignant cancer cells^{40-42,57}, including SKBR-3 cells^{58,59}, we functionalized the poly-silicon side of MMICCs with Tf-FITC in order to target cancer cells. In addition, the Au side was functionalized with pHrodo®, in order to detect intracellular pH. Results showed that internalization of bi-functional MMICCs was increased in both SKBR-3 and MCF-10A cell lines, when compared with non-functionalized MMICCs. However, this increase was significantly higher in SKBR-3, probably due to their higher TfR expression level. By contrast, MCF-10A cells have shown to display low levels of TfR expression⁴¹. Thus, these data indicate that MMICCs could be targeted to a certain cell type by using specific molecules. However, in this case MCF-10A cells showed a high capability for non-specific MMICCs uptake, which would interfere with the targeting specificity. On the other hand, the red fluorescence of pHrodo® could be visualized, indicating that MMICCs were located inside acidic compartments, which is in agreement with our data about the intracellular location studies using EEA-1 and LAMP-1 markers.

In summary, our results show that multi-material devices have a promising potential for their use in intracellular applications due to their excellent biocompatible and non-immunogenic properties, as well as for the development of different functions such as targeting and sensing. Moreover, our results highlight the importance of a prior characterization of their interactions with biological systems, not only regarding their target cells but also the cells from the neighbouring tissues, in order to develop an efficient and safe micron-sized platform for biomedical purposes.

Acknowledgements

This study was supported by grants from the Ministerio de Ciencia e Innovación (TEC2011-29140-C03), and the Generalitat de Catalunya (2014SGR-524). The authors wish to thank the Servei de Microscòpia at the Universitat Autònoma de Barcelona.

References

1. CALDORERA-MOORE, M. & PEPPAS, N. A. Micro- and nanotechnologies for intelligent and responsive biomaterial-based medical systems. *Adv. Drug Deliv. Rev.* 61, 1391-401 (2009).
2. LIM, C. T., HAN, J., GUCK, J. & ESPINOSA, H. Micro and nanotechnology for biological and biomedical applications. *Med. Biol. Eng. Comput.* 48, 941-943 (2010).
3. ROCO, M. C. Nanotechnology: convergence with modern biology and medicine. *Curr. Opin. Biotechnol.* 14, 337-346 (2003).
4. SIEGEL, R. A., NUXOLL, E. E., HILLMYER, M. A. & ZIAIE, B. Top-down and bottom-up fabrication techniques for hydrogel based sensing and hormone delivery microdevices. *Conf. Proc. ... Annu. Int. Conf. IEEE Eng. Med. Biol. Soc. IEEE Eng. Med. Biol. Soc. Annu. Conf.* 2009, 232-235 (2009).
5. NUXOLL, E. BioMEMS in drug delivery. *Adv. Drug Deliv. Rev.* 65, 1611-1625 (2013).
6. SHAWGO, R. S., RICHARDS GRAYSON, A. C., LI, Y. & CIMA, M. J. BioMEMS for drug delivery. *Curr. Opin. Solid State Mater. Sci.* 6, 329-334 (2002).
7. TAO, S. L. & DESAI, T. A. Microfabricated drug delivery systems: from particles to pores. *Adv. Drug Deliv. Rev.* 55, 315-328 (2003).
8. HILT, J. Z. & PEPPAS, N. A. Microfabricated drug delivery devices. *Int. J. Pharm.* 306, 15-23 (2005).
9. SANT, S. ET AL. Microfabrication technologies for oral drug delivery. *Adv. Drug Deliv. Rev.* 64, 496-507 (2012).
10. SANTINI, J. T., CIMA, M. J. & LANGER, R. A controlled-release microchip. *Nature* 397, 335-338 (1999).

11. SANTINI, J. T., RICHARDS, SCHEIDT, CIMA & LANGER. Microchips as Controlled Drug-Delivery Devices. *Angew. Chem. Int. Ed.* 39, 2396-2407 (2000).
12. STAPLES, M. Microchips and controlled-release drug reservoirs. *Wiley Interdiscip. Rev. Nanomed. Nanobiotechnol.* 2, 400-417 (2010).
13. BASHIR, R. BioMEMS: state-of-the-art in detection, opportunities and prospects. *Adv. Drug Deliv. Rev.* 56, 1565-1586 (2004).
14. FERNÁNDEZ-ROSAS, E. ET AL. Intracellular polysilicon barcodes for cell tracking. *Small* 5, 2433-2439 (2009).
15. FERNÁNDEZ-ROSAS, E. ET AL. Internalization and cytotoxicity analysis of silicon-based microparticles in macrophages and embryos. *Biomed. Microdevices* 12, 371-379 (2010).
16. GÓMEZ-MARTÍNEZ, R. ET AL. Intracellular Silicon Chips in Living Cells. *Small* 6, 499-502 (2010).
17. GÓMEZ-MARTÍNEZ, R. ET AL. Silicon chips detect intracellular pressure changes in living cells. *Nat Nano* 8, 517-521 (2013).
18. GRATTON, S. E. A. ET AL. The effect of particle design on cellular internalization pathways. *Proc. Natl. Acad. Sci. U. S. A.* 105, 11613-8 (2008).
19. ZAUNER, W., FARROW, N. A. & HAINES, A. M. In vitro uptake of polystyrene microspheres: effect of particle size, cell line and cell density. *J. Control. Release* 71, 39-51 (2001).
20. REJMAN, J., OBERLE, V., ZUHORN, I. S. & HOEKSTRA, D. Size-dependent internalization of particles via the pathways of clathrin- and caveolae-mediated endocytosis. *Biochem. J.* 377, 159-69 (2004).
21. CHAMPION, J. A., WALKER, A. & MITRAGOTRI, S. Role of particle size in phagocytosis of polymeric microspheres. *Pharm. Res.* 25, 1815-1821 (2008).
22. BARUA, S. ET AL. Particle shape enhances specificity of antibody-displaying nanoparticles. *Proc. Natl. Acad. Sci. U. S. A.* 110, 3270-5 (2013).
23. GENG, Y. ET AL. Shape effects of filaments versus spherical particles in flow and drug delivery. *Nat Nano* 2, 249-255 (2007).
24. KELKAR, S. S. & REINEKE, T. M. Theranostics: combining imaging and therapy. *Bioconjug. Chem.* 22, 1879-1903 (2011).

25. RAHMAN, M. ET AL. Advancement in multifunctional nanoparticles for the effective treatment of cancer. *Expert Opin. Drug Deliv.* 9, 367-381 (2012).
26. DEBBAGE, P. Targeted drugs and nanomedicine: present and future. *Curr. Pharm. Des.* 15, 153-172 (2009).
27. DURÁN, S. ET AL. Technological development of intracellular polysilicon-chromium-gold chips for orthogonal chemical functionalization. *Sensors Actuators B Chem.* 209, 212-224 (2015).
28. PATEL, N. ET AL. Immobilization of Protein Molecules onto Homogeneous and Mixed Carboxylate-Terminated Self-Assembled Monolayers. *Langmuir* 13, 6485-6490 (1997).
29. STARK, W. J. Nanoparticles in Biological Systems. *Angew. Chemie Int. Ed.* 50, 1242-1258 (2011).
30. TOMIC, S. ET AL. Size-dependent effects of gold nanoparticles uptake on maturation and antitumor functions of human dendritic cells in vitro. *PLoS One* 9, e96584 (2014).
31. BLANK, F. ET AL. Size-dependent uptake of particles by pulmonary antigen-presenting cell populations and trafficking to regional lymph nodes. *Am. J. Respir. Cell Mol. Biol.* 49, 67-77 (2013).
32. CHITHRANI, B. D., GHAZANI, A. A. & CHAN, W. C. W. Determining the size and shape dependence of gold nanoparticle uptake into mammalian cells. *Nano Lett.* 6, 662-668 (2006).
33. SCHAEUBLIN, N. M. ET AL. Does shape matter? Bioeffects of gold nanomaterials in a human skin cell model. *Langmuir* 28, 3248-58 (2012).
34. QIU, Y. ET AL. Surface chemistry and aspect ratio mediated cellular uptake of Au nanorods. *Biomaterials* 31, 7606-19 (2010).
35. FROHLICH, E. The role of surface charge in cellular uptake and cytotoxicity of medical nanoparticles. *Int. J. Nanomedicine* 7, 5577-5591 (2012).
36. PATIÑO, T., NOGUÉS, C., IBÁÑEZ, E. & BARRIOS, L. Enhancing microparticle internalization by nonphagocytic cells through the use of noncovalently conjugated polyethyleneimine. *International Journal of Nanomedicine* 7, 5671-5682 (2012).

37. SAHA, K. ET AL. Surface functionality of nanoparticles determines cellular uptake mechanisms in mammalian cells. *Small* 9, 300-5 (2013).
38. KUHN, D. A. ET AL. Different endocytotic uptake mechanisms for nanoparticles in epithelial cells and macrophages. *Beilstein J. Nanotech.* 5, 1625-1636 (2014).
39. WANG, E. C. ET AL. Differential cell responses to nanoparticle docetaxel and small molecule docetaxel at a sub-therapeutic dose range. *Nanomedicine* 10, 321-328 (2014).
40. KOLHATKAR, R., LOTE, A. & KHAMBATI, H. Active tumor targeting of nanomaterials using folic acid, transferrin and integrin receptors. *Curr. Drug Discov. Technol.* 8, 197-206 (2011).
41. HOGEMANN-SAVELLANO, D. ET AL. The transferrin receptor: a potential molecular imaging marker for human cancer. *Neoplasia* 5, 495-506 (2003).
42. CAVANAUGH, P. G., JIA, L., ZOU, Y. & NICOLSON, G. L. Transferrin receptor overexpression enhances transferrin responsiveness and the metastatic growth of a rat mammary adenocarcinoma cell line. *Breast Cancer Res. Treat.* 56, 203-217 (1999).
43. JAMES, T., MANNOOR, M. S. & IVANOV, D. V. BioMEMS -Advancing the Frontiers of Medicine. *Sensors* (Basel). 8, 6077-6107 (2008).
44. THOREK, D. L. J. & TSOURKAS, A. Size, charge and concentration dependent uptake of iron oxide particles by non-phagocytic cells. *Biomaterials* 29, 3583-3590 (2008).
45. PATIÑO, T., SORIANO, J., BARRIOS, L., IBÁÑEZ, E. & NOGUÉS, C. Surface modification of microparticles causes differential uptake responses in normal and tumoral human breast epithelial cells. *Sci. Rep.* 5, (2015).
46. BAREFORD, L. M. & SWAAN, P. W. Endocytic mechanisms for targeted drug delivery. *Adv. Drug Deliv. Rev.* 59, 748-758 (2007).
47. SHETE, H. K., PRABHU, R. H. & PATRAVALE, V. B. Endosomal escape: a bottleneck in intracellular delivery. *J. Nanosci. Nanotechnol.* 14, 460-474 (2014).
48. IVERSEN, T.-G., SKOTLAND, T. & SANDVIG, K. Endocytosis and intracellular transport of nanoparticles: Present knowledge and need for future studies. *Nano Today* 6, 176-185 (2011).

49. HE, Q., ZHANG, Z., GAO, Y., SHI, J. & LI, Y. Intracellular Localization and Cytotoxicity of Spherical Mesoporous Silica Nano- and Microparticles. *Small* 5, 2722-2729 (2009).
50. NAIR, S. ET AL. Role of size scale of ZnO nanoparticles and microparticles on toxicity toward bacteria and osteoblast cancer cells. *J. Mater. Sci. Mater. Med.* 20 (Suppl 1), S235-41 (2009).
51. KARLSSON, H. L., GUSTAFSSON, J., CRONHOLM, P. & MÖLLER, L. Size-dependent toxicity of metal oxide particles: A comparison between nano- and micrometer size. *Toxicol. Lett.* 188, 112-118 (2009).
52. NAKASHIMA, Y. ET AL. Signaling pathways for tumor necrosis factor-alpha and interleukin-6 expression in human macrophages exposed to titanium-alloy particulate debris in vitro. *J. Bone Joint Surg. Am.* 81, 603-615 (1999).
53. VALLÉS, G. ET AL. Differential inflammatory macrophage response to rutile and titanium particles. *Biomaterials* 27, 5199-5211 (2006).
54. CHOI, J. ET AL. Comparison of cytotoxic and inflammatory responses of photoluminescent silicon nanoparticles with silicon micron-sized particles in RAW 264.7 macrophages. *J. Appl. Toxicol.* 29, 52-60 (2009).
55. KUSAKA, T. ET AL. Effect of silica particle size on macrophage inflammatory responses. *PLoS One* 9, e92634 (2014).
56. WATAHA, J. C. ET AL. Sublethal concentrations of Au (III), Pd (II), and Ni(II) differentially alter inflammatory cytokine secretion from activated monocytes. *J. Biomed. Mater. Res. B. Appl. Biomater.* 69, 11-17 (2004).
57. DANIELS, T. R., DELGADO, T., HELGUERA, G. & PENICHER, M. L. The transferrin receptor part II: Targeted delivery of therapeutic agents into cancer cells. *Clin. Immunol.* 121, 159-176 (2006).
58. KAWAMOTO, M., HORIBE, T., KOHNO, M. & KAWAKAMI, K. A novel transferrin receptor-targeted hybrid peptide disintegrates cancer cell membrane to induce rapid killing of cancer cells. *BMC Cancer* 11, 359 (2011).
59. ZHENG, Q. ET AL. Expression of curcumin-transferrin receptor binding peptide fusion protein and its anti-tumor activity. *Protein Expression and Purification* 89, 181-188 (2013).



4

Discussion

The recent advances in micro- and nanotechnology have opened new and promising avenues for the biomedical field through the development of micro- and nanoplatforms able to overcome some of the major limitations of current therapies (DAVIS ET AL., 2008), as well as to combine diagnostic and treatment functions in a single entity (BANYAL ET AL., 2013; LAROUÏ ET AL., 2013; MUTHU ET AL., 2014). However, the translation of nanomedicine into real clinical applications is still in its infancy (ETHERIDGE ET AL., 2013; ANSELMO & MITRAGOTRI, 2014). In this regard, a deeper understanding of their interactions with the biological systems might help to develop more efficient and safe micro- and nanoplatforms for biomedical applications (STARK, 2011). Particularly, interactions at the cellular level are of special relevance, as the uptake efficiency, cytotoxicity and intracellular fate will determine the efficacy of micro- and nanodevices.

Several factors have proven to strongly modulate the interaction of micro- and nanoparticles at the cellular level, especially their physico-chemical properties, such as their size (NEL ET AL., 2009; PACHECO ET AL., 2013; SHANG ET AL., 2014), shape (CHITHRANI ET AL., 2006; GRATTON ET AL., 2008; BARUA ET AL., 2013) and surface properties (HAUCK ET AL., 2008; VERMA & STELLACCI, 2010). Particularly, regarding particle size, while a high number of studies have focused upon the use of nano-sized particles, less is known about micron-sized ones. In this sense, it is worth mentioning that micron-sized particles have shown to render excellent results for different applications, such as the development of multistage vectors (GODIN ET AL., 2011; BLANCO ET AL., 2011), intracellular chips (FERNÁNDEZ-ROSAS ET AL., 2009; 2010; GÓMEZ-MARTÍNEZ ET AL., 2015), microcapsules for drug delivery (SALONEN ET AL., 2005; KOHANE, 2007; SCHMIDT ET AL., 2013; PARIKH ET AL., 2014) and controlled release (PALANKAR ET AL., 2009; STUDER ET AL., 2010), siRNA sustained delivery (TANAKA ET AL., 2010) or vaccines (SINGH ET AL., 2000; KASTURI, SACHAPHIBULKIJ & ROY, 2005; BALLESTEROS ET AL., 2015; YOON ET AL., 2015). In addition, in some cases, larger particles have shown to be less cytotoxic than their nano-sized counterparts (PAN ET AL., 2007; KARLSSON ET AL., 2009; PARK ET AL., 2011). Generally, although micron-sized particles have yielded

good results for several applications in phagocytic cells, their low capacity of internalisation by non-phagocytic cells might be a limitation that needs to be overcome. However, an interesting study carried out by Barua and co-workers determined that micron-sized particles showed a higher capability of targeting due to their low non-specific uptake (BARUA ET AL., 2013), when compared with their nano-sized counterparts. Thus, the low uptake of micron-sized particles could constitute an advantage for certain purposes, such as targeting approaches. Therefore, there is a growing need to gain new insights into the interaction of micron-sized particles with cells.

Due to the lower amount of research in micron-sized particles compared with nanoparticles, as well as a high variability of experimental conditions, there is currently little knowledge about their biological interactions. Thus, in the present thesis, the main objective was to characterize the interaction of microparticles with cells, in order to assess their feasibility for future applications in biomedicine.

In our **first work**, we aimed to assess the impact of different coatings of fluorescent polystyrene microparticles (3 μm in diameter) regarding their uptake efficiency by the non-phagocytic human cervix adenocarcinoma HeLa cell line. Due to the fact that cationic particles are generally more likely to be uptaken by cells (THOREK & TSOURKAS, 2008; FRÖHLICH, 2012), we considered the use of non-viral transfection based approaches to modify the surface of microparticles. These approaches are based on the electrostatic interactions of positively charged polymers or lipids and the negatively charged DNA molecules (TROS DE ILARDUYA ET AL., 2010). Specifically, we used the cationic polymer PEI, with a molecular weight of 25 kDa, and two commercial cationic lipid based products, LipofectamineTM2000 (LF2000) and FuGENE 6.

Although some studies have already used PEI to covalently modify particles, we considered the use of free PEI (i.e. non-covalently bound to the microparticle surface), as it would represent an advantage for future microparticle-based delivery systems, since it should not interfere with the functionalization process of other molecules of interest.

Despite the fact that PEI, LF200 and FuGENE 6 have rendered excellent results regarding DNA delivery into cells, they can lead to undesirable cytotoxic effects, which need to be taken into account (GODBNEY ET AL., 1999; DUAN ET AL., 2009). Thus, aiming to find the best balance between uptake efficiency and cytotoxicity, three different PEI concentrations were tested. The highest concentration tested was set at 0.15 mM, since higher concentrations have been reported to exert dramatic cytotoxic effects (LAMBERT ET AL., 1996). By contrast, LF2000 and FuGENE 6 were used at the concentrations recommended by the manufacturers, which have already provided good results in the case of LF2000 and 1 or 3 μm -sized beads (KOBAYASHI ET AL., 2010). First, we studied the cytotoxic effect caused by the different transfection reagents in HeLa cells, and we found that whereas all treatments resulted in a high number of viable cells (<60%) with respect to the control cells, the number of cells which remained attached to the dish was dramatically decreased in some cases, such as in the LF2000 and PEI 0.15 mM treatments. For this reason, we used a combined analysis of cytotoxicity, consisting in the evaluation of the percentage of viable cells as well as the number of cells remaining attached to the culture plates after their exposure to the different treatments. This combined analysis allowed us to accurately determine the cytotoxicity of different treatments. Results showed a dose-dependent cytotoxic effect for PEI, in agreement with previous studies (DENG ET AL., 2009). In the case of LF200 and FuGENE, whereas the percentage of viable cells was high among the attached cells, a considerable number of cells were lost, indicating that their strong cytotoxicity caused cell detachment.

Once the cytotoxicity was assessed, the coating of microparticles with the different reagents was characterized by analyzing their ζ -potential. We observed a shift in the microparticle surface charge, from negative to positive, after incubation with the transfection reagents, and a dose-dependent increase of the microparticle positive surface charge when increasing PEI concentrations. In addition, we observed that the increase in positive surface charge of microparticles was higher in the case of PEI, when compared to

LF2000 and FuGENE 6 treatments. In order to assess whether PEI could modify the surface of microparticles which are already functionalised, we used functionalised non-fluorescent carboxylated particles with an Alexa Fluor®594 conjugated IgG. Zeta potential analyses determined that PEI could also interact with the functionalised particles and increase their positive surface charge.

Next, we studied the internalisation of microparticles by HeLa cells, using two different approaches: FC and CSLM. Whereas FC allowed analysing a higher number of cells, it did not discriminate between cells with internalised particles and cells with particles attached to their membrane. For this reason, we used CSLM in order to accurately distinguish the internalised microparticles from those bound to the cell surface. Results obtained by FC showed that all treatments increased the percentage of cells associated with microparticles, PEI 0.05 mM (25.9%) and LF2000 (20.4%) being the most effective treatments. This increase on PEI- and LF2000-coated cell-microparticle association in comparison with non-coated microparticles (3.7%) could be related to the change on their surface charge, as positively charged particles are more likely to be uptaken by cells than those negatively charged (THOREK & TSOURKAS, 2008; VERMA & STELLACCI, 2010; FRÖHLICH, 2012). Surprisingly, even though the ζ -potential of microparticles increased when higher concentrations of PEI were used, cell-microparticle association decreased. On the other hand, in spite of lower internalisation, higher PEI concentrations facilitated microparticle-cell contact, as a higher amount of particles bound to the cell surface were observed. Thus, the decreased particle internalisation at higher PEI concentrations could be related to the cytotoxic effect of PEI, especially regarding membrane damage induction, in agreement with that described by other groups (HELANDER ET AL., 1997; GRANDINETTI ET AL., 2012). When the cytotoxic effect was considered, 0.05 mM PEI was the most effective treatment with regard to microparticle internalisation. Therefore, we used this treatment for the following analyses of the intracellular fate of microparticles, once they had been internalised.

One of the main advantages of using PEI when used as a transfection reagent is the proton-sponge effect (described in the Introduction, Section 1.3.3.), which leads to disruption of the endolysosomal compartment and subsequent cytosolic release of its contents (BOUSIFF ET AL., 1995; SONAWANE ET AL., 2003; CREUSAT ET AL., 2010). TEM analyses showed that most of the internalised particles were tightly surrounded by a single membrane, which was positive for the LAMP-1 marker, indicating that they were actually located within the lysosomal compartment. Besides, some particles were surrounded by a double membrane structure, suggesting that an autophagic process could be taking place, as previously described when using 1- μm polystyrene microparticles coated with LF2000 (KOBAYASHI ET AL., 2010). The results obtained with TEM were further confirmed by CSLM, through immunofluorescence localization of EEA-1 and LAMP-1 markers, which allowed performing a quantitative assessment of microparticles that were surrounded by either an endosomal or lysosomal membrane. Data showed that up to 83% of microparticles were located inside lysosomes and no endosomal association was found. Related to this, it is worth mentioning that Kobayashi and co-workers reported that cationic lipids facilitate the endosomal escape of 1 μm polystyrene particles, leading to the induction of an autophagic process, the particles being surrounded by an autophagosome after their release into the cytosol (KOBAYASHI ET AL., 2010). Therefore, in our case, those particles that were not associated with lysosome markers could be either located free in the cytosol or be involved in an autophagic process.

In summary, the first work demonstrated that the use of transfection reagents can significantly improve the uptake of 3 μm polystyrene microparticles in the non-phagocytic HeLa cell line. However, their intrinsic cytotoxicity is a crucial factor that needs to be considered. In this regard, we found that PEI at a 0.05 mM concentration offered an excellent balance between cytotoxicity and microparticle internalisation efficiency. Moreover, the effect of PEI on the increase of positive charges on the surface microparticles was maintained when antibody-functionalised particles were used. With respect to microparticle in-

ternalisation, we observed that not only the surface charge is a key factor, but also cytotoxicity. Finally, despite PEI having a great capability for the delivery of DNA into the cytosol due to its proton sponge effect, the great majority of particles coated with PEI remained trapped into the lysosomal compartment.

Apart from particle design, and despite having received less attention in the literature, the cell line is a crucial factor when studying particle-cell interactions. In this regard, several attempts have been performed to target micro- or nanoparticles to a specific cell type, through their surface modification using specific peptides or antibodies (EL-SAYED ET AL., 2006; GU ET AL., 2007; SINGH & LILLARD, 2009; FAY & SCOTT, 2011; ZHONG ET AL., 2014). On the other hand, it has been shown that cell lines can also respond differently to particles functionalised with non-targeting molecules (SAHA ET AL., 2013). These findings suggest that the cell type effect is a crucial factor regarding particle-cell interactions that needs to be thoroughly characterized and taken into account when designing new micro- and nanoplatforms for biomedical applications.

Thus, in our **second work**, we aimed to evaluate the cell type effect with regard to non-specific surface modifications of non-fluorescent polystyrene microparticles. The study was carried out by using two different cell lines: the human breast adenocarcinoma derived SKBR-3 cell line and the human breast epithelial derived MCF-10A cell line. Since antibodies are one of the most used molecules in particle functionalization, we used a fluorescent secondary IgG antibody, which was not specific for any of these two cell types. Moreover, we used PEI to further modify the surface of microparticles and study its effect on particle-cell interactions in both cell lines, as in our previous work it was proven to be a good approach for microparticle delivery strategies. In this case, we used two types of PEI, 25 kDa and 750 kDa PEI, both differing in their structure and molecular weight, as these two parameters have been described to modulate cell interactions (NEU ET AL., 2005). Moreover, Kobayashi and co-workers reported that PEI with a higher molecular weight can facilitate the escape of microparticles into the cell cytosol more efficiently than a lower molecular weight PEI (KOBAYASHI ET AL., 2010).

Since in our first work we observed that the cytotoxicity was a crucial factor when studying the effect of surface modifications on particle-cell interactions, the first step was to determine the cytotoxicity of 25 kDa and 750 kDa PEI in both SKBR-3 and MCF-10A cells. We chose to work at a 0.05 mM concentration, since this rendered a good balance between cytotoxicity and internalisation efficiency in our previous work. No cytotoxic effect was observed for any of the cell or PEI types. Characterization of microparticles showed that after treatments with PEI, the great majority of particles (80%) were monodisperse. In addition, the ζ -potential of microparticles changed to positively charged when coated with either 25 or 750 kDa PEI, this change being significantly more relevant in the case of 750 kDa PEI. This increased surface charge by 750 kDa PEI with respect to 25 kDa PEI was probably due to a higher number of protonable amine groups.

With regard to microparticle internalisation, the fact that fluorescence of microparticles came from their surface instead of their core allowed us to use a trypan-blue (TB) based quenching technique (VRANIC ET AL., 2013). With this technique, we were able to accurately discriminate between cells with internalised particles and those with particles attached to their membranes, without the need of using CSLM. Moreover, it allowed discarding dead cells from the analysis, as TB only accumulates in dead cells. A clear difference between cell lines was observed with regard to microparticle internalisation efficiency. On the one hand, SKBR-3 internalised better the positively charged microparticles, whereas the opposite was found for MCF-10A. These results are in agreement with previous findings, where MCF-10A showed a great capability for internalizing negatively charged quantum dots (XIAO ET AL., 2010). In this case, this differential uptake could not be attributed to a cytotoxic effect, as it was the case of our first work, since no differences regarding cell viability were found for any of the PEI treatments. For this reason, we investigated whether these differences could be related to a distinct mechanism of internalisation through the use of two different endocytic inhibitors. On the one hand, we used Cytochalasin D (CD) to inhibit the internalisation of microparticles by macropi-

nocytosis (SCHLIWA, 1982; WAKATSUKI ET AL., 2001). On the other hand, we used dynasore to inhibit dynamin-dependent internalisation processes (MACIA ET AL., 2006). Results showed significant differences between the two cell lines with regard to the mechanism of internalisation. Whereas SKBR-3 cells internalised all types of microparticles by the macropinocytic pathway, MCF-10A showed different mechanisms of internalisation for the different types of microparticles. Specifically, both CD and Dyn inhibited the uptake of non-coated particles but no inhibition of PEI-coated particles could be achieved by either CD or Dyn. This indicated that particles could be uptaken by other alternative actin- and dynamin-independent mechanisms in MCF-10A cells.

Taken together, these results suggest that both surface properties of microparticles and the cell type are crucial factors for the modulation of particle-cell interactions, not only in terms of internalisation efficiency but also with regard to the mechanism of internalisation. As different mechanisms of internalisation were observed for the different cell lines and types of microparticles, their intracellular fate was assessed. The great majority of particles were found in the lysosomal compartment in both cell lines. Thus, despite using PEI with a higher molecular weight, the delivery of microparticles into the cytosol could not be achieved. Hence, even though PEI has demonstrated an excellent capability of releasing DNA and nanoparticles into the cytosol (BOUSIFF ET AL., 1995), this endolysosomal escape is not possible in the case of larger particles. Future research regarding the delivery of large microparticles or their cargo into the cytosol should therefore be focused on the development of alternative approaches that allow their endolysosomal escape.

Therefore, in this second work we found that non-tumoral and tumoral human breast cells have different uptake responses to different surface modifications of microparticles, not only regarding internalisation efficiency but also the mechanism of internalisation. Thus, the design of new micro- and nano-platforms must take into account the surface properties of particles as well as the characteristics of the target cell in order to improve specific cell delivery and diminish undesirable side effects on the healthy neighbouring cells and tissues.

One particularly interesting example of micron-sized devices are the so-called biological microelectromechanical systems (BioMEMs), which have shown a great potential for several biomedical applications such as drug delivery (SHAWGO ET AL., 2002; TAO & DESAI, 2003; HILT & PEPPAS, 2005; SANT ET AL., 2012), controlled-release (SANTINI ET AL., 1999; SANTINI ET AL., 2000; STAPLES, 2010) and diagnostics (BASHIR, 2004). In this sense, we have reported the development of multi-material intracellular chips, which can be functionalised with different molecules with a precise control over their spatial distribution (DURÁN ET AL., 2015). The conjugation of different molecules in a single platform allows performing multiple functions, which is a main goal in biomedicine (DEBBAGE, 2009; KELKAR & REINEKE, 2011; RAHMAN ET AL., 2012).

As the data obtained from our two previous works pointed out that the characterization of particle-cell interactions is essential when developing a novel micro- or nanosystem, the **third work** aimed to explore the potential of multi-material intracellular chips (MMICCs) for biological applications. This was conducted by assessing the interactions of these chips with cells, in terms of biocompatibility, uptake, intracellular fate and inflammatory cytokine release. Again, we chose two cell lines, SKBR-3 and MCF-10A, as they showed to be a good model because of their different nature (tumorigenic vs. non-tumorigenic) as well as their differential response to micron-sized particles. In agreement with our second work, we found that MMICCs internalisation was higher in MCF-10A than in SKBR-3 cells.

In our first work, the cytotoxic effect of transfection reagents directly affected the uptake of microparticles by cells. Thus, in order to provide a deeper understanding about the differences on cellular responses to micro- or nanoparticles, biocompatibility is a key factor to be taken into account, as it could play a relevant role on particle-cell interactions. On the one hand, a lower cytotoxicity of micron-sized particles compared to nano-sized ones has been attributed to a lower uptake efficiency (HE ET AL., 2009). Besides, the study carried out by Karlsson and co-workers showed that the cytotoxicity of micro- and nanomaterials not only relies on the size of particles but also on the material

composition (KARLSSON ET AL., 2009). However, these authors did not check the particle uptake efficiency. In our case, MCF-10A showed to internalise a high number of MMICCs. Thus, we wondered whether MMICCs would induce a higher cytotoxic effect on MCF-10A than in SKBR-3 cells. On the other hand, a higher cytotoxicity resulted in a decreased microparticle uptake in our first work.

Thus, the biocompatibility of MMICCs in both SKBR-3 and MCF-10A cell lines was assessed in terms of cell viability, morphology and adhesion. No differences were found for any of these parameters when MMICCs exposed cells were compared with control cells, meaning that MMICCs were biocompatible for both cell lines, regardless of their uptake rates. These results also discarded the possibility that the internalisation in SKBR-3 cells was lower due to any toxic effect caused by MMICCs. Altogether, these findings indicate that whereas the internalisation efficiency of MMICCs depends on the cell line, they do not lead to cytotoxic effects in any of these two cell lines, these results being consistent with those obtained in our second work.

With regard to intracellular location, MMICCs were found either in the endosomal or the lysosomal compartment, regardless of the cell type. These results are particularly relevant, as for those applications where the endolysosomal compartment is not the target, strategies for the release of MMICCs into the cytosol will be required.

In certain cases, the presence of foreign materials inside the organism can lead to an undesirable inflammatory immune response. In this sense, it has been shown that macrophages exposed to several materials, including titanium (NAKASHIMA ET AL., 1999; VALLÉS ET AL., 2006), silicon (CHOI ET AL., 2009) and amorphous silica (KUSAKA ET AL., 2014), and metal ions such as Au, Pd and Ni (WATAHA ET AL., 2004) can release human inflammatory cytokines. Since MMICCs contain different materials (polysilicon, gold and chromium), we assessed the release of different inflammatory cytokines by macrophages incubated with MMICCs. Results showed no induction of inflammatory cytokines release by macrophages at either 5 or 24h of incubation with MMICCs.

Finally, in order to render the chips multifunctional, as a proof-of-concept approach, MMICCs were functionalised with two different molecules by using orthogonal chemistry techniques. This approach allowed us to precisely provide a controlled spatial regulation of the functionalised molecules, as the gold and polysilicon surfaces were functionalised with different molecules. On the one hand, the gold side was functionalised with the commercial pH sensor pHrodo®. On the other hand, the polysilicon surface was functionalised with transferrin (Tf) to target cancer cells, since the latter have shown to overexpress the Tf receptor in many cases (DANIELS ET AL., 2006). Uptake of functionalised MMICCs was increased for both cell lines, when compared with non-functionalised MMICCs. However, this increase was higher in the case of SKBR-3 cells and could be attributed to its higher levels of Tf receptor expression (KAWAMOTO ET AL., 2011). In spite of this, the fact that the MCF-10A cell line had a great capability for non-specific uptake of MMICCs did not allow to achieve an effective targeting.

In summary, all three works have provided an integrative understanding about the relationship between certain characteristics of microparticles and cell responses. We observed that the surface of microparticles, as well as their cytotoxicity, plays a key role on their internalisation by non-phagocytic cells. On the other hand, the cell type showed to be equally important regarding the cell response to a determined type of particle. Therefore, it is essential to characterize the biological interactions of micron-sized platforms, in order to develop safe and efficient systems for their application in biomedicine. Moreover, the obtained results provide promising outcomes for the use of micron-sized platforms in biomedicine, as in general they have proven to render high biocompatibility. In addition, by tuning the surface of microparticles, their uptake can be enhanced in non-phagocytic cells and they can be selectively delivered to a certain cell type. However, the non-specific uptake capability of not only the target cells but also the neighbouring cells should be characterized when designing a micro- or nanodevice for biomedical purposes.



5

Conclusions

- I.** Microparticle coating with LF2000, FuGENE and Pei significantly increases microparticle positive surface charges, leading to a higher uptake by non-phagocytic human cervix adenocarcinoma HeLa cells.
- II.** Microparticle coating with PEI 25kDa at a 0.05 mM concentration showed the best balance between internalisation efficiency and cytotoxicity in HeLa cells.
- III.** Tumoral SKBR-3 cells showed an enhanced uptake of positively charged microparticles, whereas the opposite was observed for non-tumoral MCF-10A cells.
- IV.** SKBR-3 cells internalised microparticles through macropinocytosis, regardless of their surface properties. By contrast, MCF10A cells showed distinct internalisation mechanisms depending on the surface properties of microparticles.
- V.** P-Si-Cr-Au MMICCs are promising candidates for biomedical applications, as they are efficiently uptaken by non-phagocytic cells, they show high biocompatibility and no induction of inflammatory responses.
- VI.** Regardless of the surface properties and cell type, the majority of microparticles were observed to be located within the endolysosomal compartments, indicating the need for developing new strategies for their delivery into the cytosol.
- VII.** Dually-functionalised MMICCs can be used for multi-functional purposes such as tumoral cells targeting and intracellular pH sensing.



6

References

- ACHARYA S & SAHOO SK, 2011.** PLGA nanoparticles containing various anti-cancer agents and tumour delivery by EPR effect. *Advanced Drug Delivery Reviews*, 63, pp. 170-183.
- ADEREM A & UNDERHILL DM, 1999.** Mechanisms of phagocytosis in macrophages. *Annual review of immunology*, 17, pp. 593-623.
- ADLAKHA-HUTCHEON G, BALLY MB, SHEW CR & MADDEN TD, 1999.** Controlled destabilization of a liposomal drug delivery system enhances mitoxantrone antitumor activity. *Nature Biotechnology*, 17, pp. 775-779.
- AGGARWAL P, HALL JB, MCLELAND CB, DOBROVOLSKAIA MA & MCNEIL SE, 2009.** Nanoparticle interaction with plasma proteins as it relates to particle biodistribution, biocompatibility and therapeutic efficacy. *Advanced drug delivery reviews*, 61, pp. 428-437.
- ALBANESE A, TANG PS, & CHAN WCW, 2012.** The effect of nanoparticle size, shape, and surface chemistry on biological systems. *Annual Review of Biomedical Engineering*, 14, pp. 1-16.
- ALBERTS B, JOHNSON A, LEWIS J, RAFF M, ROBERTS K ET AL., 2014.** Molecular biology of the cell, 6th ed. Chapter 11, membrane transport of small molecules and the electrical properties of membranes. *Garland science*. pp. 651-694
- ALKILANY AM & MURPHY CJ, 2010.** Toxicity and cellular uptake of gold nanoparticles: what we have learned so far? *Journal of nanoparticle research*, 12, pp. 2313-2333.
- ALLEN TM & CULLIS PR, 2013.** Liposomal drug delivery systems: from concept to clinical applications. *Advanced drug delivery reviews*, 65, pp. 36-48.
- ANGLIN EJ, CHENG L, FREEMAN WR & SAILOR MJ, 2008.** Porous silicon in drug delivery devices and materials. *Advanced Drug Delivery Reviews*, 60, pp. 1266-1277.
- ANGUISSOLA S, GARRY D, SALVATI A, O'BRIEN PJ & DAWSON KA, 2014.** High content analysis provides mechanistic insights on the pathways of toxicity induced by amine-modified polystyrene nanoparticles. *PloS ONE*, 9, p. e.108025.

- ANSELMO AC & MITRAGOTRI S, 2014.** An overview of clinical and commercial impact of drug delivery systems. *Journal of Controlled Release*, 190, pp. 15-28.
- ARVIZO RR, MIRANDA OR, MOYANO DF, WALDEN CA, GIRI K ET AL., 2011.** Modulating pharmacokinetics, tumor uptake and biodistribution by engineered nanoparticles. *PloS ONE*, 6, p. e.24374.

B

- BALLESTEROS NA, ALONSON M, SAINT-JEAN SR & PEREZ-PRIETO SI, 2015.** An oral DNA vaccine against infectious haematopoietic necrosis virus (IHNV) encapsulated in alginate microspheres induces dose-dependent immune responses and significant protection in rainbow trout (*Oncorhynchus mykiss*). *Fish & shellfish immunology*, 45, pp. 877-888.
- BANYAL S, MALIK P, TULI HS & MUKHERJEE TK, 2013.** Advances in nanotechnology for diagnosis and treatment of tuberculosis. *Current opinion in pulmonary medicine*, 19, pp. 289-297.
- BAREFORD LM & SWAAN PW, 2007.** Endocytic mechanisms for targeted drug delivery. *Advanced drug delivery reviews*, 59, pp. 748-58.
- BARGHEER D, NIELSEN J, GÉBEL G, HEINE M, SALMEN SC ET AL., 2015.** The fate of a designed protein corona on nanoparticles in vitro and in vivo. *Beilstein Journal of Nanotechnology*, 6, pp. 36-46.
- BARUA S, YOO JW, KOLHAR P, WAKANKAR A, GOKARN YR ET AL., 2013.** Particle shape enhances specificity of antibody-displaying nanoparticles. *Proceedings of the National Academy of Sciences of the United States of America*, 110, pp. 3270-5.
- BASHIR R, 2004.** BioMEMS: state-of-the-art in detection, opportunities and prospects. *Advanced drug delivery reviews*, 56, pp. 1565-1586.
- BENJAMINSEN RV, MATTEBJERG MA, HENRIKSEN JR, MOGHIMI SM, ANDRESEN TL, 2013.** The possible proton sponge effect of polyethylenimine (PEI) does not include change in lysosomal pH. *Molecular Therapy*, 21, pp. 149-157.
- BLANCO E, HSIAO A, MANN AP, LANDRY MG, MERIC-BERNSTAM F ET AL., 2011.** Nanomedicine in cancer therapy: innovative trends and prospects. *Cancer science*, 102, pp. 1247-1252.

- BLANK F, STUMBLES PA, SEYDOUX E, HOLT PG, FINK A ET AL., 2013.** Size-dependent uptake of particles by pulmonary antigen-presenting cell populations and trafficking to regional lymph nodes. *American journal of respiratory cell and molecular biology*, 49, pp. 67-77.
- BOAL AK, ILHAN F, DEROUCHY JE, THURN-ABRECHT T, RUSSELL TP ET AL., 2000.** Self-assembly of nanoparticles into structured spherical and network aggregates. *Nature*, 404, pp. 746-748.
- BOLHASSANI A, JAVANZAD S, SALEH T, HASHEMI M, AGHASEDEGHI MR ET AL., 2014.** Polymeric nanoparticles: potent vectors for vaccine delivery targeting cancer and infectious diseases. *Human vaccines & immunotherapeutics*, 10, pp. 321-332.
- BONIFACINO JS & ROJAS R, 2006.** Retrograde transport from endosomes to the trans-Golgi network. *Nature reviews. Molecular cell biology*, 7, pp. 568-579.
- BOSMAN AW, JANSSEN HM & MEIJER EW, 1999.** About dendrimers: structure, physical properties, and applications. *Chemical Reviews*, 99, pp. 1665-1688.
- BOUSIFF O, LEZOUALC'H F, ZANTA MA, MERGNY MD, SCHERMAN D ET AL., 1995.** A versatile vector for gene and oligonucleotide transfer into cells in culture and in vivo: Polyethylenimine. *Proceedings of the National Academy of Sciences*, 92, pp. 7297-7301.
- BRADBURNE CE, DELEHANTY JB, GEMMILL KB, MEI BC, MATTOUSSI H ET AL., 2013.** Cytotoxicity of quantum dots used for in vitro cellular labeling: role of QD surface ligand, delivery modality, cell type, and direct comparison to organic fluorophores. *Bioconjugate Chemistry*, 24, pp. 1570-1583.
- BROCK R, 2014.** The uptake of arginine-rich cell-penetrating peptides: putting the puzzle together. *Bioconjugate Chemistry*, 25, pp. 863-868.
- BRUS LE, 1984.** Electron-electron and electron-hole interactions in small semiconductor crystallites: The size dependence of the lowest excited electronic state. *The Journal of Chemical Physics*, 80, 4403.
- DEL BURGO LS, PEDRAZ JL & ORIVE G, 2014.** Advanced nanovehicles for cancer management. *Drug discovery today*, 19, pp 1659-1670.

- CABALLERO L, MENA J, MORALES-ALVAREZ A, KOGAN MJ & MELO F, 2015. Assessment of the nature interactions of beta-amyloid protein by a nanoprobe method. *Langmuir*, 31, pp. 299-306.
- CALVO P, VILA-JATO JL & ALONSO MJ, 1997. Evaluation of cationic polymer-coated nanocapsules as ocular drug carriers. *International Journal of Pharmaceutics*, 153, pp. 41-50.
- CANNON GJ & SWANSON JA, 1992. The macrophage capacity for phagocytosis. *Journal of cell science*, 101, pp. 907-913.
- CAVALLI R, GASCO MR, CHETONI P, BURGALASSI S & SAETTONE MF, 2002. Solid lipid nanoparticles (SLN) as ocular delivery system for tobramycin. *International Journal of Pharmaceutics*, 238, pp. 241-245.
- CEDERVALL T, LYNCH I, LINDMAN S, BERGGARD T, THULIN E ET AL., 2007. Understanding the nanoparticle-protein corona using methods to quantify exchange rates and affinities of proteins for nanoparticles. *Proceedings of the National Academy of Sciences*, 104, pp. 2050-2055.
- CHAMPION JA, WALKER A & MITRAGOTRI S, 2008. Role of particle size in phagocytosis of polymeric microspheres. *Pharmaceutical research*, 25, pp. 1815-1821.
- CHAUHAN VP & JAIN RK, 2013. Strategies for advancing cancer nanomedicine. *Nat Mater*, 12, pp. 958-962.
- CHEN D, DOUGHERTY CA, ZHU K & HONG H, 2015. Theranostic applications of carbon nanomaterials in cancer: Focus on imaging and cargo delivery. *Journal of controlled release*, 210, pp. 230-245.
- CHEN J, HESSLER JA, PUTCHAKAYALA K, PANAMA BK, KHAN DP ET AL., 2009. Cationic nanoparticles induce nanoscale disruption in living cell plasma membranes. *The journal of physical chemistry B*, 113, pp. 11179-11185.
- CHIMINI G & CHAVRIER P, 2000. Function of Rho family proteins in actin dynamics during phagocytosis and engulfment. *Nature cell biology*, 2, pp. E191-E196.
- CHITHRANI BD, GHAZANI AA & CHAN WCW, 2006. Determining the size and shape dependence of gold nanoparticle uptake into mammalian cells. *Nano letters*, 6, pp. 662-668.

- CHOI J, ZHANG Q, REJPA V, WANG NS, STRATMEYER ME ET AL., 2009.** Comparison of cytotoxic and inflammatory responses of photoluminescent silicon nanoparticles with silicon micron-sized particles in RAW 264.7 macrophages. *Journal of applied toxicology*, 29, pp. 52-60.
- CHOU LYT, MING K & CHAN WCW, 2011.** Strategies for the intracellular delivery of nanoparticles. *Chemical Society Reviews*, 40, pp. 233-245.
- CHU Z, ZHANG S, ZHANG B, ZHANG C ET AL, 2014.** Unambiguous observation of shape effects on cellular fate of nanoparticles. *Scientific reports*, 4, p. 4495.
- CONNER SD, & SCHMID SL, 2003.** Regulated portals of entry into the cell. *Nature*, 422, pp. 37-44.
- CONNOR EE, MWAMUKA J, GOLE A, MURPHY CJ & WYATT MD, 2005.** Gold nanoparticles are taken up by human cells but do not cause acute cytotoxicity. *Small*, 1, pp. 325-7.
- COOPER GM & HAUSMAN RE, 2013.** The cell: a molecular approach, 6th ed. Chapter 13: the plasma membrane. *Sinauer associates, Inc.*, pp. 515-556
- COPOLOVICI DM, LANGEL K, ERISTE E & LANGEL Ü, 2014.** Cell-penetrating peptides: design, synthesis, and applications. *ACS Nano*, 8, pp. 1972-1994.
- CORADEGHINI R, GIORIA S, GARCÍA CP, NATIVO P, FRANCHINI F ET AL., 2013.** Size-dependent toxicity and cell interaction mechanisms of gold nanoparticles on mouse fibroblasts. *Toxicology Letters*, 217, pp. 205-216.
- CREUSAT G, RINALDI AS, WEISS E, ELBAGHDADI R, REMY JS ET AL., 2010.** Proton sponge trick for pH-sensitive disassembly of polyethylenimine-based siRNA delivery systems. *Bioconjugate Chemistry*, 21, pp. 994-1002.

D

- DANIELS TR, DELGADO T, HELGUERA G & PENICHER ML, 2006.** The transferrin receptor part II: Targeted delivery of therapeutic agents into cancer cells. *Clinical Immunology*, 121, pp. 159-176.
- DAUSEND J, MUSYANOVYH A, DASS M, WALTHER P, SCHREZENMEIER H ET AL., 2008.** Uptake mechanism of oppositely charged fluorescent nanoparticles in HeLa cells. *Macromolecular bioscience*, 8, pp. 1135-43.

- DAVID R, ERDMANN M, FORNOF AR & GAUB HE, 2014.** Functionalization of cantilever tips with nucleotides by the phosphoramidite method. *ChemMedChem*, 9, pp. 2049-2051.
- DAVIS ME, CHEN Z & SHIN DM, 2008.** Nanoparticle therapeutics: an emerging treatment modality for cancer. *Nat Rev Drug Discov*, 7, pp. 771-782.
- DAWIDCZYK CM, RUSSELL LM & SEARSON PC, 2014.** Nanomedicines for cancer therapy: state-of-the-art and limitations to pre-clinical studies that hinder future developments. *Frontiers in chemistry*, 2, p. 69.
- DEBBAGE P, 2009.** Targeted drugs and nanomedicine: present and future. *Current pharmaceutical design*, 15, pp. 153-172.
- DECUZZI P, LEE S, BHUSHAN B & FERRARI M, 2005.** A theoretical model for the margination of particles within blood vessels. *Annual Biomedical Engineering*, 33, pp. 179-190.
- DECUZZI P, PASQUALINI R, ARAP W & FERRARI M, 2009.** Intravascular delivery of particulate systems: does geometry really matter? *Pharmacological research*, 26, pp. 235-243.
- DENG R, YUE Y, JIN F, CHEN Y, KUNG HF ET AL., 2009.** Revisit the complexation of PEI and DNA - how to make low cytotoxic and highly efficient PEI gene transfection non-viral vectors with a controllable chain length and structure? *Journal of controlled release*, 140, pp. 40-46.
- DERFUS AM, CHAN WCW & BHATIA SN, 2004.** Probing the cytotoxicity of semiconductor quantum dots. *Nano Letters*, 4, pp. 11-18.
- DING Y, JIANG Z, SAHA K, KIM CS, KIM ST ET AL., 2014.** Gold nanoparticles for nucleic acid delivery. *Molecular Therapy*, 22, pp. 1075-1083.
- DONKURU M, BADEA I, WETTING S, VERRALL R, ELSABAHY M ET AL., 2010.** Advancing nonviral gene delivery: lipid- and surfactant-based nanoparticle design strategies. *Nanomedicine (London, England)*, 5, pp. 1103-1127.
- DOWLING AP, 2004.** Development of nanotechnologies. *Materials Today*, 7, pp. 30-35.
- DREXLER K.E, 1981.** Molecular engineering: An approach to the development of general capabilities for molecular manipulation. *Proceedings of the National Academy of Sciences of the United States of America*, 78, pp. 5275-5278.

- DUAN Y, ZHANG S, WANG B, YANG B & ZHI D, 2009.** The biological routes of gene delivery mediated by lipid-based non-viral vectors. *Expert opinion on drug delivery*, 6, pp. 1351-1361.
- DURÁN S, DUCH M, PATIÑO T, TORRES A ET AL., 2015.** Technological development of intracellular polysilicon-chromium-gold chips for orthogonal chemical functionalization. *Sensors and Actuators B: Chemical*, 209, pp. 212-224.
- DUTTA D & DONALDSON JG, 2012.** Search for inhibitors of endocytosis: Intended specificity and unintended consequences. *Cellular Logistics*, 2, pp. 203-208.

E

- EKIMOV AI, EFROS AL & ONUSHCHENKO AA, 1985.** Quantum size effect in semiconductor microcrystals. *Solid State Communications*, 56, pp. 921-924.
- EL-SAYED IH, HUANG X & EL-SAYED M, 2006.** Selective laser photo-thermal therapy of epithelial carcinoma using anti-EGFR antibody conjugated gold nanoparticles. *Cancer letters*, 239, pp. 129-35.
- ELIYAHU H, BARENHOLZ Y & DOMB AJ, 2005.** Polymers for DNA delivery. *Molecules*, 10(1), pp. 34-64.
- ELSABAHY M, WAZEN N, BAYÓ-PUXAN N, DELAVEY G, SERVANT M ET AL., 2009.** Delivery of nucleic acids through the controlled disassembly of multifunctional nanocomplexes. *Advanced Functional Materials*, 19, pp. 3862-3867.
- ETHERIDGE ML, CAMPBELL SA, ERDMAN AG, HAYNES CL, WOLF SM ET AL., 2013.** The big picture on nanomedicine: the state of investigational and approved nanomedicine products. *Nanomedicine: nanotechnology, biology, and medicine*, 9, pp. 1-14.

F

- FAY F & SCOTT CJ, 2011.** Antibody-targeted nanoparticles for cancer therapy. *Immunotherapy*, 3, pp. 381-394.
- FERNÁNDEZ-ROSAS E, GÓMEZ R, IBÁÑEZ E, BARRIOS L, DUCH M ET AL., 2010.** Internalization and cytotoxicity analysis of silicon-based microparticles in macrophages and embryos. *Biomedical microdevices*, 12, pp. 371-379.

- FERNÁNDEZ-ROSAS E, GÓMEZ R, IBÁÑEZ E, BARRIOS L, DUCH M ET AL., 2009.** Intracellular polysilicon barcodes for cell tracking. *Small*, 5(21), pp. 2433-2439.
- FERRARI M, 2005.** Cancer nanotechnology: opportunities and challenges. *Nature reviews. Cancer*, 5, pp. 161-71.
- FEYNMAN RP, 1992.** There 's plenty of room at the bottom. *Journal of Microelectromechanical Systems*, 1, pp. 60-66.
- FISCHER D, LI Y, AHLEMAYER B, KRIEGLSTEIN J & KISSEL T, 2003.** In vitro cytotoxicity testing of polycations: influence of polymer structure on cell viability and hemolysis. *Biomaterials*, 24, pp. 1121-1131.
- FRÖHLICH E, 2013.** Cellular targets and mechanisms in the cytotoxic action of non-biodegradable engineered nanoparticles. *Current drug metabolism*, 14, pp. 976-988.
- FRÖHLICH E, 2012.** The role of surface charge in cellular uptake and cytotoxicity of medical nanoparticles. *International journal of nanomedicine*, 7, pp. 5577-5591.

G

- GENTILE F, CHIAPPINI C, FINE D, BHAVANE RC, PELUCCIO MS ET AL., 2008.** The effect of shape on the margination dynamics of non-neutrally buoyant particles in two-dimensional shear flows. *Journal of Biomechanics*, 41, pp. 2312-2318
- GODBAY WT, WU KK & MIKOS AG, 1999.** Poly(ethylenimine) and its role in gene delivery. *Journal of controlled release*, 60(2-3), pp. 149-160.
- GODIN B, TASCIOTTI E, LIU X, SERDA RE, FERRARI M ET AL, 2011.** Multistage nanovectors: from concept to novel imaging contrast agents and therapeutics. *Accounts of chemical research*, 44, pp. 979-989.
- GÓMEZ-MARTÍNEZ R, HERNÁNDEZ-PINTO, DUCH M, VÁZQUEZ P, ZINOVIEV K ET AL., 2013.** Silicon chips detect intracellular pressure changes in living cells. *Nature Nanotechnology*, 8, pp. 517-521.
- GONZÁLEZ O, SMITH RL & GOODMAN SB, 1996.** Effect of size, concentration, surface area, and volume of polymethylmethacrylate particles on human macrophages in vitro. *Journal of biomedical materials research*, 30, pp. 463-473.

- GRANDINETTI G, SMITH AE & REINEKE TM, 2012.** Membrane and nuclear permeabilization by polymeric pDNA vehicles: efficient method for gene delivery or mechanism of cytotoxicity? *Molecular pharmaceutics*, 9, pp. 523-538.
- GRATTON SE, ROPP PA, POHLHAUS PD, LUFT JC, MADDEN VJ ET AL., 2008.** The effect of particle design on cellular internalization pathways. *Proceedings of the National Academy of Sciences of the United States of America*, 105, pp. 11613-8.
- GU FX, KARNIK R, WANG AZ, ALEXIS F, NISSENBAUM EL ET AL., 2007.** Targeted nanoparticles for cancer therapy. *Nano Today*, 2, pp. 14-21.
- GUNDELFINGER ED, KESSELS MM & QUALMANN B, 2003.** Temporal and spatial coordination of exocytosis and endocytosis. *Nature Reviews Molecular Cell Biology*, 4, pp. 127-139.

H

- HAN T & DAS DB, 2015.** Potential of combined ultrasound and microneedles for enhanced transdermal drug permeation: A review. *European journal of pharmaceutics and biopharmaceutics*, 89C, pp. 312-328.
- HAUCK TS, GHAZANI A & CHAN WCW, 2008.** Assessing the effect of surface chemistry on gold nanorod uptake, toxicity, and gene expression in mammalian cells. *Small*, 4, pp. 153-9.
- HAYASHI K, NAKAMURA M, SAKAMOTO W, YOGO T, MIKI H ET AL., 2013.** Superparamagnetic nanoparticle clusters for cancer theranostics combining magnetic resonance imaging and hyperthermia treatment. *Theranostics*, 3, pp. 366-376.
- HE Q, ZHANG Z, GAO Y, SHI J & LI Y, 2009.** Intracellular localization and cytotoxicity of spherical mesoporous silica nano- and microparticles. *Small*, 5, pp. 2722-2729.
- HELANDER IM, ALAKOMI HL, LATVA-KALA K & KOSKI P, 1997.** Polyethyleneimine is an effective permeabilizer of gram-negative bacteria. *Microbiology*, 143, pp. 3193-3199.
- HELDIN CH, RUBIN K, PIETRAS K, & OSTMAN A.** High interstitial fluid pressure: an obstacle in cancer therapy. *Nature Reviews Cancer*, 4, pp. 806-813.

- HILT JZ & PEPPAS NA, 2005.** Microfabricated drug delivery devices. *International Journal of Pharmaceutics*, 306, pp. 15-23.
- HOFMANN S, SHARMA R, DUCATI C, DU G, MATTEVI C ET AL., 2007.** In situ observations of catalyst dynamics during surface-bound carbon nanotube nucleation. *Nano Letters*, 7, pp. 602-608.
- HUANG C, NEOH KG, KANG ET & SHUTER B, 2011.** Surface modified superparamagnetic iron oxide nanoparticles (SPIONs) for high efficiency folate-receptor targeting with low uptake by macrophages. *Journal of Materials Chemistry*, 21, pp. 16094-16102.
- HUANG X & EL-SAYED M, 2011.** Plasmonic photo-thermal therapy (PPTT). *Alexandria Journal of Medicine*, 47, pp. 1-9.
- HUOTARI J & HELENIUS A, 2011.** Endosome maturation. *The EMBO Journal*, 30, pp. 3481-3500.

I

- IJIMA S, 1991.** Helical microtubules of graphitic carbon. *Nature*, 354, pp. 56-58.
- IMPERIALE JC, NEJAMKIN P, DEL SOLE MJ, LANNUSSE CE & SOSNIK A, 2015.** Novel protease inhibitor-loaded Nanoparticle-in-Microparticle Delivery System leads to a dramatic improvement of the oral pharmacokinetics in dogs. *Biomaterials*, 37, pp. 383-394.
- IYERSEN TG, SKOTLAND T & SANDVIG K, 2011.** Endocytosis and intracellular transport of nanoparticles: Present knowledge and need for future studies. *Nano Today*, 6, pp. 176-185.

J

- JAIN GK, WARSJI MH, NIRMAL J, GARG V, PATHAN SA ET AL., 2012.** Therapeutic stratagems for vascular degenerative disorders of the posterior eye. *Drug discovery today*, 17, pp. 748-759.
- JAIN NK, MISHRA V & MEHRA NK, 2013.** Targeted drug delivery to macrophages. *Expert opinion on drug delivery*, 10, pp. 353-67.

JAIN S, HIRST DG & O'SULLIVAN JM, 2012. Gold nanoparticles as novel agents for cancer therapy. *The British Journal of Radiology*, 85, pp. 101-113.

K

KAMINSKAS LM, MCLEOD VM, KELLY BD, SBERNA G ET AL, 2015. A comparison of changes to doxorubicin pharmacokinetics, antitumor activity, and toxicity mediated by PEGylated dendrimer and PEGylated liposome drug delivery systems. *Nanomedicine: Nanotechnology, Biology and Medicine*, 8, pp. 103-111.

KARLSSON HL, GUSTAFSSON J, CRONHOLM P & MÖLLER L, 2009. Size-dependent toxicity of metal oxide particles—A comparison between nano- and micrometer size. *Toxicology Letters*, 188, pp. 112-118.

KASTURI SP, SACHAPHIBULKIJ K & ROY K, 2005. Covalent conjugation of polyethyleneimine on biodegradable microparticles for delivery of plasmid DNA vaccines. *Biomaterials*, 26, pp. 6375-6385.

KELKAR SS, & REINEKE TM, 2011. Theranostics: combining imaging and therapy. *Bioconjugate chemistry*, 22, pp. 1879-1903.

KENNEDY LC, BICKFORD LR, LEWINSKI NA, COUGHLIN AJ, HU Y ET AL., 2011. A new era for cancer treatment: gold-nanoparticle-mediated thermal therapies. *Small*, 7, pp. 169-183.

KESHARWANI P, MISHRA V & JAIN NK, 2015. Validating the anticancer potential of carbon nanotube-based therapeutics through cell line testing. *Drug discovery today*, 20, pp 1049-1060.

KIM JA, ABERG C, DE CÁRCER G, MALUMBRES M, SALVATI A ET AL., 2013. Low dose of amino-modified nanoparticles induces cell cycle arrest. *ACS nano*, 7, pp. 7483-7494.

KIM ST, JANG DJ, KIM JH, PARK JY, LIM JS ET AL., 2009. Topical administration of cyclosporin A in a solid lipid nanoparticle formulation. *Die Pharmazie*, 64, pp. 510-514.

KING-HEIDEN TC, WIECINSKI PN, MANGHAM A, METZ KM, NESBIT D ET AL., 2009. Quantum Dot Nanotoxicity Assessment Using the Zebrafish Embryo. *Environmental Science & Technology*, 43, pp. 1605-1611.

- KIRKHAM M & PARTON RG, 2005.** Clathrin-independent endocytosis: new insights into caveolae and non-caveolar lipid raft carriers. *Biochimica et biophysica acta*, 1746, pp. 349-363.
- KOBAYASHI S, KOJIDANI T, OSAKADA H, YAMAMOTO A, YOSHIMORI T ET AL., 2010.** Artificial induction of autophagy around polystyrene beads in nonphagocytic cells. *Autophagy*, 6, pp. 36-45.
- KOHANE DS, 2007.** Microparticles and nanoparticles for drug delivery. *Biotechnology and Bioengineering*, 96, pp. 203-209.
- KOYNOVA R & TENCHOV B, 2011.** Recent patents in cationic lipid carriers for delivery of nucleic acids. *Recent patents on DNA & gene sequences*, 5, pp. 8-27.
- KROTO HW, HEATH JR, O'BRIEN SC, CURL RF & SMALLEY RE, 1985.** C60: Buckminsterfullerene. *Nature*, 318, pp. 162-163.
- KÜHN DA, VANHECKE D, MICHEN B, BLANK F, GEHR P ET AL., 2014.** Different endocytotic uptake mechanisms for nanoparticles in epithelial cells and macrophages. *Beilstein Journal of Nanotechnology*, 5, pp. 1625-1636.
- KUSAKA T, NAKAYAMA M, NAKAMURA K, ISHIMIYA M, FURUSAWA E ET AL., 2014.** Effect of silica particle size on macrophage inflammatory responses. *PloS one*, 9, p. e92634.

L

- LABALA S, MANDAPALLI PK, KURUMADDALI A & VENUGANTI VV, 2015.** Layer-by-layer polymer coated gold nanoparticles for topical delivery of imatinib mesylate to treat melanoma. *Molecular pharmaceuticals*, 12, pp. 878-888.
- LAMBERT RC, MAULET Y, DUPONT JL, MYKITA S, CRAIG P ET AL., 1996.** Polyethylenimine-mediated DNA transfection of peripheral and central neurons in primary culture: probing Ca²⁺ channel structure and function with antisense oligonucleotides. *Molecular and cellular neurosciences*, 7, pp. 239-246.
- LANKOFF A, SANDBERG WG, WĘGIEREK-CIUK A, LISOWSKA H, REFSNES M, ET AL., 2012.** The effect of agglomeration state of silver and titanium dioxide nanoparticles on cellular response of HepG2, A549 and THP-1 cells. *Toxicology letters*, 208, pp. 197-213.

- LAROUÏ H, RAKHYA P, XIAO B, VIENNOIS E & MERLIN D, 2013.** Nanotechnology in diagnostics and therapeutics for gastrointestinal disorders. *Digestive and liver disease*, 45, pp. 995-1002.
- LARSEN EKV, NIELSEN T, WITTENBORN T, BIERKEDAL H, VORUP-JENSEN T ET AL., 2009.** Size-dependent accumulation of PEGylated silane-coated magnetic iron oxide nanoparticles in murine tumors. *ACS Nano*, 3, pp. 1947-1951.
- LESNIAK A, FENAROLI F, MONOPOLI MP, ABERG C, DAWSON KA ET AL., 2012.** Effects of the presence or absence of a protein corona on silica nanoparticle uptake and impact on cells. *ACS Nano*, 6, pp. 5845-5857.
- LI D, TANG X, PULLI B, LIN C, ZHAO P ET AL., 2014.** Theranostic nanoparticles based on bioreducible polyethylenimine-coated iron oxide for reduction-responsive gene delivery and magnetic resonance imaging. *International journal of nanomedicine*, 9, pp. 3347-3361.
- LI P, LI D, ZHANG L, LI G & WANG E, 2008.** Cationic lipid bilayer coated gold nanoparticles-mediated transfection of mammalian cells. *Biomaterials*, 29, pp. 3617-3624.
- LI X, JIANG L, ZHAN Q, QIAN J & HE S, 2009.** Localized surface plasmon resonance (LSPR) of polyelectrolyte-functionalized gold-nanoparticles for biosensing. *Colloids and Surfaces A: Physicochemical and Engineering Aspects*, 332, pp. 172-179.
- LIECHTY WB, KRYSZCIO DR, SLAUGHTER BV & PEPPAS N, 2010.** Polymers for drug delivery systems. *Annual review of chemical and biomolecular engineering*, 1, pp. 149-173.
- LIPO A, CONJUSTEAU A, TSYBOULSKI D, ERMOLINSKY B, KAZANSKY A ET AL., 2012.** Biocompatible Gold Nanorod Conjugates for Preclinical Biomedical Research. *Journal of nanomedicine & nanotechnology*, 2, pp. 1-10.
- LOOS C, SYROVETS T, MUSYANOVYCH A, MAILÄNDER V, LANDFESTER K ET AL., 2014.** Functionalized polystyrene nanoparticles as a platform for studying bio-nano interactions. *Beilstein journal of nanotechnology*, 5, pp. 2403-2412.
- LU F, WU SH, HUNG Y & MOU CY, 2009.** Size effect on cell uptake in well-suspended, uniform mesoporous silica nanoparticles. *Small*, 5, pp. 1408-1413.

- LUNOV O, SYROVETS T, LOOS C, NIENHAUS GU, MAINLÄNDER V ET AL., 2011. Amino-functionalized polystyrene nanoparticles activate the NLRP3 inflammasome in human macrophages. *ACS Nano*, 5, pp. 9648-9657.
- LUZIO JP, PRYOR PR & BRIGHT NA, 2007. Lysosomes: fusion and function. *Nature Reviews Molecular Cell Biology*, 8, pp. 622-632.
- LV H, ZHANG S, WANG B, CUI S & YAN J, 2006. Toxicity of cationic lipids and cationic polymers in gene delivery. *Journal of controlled release*, 114, pp. 100-109.

M

- MA X, ZHAO Y, WOEI K & ZHAO Y, 2013. Integrated hollow mesoporous silica nanoparticles for target drug/siRNA co-delivery. *Chemistry*, 19, pp. 15593-15603.
- MACIA E, EHRLICH M, MASSOL R, BOUCROT E, BRUNNER C ET AL., 2006. Dynasore, a cell-permeable inhibitor of dynamin. *Developmental cell*, 10, pp. 839-50.
- MAEDA H, 2010. Tumor-selective delivery of macromolecular drugs via the EPR effect: background and future prospects. *Bioconjugate chemistry*, 21, pp. 797-802.
- MAGENAU A, BENZING C, PROSCHOGO N, DON AS, HEJAZI L ET AL., 2011. Phagocytosis of IgG-coated polystyrene beads by macrophages induces and requires high membrane order. *Traffic*, 12, pp. 1730-1743.
- MAHMOUDI M, SANT S, WANG B, LAURENT S & SEN T, 2011. Superparamagnetic iron oxide nanoparticles (SPIONs): Development, surface modification and applications in chemotherapy. *Advanced Drug Delivery Reviews*, 63, pp. 24-46.
- MAILÄNDER V & LANDFESTER K, 2009. Interaction of nanoparticles with cells. *Biomacromolecules*, 10, pp. 2379-2400.
- MARETTI E, ROSSI T, BONDI M, CROCE MA, HANUSKOVA M ET AL., 2014. Inhaled solid lipid microparticles to target alveolar macrophages for tuberculosis. *International Journal of Pharmaceutics*, 462, pp. 74-82.
- MEDINTZ IL, UYEDA HT, GOLDMAN ER & MATTOUSSI H, 2005. Quantum dot bioconjugates for imaging, labelling and sensing. *Nature Materials*, 4, pp. 435-446.

- MEHRA NK, JAIN K & JAIN NK, 2015.** Pharmaceutical and biomedical applications of surface engineered carbon nanotubes. *Drug discovery today*, 20, pp. 750-759.
- MELLMAN I, 1996.** Endocytosis and molecular sorting. *Annual Review of Cell and Developmental Biology*, 12(1), pp. 575-625.
- MENG H, MAI WX, ZHANG H, XUE M, XIA T ET AL., 2013.** Codelivery of an optimal drug/siRNA combination using mesoporous silica nanoparticles to overcome drug resistance in breast cancer in vitro and in vivo. *ACS nano*, 7, pp. 994-1005.
- MERISKO-LIVERSIDGE EM & LIVERSIDGE GG, 2008.** Drug nanoparticles: formulating poorly water-soluble compounds. *Toxicologic Pathology*, 36, pp. 43-48.
- MOGHIMI SM, HUNTER AC & MURRAY JC, 2005.** Nanomedicine: current status and future prospects. *The FASEB Journal*, 19, pp. 311-330.
- MONOPOLI MP, WALCZYK D, CAMPBELL A, ELIA G, LYNCH I ET AL., 2011.** Physical-chemical aspects of protein corona: relevance to in vitro and in vivo biological impacts of nanoparticles. *Journal of the American Chemical Society*, 133, pp. 2525-2534.
- MONTON H, PAROLO C, ARANDA-RAMOS A, MERKOÇI A & NOGUÉS C, 2015.** Annexin-V/quantum dot probes for multimodal apoptosis monitoring in living cells: improving bioanalysis using electrochemistry. *Nanoscale*, 7, pp. 4097-4104.
- MONTON H, ROLDÁN M, MERKOÇI A, ROSSINYOL E, CASTELL O ET AL., 2012.** The use of quantum dots for immunochemistry applications. *Methods in molecular biology*, 906, pp. 185-192.
- MÜLLER-GOYMANN CC, 2004.** Physicochemical characterization of colloidal drug delivery systems such as reverse micelles, vesicles, liquid crystals and nanoparticles for topical administration. *European Journal of Pharmaceutics and Biopharmaceutics*, 58, pp. 343-356.
- MUNDRA RV, WU X, SAUER J, DORDICK JS & KANE RS, 2014.** Nanotubes in biological applications. *Current opinion in biotechnology*, 28, pp. 25-32.
- MUTHU MS, LEONG DT, MEI L & FENG SS, 2014.** Nanotheranostics - application and further development of nanomedicine strategies for advanced theranostics. *Theranostics*, 4, pp. 660-677.

N

- NAKASHIMA Y, SUN DH, TRINIDADE MC, MALONEY WJ, GOODMAN SB ET AL., 1999.** Signaling pathways for tumor necrosis factor-alpha and interleukin-6 expression in human macrophages exposed to titanium-alloy particulate debris in vitro. *The Journal of bone and joint surgery. American volume*, 81, pp. 603-615.
- NANJWADE BK, BECHRA HM, DERKAR GK, MANVI FV, NANJWADE VK, 2009.** Dendrimers: Emerging polymers for drug-delivery systems. *European Journal of Pharmaceutical Sciences*, 38, pp. 185-196.
- NEL AE, MÄDLER L, VELEGOL D, XIA T, HOEK EMV ET AL., 2009.** Understanding biophysicochemical interactions at the nano-bio interface. *Nature materials*, 8, pp. 543-57.
- NEU M, FISCHER D & KISSEL T, 2005.** Recent advances in rational gene transfer vector design based on poly(ethyleneimine) and its derivatives. *The journal of gene medicine*, 7, pp. 992-1009.

O

- O'HAGAN DT, MCGEE JP, HOLMGREN J, MOWAT AM, DONACHIE AM ET AL., 1993.** Biodegradable microparticles for oral immunization. *Vaccine*, 11, pp. 149-154.

P

- PACHECO P, WHITE D & SULCHEK T, 2013.** Effects of microparticle size and Fc density on macrophage phagocytosis. *PloS one*, 8, p. e60989.
- PALANKAR R, SKIRTACH AG, KREFT O, BÉDARD M, GARSTKA M ET AL., 2009.** Controlled intracellular release of peptides from microcapsules enhances antigen presentation on MHC class I molecules. *Small*, 5, pp. 2168-2176.
- PAN X, GUAN J, YOO JW, EPSTEIN AJ, LEE LJ ET AL., 2008.** Cationic lipid-coated magnetic nanoparticles associated with transferrin for gene delivery. *International journal of pharmaceuticals*, 358, pp. 263-270.
- PAN Y, NEUSS S, LEIFERT A, FISCHLER M, WEN F ET AL., 2007.** Size-dependent cytotoxicity of gold nanoparticles. *Small*, 3, pp. 1941-9.

- PARIKH R, DALWADI S, ABOTI P & PATEL L, 2014.** Inhaled microparticles of anti-tubercular antibiotic for in vitro and in vivo alveolar macrophage targeting and activation of phagocytosis. *Journal of Antibiotics*, 67, pp. 387-394.
- PARK J, DVORACEK C, LEE KH, GALLOWAY JF ET AL., 2011.** CuInSe/ZnS Core/Shell NIR quantum dots for biomedical imaging. *Small*, 7, pp. 3148-3152.
- PARK MV, NEIGH AM, VERMEULEN JP, DE LA FONTEYNE LJ ET AL., 2011.** The effect of particle size on the cytotoxicity, inflammation, developmental toxicity and genotoxicity of silver nanoparticles. *Biomaterials*, 32, pp. 9810-9817.
- PATEL HM & MOGHIMI SM, 1998.** Serum-mediated recognition of liposomes by phagocytic cells of the reticuloendothelial system - The concept of tissue specificity. *Advanced Drug Delivery Reviews*, 32, pp. 45-60
- PATIÑO T, MAHAJAN U, PALANKAR R, MEDVEDEV N, WALOWSKI J ET AL., 2015.** Multifunctional gold nanorods for selective plasmonic photothermal therapy in pancreatic cancer cells using ultra-short pulse near-infrared laser irradiation. *Nanoscale*, 7, pp. 5328-5337.
- PEER D, KARP JM, HONG S, FAROKHZAD OC ET AL., 2007.** Nanocarriers as an emerging platform for cancer therapy. *Nature Nanotechnology*, 2, pp. 751-760.
- PELKMANS L, PUNTENER D & HELENIUS A, 2002.** Local actin polymerization and dynamin recruitment in SV40-induced internalization of caveolae. *Science*, 296, pp. 535-539.
- PERACCHIA MT, FATTAL E, DESMAËLE D, BESNARD M, NOËL JP ET AL., 1999.** Stealth® PEGylated polycyanoacrylate nanoparticles for intravenous administration and splenic targeting. *Journal of Controlled Release*, 60, pp. 121-128.
- PFEFFER SR, 2009.** Multiple routes of protein transport from endosomes to the trans Golgi network. *FEBS letters*, 583, pp. 3811-3816.

Q

- QIU Y, LIU Y, WANG L, XU L, BAI R ET AL., 2010.** Surface chemistry and aspect ratio mediated cellular uptake of Au nanorods. *Biomaterials*, 31, pp. 7606-19.
- QUINN HL, KEARNEY MC, COURTENAY AJ ET AL. 2014.** The role of microneedles for drug and vaccine delivery. *Expert opinion on drug delivery*, 11, pp. 1769-1780.

R

- RAHMAN M, AHMAD MZ, KAZMI I, AKHTER S, AFZAI M ET AL., 2012.** Advancement in multifunctional nanoparticles for the effective treatment of cancer. *Expert opinion on drug delivery*, 9, pp. 367-381.
- RAMÓN-AZCÓN J, AHADIAN S, OBREGÓN R, SHIKU H, RAMALINGAM M ET AL., 2014.** Applications of carbon nanotubes in stem cell research. *Journal of biomedical nanotechnology*, 10, pp. 2539-2561.
- REJMAN J, OBERLE V, ZUHORN IS & HOEKSTRA D, 2004.** Size-dependent internalization of particles via the pathways of clathrin- and caveolae-mediated endocytosis. *The Biochemical journal*, 377, pp. 159-69.
- RITZ S, SCHÖTTLER S, KOTMAN N, BAIER G, MUSYANOVYCH A ET AL., 2015.** Protein corona of nanoparticles: distinct proteins regulate the cellular uptake. *Biomacromolecules*, 16, pp 1311-1321.
- ROGACH A, SUSHA A, CARUSO F, SUKHORUKOV G, KORNOWSKI A ET AL., 2000.** Nano- and microengineering: 3-D colloidal photonic crystals prepared from sub- μm -sized polystyrene latex spheres pre-coated with luminescent polyelectrolyte/nanocrystal shells. *Advanced Materials*, 12, pp. 333-337.
- ROY K, MAO HQ, HUANG SK, LEONG KW ET AL., 1999.** Oral gene delivery with chitosan-DNA nanoparticles generates immunologic protection in a murine model of peanut allergy. *Nature Medicine*, 5, pp. 387-391.

S

- SAFTIG P & KLUMPERMAN J, 2009.** Lysosome biogenesis and lysosomal membrane proteins: trafficking meets function. *Nature Reviews Molecular Cell Biology*, 10, pp. 623-635.
- SAHA K, KIM ST, YAN B, MIRANDA OR, ALFONSO FS ET AL., 2013.** Surface functionality of nanoparticles determines cellular uptake mechanisms in mammalian cells. *Small*, 9, pp. 300-305.
- SAKULKHU U, MAHMOUDI M, MAURIZI L, SALAKLANG J & HOFMANN H, 2014.** Protein corona composition of superparamagnetic iron oxide nanoparticles with various physico-chemical properties and coatings. *Scientific Reports*, 4, p. 5020.

- SALONEN J, LAITINEN L, KAUKONEN AM, TUURA J, BJÖRKQVIST M ET AL., 2005.** Mesoporous silicon microparticles for oral drug delivery: Loading and release of five model drugs. *Journal of Controlled Release*, 108, pp. 362-374.
- SALVATI A, PITEK AS, MONOPOLI MP, PRAPAINOP K ET AL, 2013.** Transferrin-functionalized nanoparticles lose their targeting capabilities when a biomolecule corona adsorbs on the surface. *Nature Nanotechnology*, 8, pp. 137-143.
- SANDVIG K, TORGENSEN ML, RAA HA & VAN DEURS B, 2008.** Clathrin-independent endocytosis: from nonexisting to an extreme degree of complexity. *Histochemistry and cell biology*, 129, pp. 267-276.
- SANDVIG K & VAN DEURS B, 2005.** Delivery into cells: lessons learned from plant and bacterial toxins. *Gene Therapy*, 12, pp. 865-872.
- SANNA V, PALA N & SECHI M, 2014.** Targeted therapy using nanotechnology: focus on cancer. *International journal of nanomedicine*, 9, pp. 467-483.
- SANT S, TAO SL, FISHER OZ, XU Q ET AL., 2012.** Microfabrication technologies for oral drug delivery. *Advanced drug delivery reviews*, 64, pp. 496-507.
- SANTINI JT, CIMA MJ & LANGER R, 1999.** A controlled-release microchip. *Nature*, 397, pp. 335-338.
- SANTINI JT, RICHARDS AC, SCHEIDT R, CIMA MJ & LANGER R, 2000.** Microchips as Controlled Drug-Delivery Devices. *Angewandte Chemie*, 39, pp. 2396-2407.
- SANVICENS N & MARCO MP, 2008.** Multifunctional nanoparticles: properties and prospects for use in human medicine. *Trends in biotechnology*, 26, pp. 425-433.
- SARKAR A, GHOSH M & SIL PC, 2014.** Nanotoxicity: oxidative stress mediated toxicity of metal and metal oxide nanoparticles. *Journal of nanoscience and nanotechnology*, 14, pp. 730-743.
- SCHLIWA M, 1982.** Action of cytochalasin D on cytoskeletal networks. *The Journal of cell biology*, 92, pp. 79-91.
- SCHMIDT C, LAUTENSCHLAEGER C, COLLNOT EM, SCHUMANN M, BOJARSKI C ET AL., 2013.** Nano- and microscaled particles for drug targeting to inflamed intestinal mucosa: A first in vivo study in human patients. *Journal of Controlled Release*, 165, pp. 139-145.

- SEYRANTEPE V, IANELLO A, LIANG F, KANSHIN E, JAYANTH P ET AL., 2010.** Regulation of Phagocytosis in Macrophages by Neuraminidase 1. *Journal of Biological Chemistry*, 285, pp. 206-215.
- SHANG L, NIENHAUS K & NIENHAUS G, 2014.** Engineered nanoparticles interacting with cells: size matters. *Journal of Nanobiotechnology*, 12, p. 5.
- SHAWGO RS, GRAYSON ACR, LI Y & CIMA MJ, 2002.** BioMEMS for drug delivery. *Current Opinion in Solid State and Materials Science*, 6, pp. 329-334.
- SHETE HK, PRABHU RH & PATRAVALE VB, 2014.** Endosomal escape: a bottleneck in intracellular delivery. *Journal of nanoscience and nanotechnology*, 14, pp. 460-474.
- SHRESTHA R, ELSABAHY M, FLOREZ-MALAVAR S, SAMARAJEEWA S & WOOLEY KL, 2012.** Endosomal escape and siRNA delivery with cationic shell crosslinked knedel-like nanoparticles with tunable buffering capacities. *Biomaterials*, 33, pp. 8557-8568.
- SINGH M, BRIONES M, OTT G & O'HAGAN D, 2000.** Cationic microparticles: A potent delivery system for DNA vaccines. *Proceedings of the National Academy of Sciences of the United States of America*, 97, pp. 811-6.
- SINGH R & LILLARD JWJ, 2009.** Nanoparticle-based targeted drug delivery. *Experimental and molecular pathology*, 86, pp. 215-223.
- SONAWANE ND, SZOKA FCJ & VERKMAN AS, 2003.** Chloride accumulation and swelling in endosomes enhances DNA transfer by polyamine-DNA polyplexes. *The Journal of biological chemistry*, 278, pp. 44826-44831.
- STAPLES M, 2010.** Microchips and controlled-release drug reservoirs. *Wiley interdisciplinary reviews. Nanomedicine and nanobiotechnology*, 2, pp. 400-417.
- STARK WJ, 2011.** Nanoparticles in Biological Systems. *Angewandte Chemie International Edition*, 50, pp. 1242-1258.
- STEPHENS DJ & PEPPERKOK R, 2001.** The many ways to cross the plasma membrane. *Proceedings of the National Academy of Sciences*, 98, pp. 4295-4298.
- STUDER D, PALANKAR R, BÉDARD M, WINTERHALTER M & SPRINGER S, 2010.** Retrieval of a metabolite from cells with polyelectrolyte microcapsules. *Small*, 6, pp. 2412-2419.

SUN X & ZHANG N, 2010. Cationic polymer optimization for efficient gene delivery. *Mini reviews in medicinal chemistry*, 10, pp. 108-125.

SWANSON JA & WATTS C, 1995. Macropinocytosis. *Trends in cell biology*, 5, pp. 424-428.

T

TAN J, SHAH S, THOMAS A, OU-YANG HD & LIU Y, 2013. The influence of size, shape and vessel geometry on nanoparticle distribution. *Microfluidics Nanofluidics*, 14, pp. 77-87.

TANAKA T, MANGALA LS, VIVAS-MEJIA PE, NIEVES-ALICEA R, MANN AP ET AL., 2010. Sustained Small Interfering RNA Delivery by Mesoporous Silicon Particles. *Cancer research*, 70, pp. 3687-3696.

TANIGUCHI N, 1974. On the Basic Concept of "Nano-Technology." *Bulletin of the Japan Society of Precision Engineering*, pp. 18-23.

TAO SL & DESAI TA, 2003. Microfabricated drug delivery systems: from particles to pores. *Advanced Drug Delivery Reviews*, 55, pp. 315-328.

TASCIOTTI E, LIU X, BHAVANE R, PLANT K, LEONARD AD ET AL., 2008. Mesoporous silicon particles as a multistage delivery system for imaging and therapeutic applications. *Nature Nanotechnology*, 3, pp. 151-157

TEKLE C, DEURS BV, SANDVIG K & IVERSEN TG, 2008. Cellular trafficking of quantum dot-ligand bioconjugates and their induction of changes in normal routing of unconjugated ligands. *Nano letters*, 8, pp. 1858-1865.

THIELE L, MERKLE HP & WALTER E, 2003. Phagocytosis and phagosomal fate of surface-modified microparticles in dendritic cells and macrophages. *Pharmaceutical research*, 20, pp. 221-8.

THOMAS TP, MAJOROS I, KOTLYAR A, MULLEN D, BANASZAK MM ET AL., 2009. Cationic poly(amidoamine) dendrimer induces lysosomal apoptotic pathway at therapeutically relevant concentrations. *Biomacromolecules*, 10, pp. 3207-3214.

THOREK DLJ & TSOURKAS A, 2008. Size, charge and concentration dependent uptake of iron oxide particles by non-phagocytic cells. *Biomaterials*, 29, pp. 3583-3590.

- TIWARI PM, VIG K, DENNIS VA & SINGH SR, 2011.** Functionalized Gold Nanoparticles and Their Biomedical Applications. *Nanomaterials*, 1, pp. 31-63.
- TOMIC S, DOKIC J, VASILIJIC S, OGRINC N, RUDOLF R ET AL., 2014.** Size-dependent effects of gold nanoparticles uptake on maturation and antitumor functions of human dendritic cells in vitro. *PloS one*, 9, p. e96584.
- TROS DE ILARDUYA C, SUN Y & DUZGUNES N, 2010.** Gene delivery by lipoplexes and polyplexes. *European journal of pharmaceutical sciences*, 40, pp. 159-170.
- TSONG TY, 1991.** Electroporation of cell membranes. *Biophys. J.* 60, pp. 297-306.

U

- UL-AIN Q, SHARMA S & KHULLER GK, 2003.** Chemotherapeutic potential of orally administered poly(lactide-co-glycolide) microparticles containing isoniazid, rifampin, and pyrazinamide against experimental tuberculosis. *Anti-microbial agents and chemotherapy*, 47, pp. 3005-3007.
- UNDERHILL DM & GOODRIDGE HS, 2012.** Information processing during phagocytosis. *Nature Reviews Immunology*, 12, pp. 492-502.
- URBANSKA AM, KARAGIANNIS ED, GUAJARDO G, LANGER RS & ANDERSON DG, 2012.** Therapeutic effect of orally administered microencapsulated oxaliplatin for colorectal cancer. *Biomaterials*, 33, pp. 4752-4761.

V

- VALDIGLESIAS V, KILIÇ G, COSTA C, FERNÁNDEZ-BERTÓLEZ N ET AL., 2015.** Effects of iron oxide nanoparticles: cytotoxicity, genotoxicity, developmental toxicity, and neurotoxicity. *Environmental and molecular mutagenesis*, 56, pp. 125-148.
- VALLÉS G, GONZÁLEZ-MELENDI P, GONZÁLEZ-CARRASCO JL, SALDAÑA L, SÁNCHEZ-SABATÉ E ET AL., 2006.** Differential inflammatory macrophage response to rutile and titanium particles. *Biomaterials*, 27, pp. 5199-5211.
- VAN MIDWOUT PM, JANSE A, MEREMA MT, GROOTHUIS GMM & VERPOORTE E, 2012.** Comparison of biocompatibility and adsorption properties of different plastics for advanced microfluidic cell and tissue culture models. *Analytical chemistry*, 84, pp. 3938-3944.

- VARELA JA, BEXIGA MG, ABERG C, SIMSON JC & DAWSON KA, 2012.** Quantifying size-dependent interactions between fluorescently labeled polystyrene nanoparticles and mammalian cells. *Journal of nanobiotechnology*, 10, p. 39.
- VELEV OD & KALER EW, 1999.** In situ assembly of colloidal particles into miniaturized biosensors. *Langmuir*, 15, pp. 3693-3698.
- VENKATESAN J, PALLELA R & KIM SK, 2014.** Applications of carbon nanomaterials in bone tissue engineering. *Journal of biomedical nanotechnology*, 10, pp. 3105-3123.
- VERMA A & STELLACCI F, 2010.** Effect of surface properties on nanoparticle-cell interactions. *Small*, 6, pp. 12-21.
- VRANIC S, BOGGETTO N, CONTREMOULINS V, MORNET S, REINHARDT N, 2013.** Deciphering the mechanisms of cellular uptake of engineered nanoparticles by accurate evaluation of internalization using imaging flow cytometry. *Particle and fibre toxicology*, 10, p. 2.

W

- WAKATSUKI T, SCHWAB B, THOMPSON NC & ELSON EL, 2001.** Effects of cytochalasin D and latrunculin B on mechanical properties of cells. *Journal of cell science*, 114, pp. 1025-1036.
- WALCZYK D, BOMBELLI FB, MONOPOLI MP ET AL., 2010.** What the cell “sees” in bionanoscience. *Journal of the American Chemical Society*, 132, pp. 5761-8.
- WANG J ET AL., 2015.** Size- and surface chemistry-dependent pharmacokinetics and tumor accumulation of engineered gold nanoparticles after intravenous administration. *Metallomics: integrated biometal science*, 7, pp. 516-524.
- WANG J, BAI R, YANG R, LIU J, TANG J ET AL., 2010.** The complex role of multivalency in nanoparticles targeting the transferrin receptor for cancer therapies. *Journal of the American Chemical Society*, 132, pp. 11306-11313.
- WANG T, HARTNER WC, GILLESPIE JW, PRAVEEN KP, YANG S ET AL., 2014.** Enhanced tumor delivery and antitumor activity in vivo of liposomal doxorubicin modified with MCF-7-specific phage fusion protein. *Nanomedicine: nanotechnology, biology, and medicine*, 10, pp. 421-430.

- WATAHA JC, LEWIS JB, VOLKMANN KR, LOCKWOOD PE, MESSER RL ET AL., 2004.** Sublethal concentrations of Au (III), Pd (II), and Ni(II) differentially alter inflammatory cytokine secretion from activated monocytes. *Journal of biomedical materials research. Part B, Applied biomaterials*, 69, pp. 11-17.
- WICKI A, WITZIGMANN D, BALASUBRAMANIAN V & HUWYLER J, 2015.** Nanomedicine in cancer therapy: Challenges, opportunities, and clinical applications. *Journal of Controlled Release*, 200, pp. 138-157.
- WIN KY & FENG SS, 2005.** Effects of particle size and surface coating on cellular uptake of polymeric nanoparticles for oral delivery of anticancer drugs. *Biomaterials*, 26, pp. 2713-2722.

X

- XIA T, KOVOCHICH M, LIONG M, ZINK JI & NEL AE, 2008.** Cationic polystyrene nanosphere toxicity depends on cell-specific endocytic and mitochondrial injury pathways. *ACS nano*, 2, pp. 85-96.
- XIAO Y, FORRY SP, GAO X, HOLBROOK RD, TELFORD WG ET AL., 2010.** Dynamics and mechanisms of quantum dot nanoparticle cellular uptake. *Journal of nanobiotechnology*, 8, p. 13.
- XU Y & SZOKA FC, 1996.** Mechanism of DNA Release from Cationic Liposome/DNA Complexes Used in Cell Transfection, *Biochemistry*, 35, pp. 5616-5623.

Y

- YAMEEN B, CHOI WI, VILOS C, SWAMI A, SHI J ET AL., 2014.** Insight into nanoparticle cellular uptake and intracellular targeting. *Journal of controlled release*, 190, pp. 485-499.
- YAN Y, GAUSE KT, KAMPHUIS MM, ANG CS, O'BRIEN-SIMPSON NM ET AL., 2013.** Differential roles of the protein corona in the cellular uptake of nanoporous polymer particles by monocyte and macrophage cell lines. *ACS nano*, 7, pp. 10960-70.
- YANG P, GAI S & LIN J, 2012.** Functionalized mesoporous silica materials for controlled drug delivery. *Chemical Society Reviews*, 41, pp. 3679-3698.

- YOFFE S, LESHUK T, EVERETT P & GU F, 2013.** Superparamagnetic iron oxide nanoparticles (SPIONs): synthesis and surface modification techniques for use with MRI and other biomedical applications. *Current pharmaceutical design*, 19, pp. 493-509.
- YOON YM, LEWIS JS, CARSTENS MR, CAMPBELL-THOMPSON M, WASSERFALL CH ET AL., 2015.** A combination hydrogel microparticle-based vaccine prevents type 1 diabetes in non-obese diabetic mice. *Scientific reports*, 5, p. 13155.

Z

- ZAUNER W, FARROW NA & HAINES AM., 2001.** In vitro uptake of polystyrene microspheres: effect of particle size, cell line and cell density. *Journal of controlled release*, 71, pp. 39-51.
- ZHANG L, SINCLAIR A, CAO Z, ELLA-MENYE JR, XU X ET AL., 2013.** Hydrolytic cationic ester microparticles for highly efficient DNA vaccine delivery. *Small*, 9, pp. 3439-44.
- ZHANG Y, XU D, LI W, YU J & CHEN Y ET AL., 2012.** Effect of Size, Shape, and Surface Modification on Cytotoxicity of Gold Nanoparticles to Human HEp-2 and Canine MDCK Cells. *Journal of Nanomaterials*, 2012, pp. 1-7.
- ZHANG Y & YU LC, 2008.** Microinjection as a tool of mechanical delivery. *Current opinion in biotechnology*, 19, pp. 506-510.
- ZHONG Y, MENG F, DENG C & ZHONG Z, 2014.** Ligand-directed active tumor-targeting polymeric nanoparticles for cancer chemotherapy. *Biomacromolecules*, 15, pp. 1955-1969.
- ZOLNIK BS, GONZÁLEZ-FERNÁNDEZ A, SADRIEH N & DOBROVOLSKAIA MA, 2010.** Nanoparticles and the immune system. *Endocrinology*, 151, pp. 458-465.

